2019

Quantitative diatom-based proxy for sea ice extent in the Bering and Chukchi seas

Anna Nesterovich
Iowa State University

Quantitative diatom-based proxy for sea ice extent in the Bering and Chukchi seas

by

Anna Nesterovich

A dissertation submitted to the graduate faculty

in partial fulfillment of the requirements for the degree of

DOCTOR OF PHILOSOPHY

Co-majors: Geology; Environmental Sciences

Program of Study Committee:
Beth E. Caissie, Major Professor
William J. Gutowski
Chris Harding
Alan David Wanamaker Jr.
Yuyu Zhou
Philip M. Dixon

The student author, whose presentation of the scholarship herein was approved by the program of study committee, is solely responsible for the content of this dissertation. The Graduate College will ensure this dissertation is globally accessible and will not permit alterations after a degree is conferred.

Iowa State University

Ames, Iowa

2019

DEDICATION

For every young diatomist despairing in the taxonomical swamp: You can make it. Just remember that swamps are beautiful.

TABLE OF CONTENTS

Page

LIST OF FIGURES v

LIST OF TABLES viii

ACKNOWLEDGMENTS ix

ABSTRACT xi

CHAPTER 1. INTRODUCTION 1
Motivation 1
Arctic Sea Ice 2
Sea Ice Proxies 5
Diatom-based Sea Ice Proxies 6
Thesis organization 9
References 11

CHAPTER 2. TAXONOMY AND ULTRASTRUCTURE OF *SINERIMA*, A NEW GENUS OF DIATOMS (BACILLARIOPHYTA), WITH A DESCRIPTION OF A NEW SPECIES, *S. MARIGELA* 19
Abstract 19
Introduction 19
Material and Methods 22
Samples 22
Microscopy 23
Statistical Analysis 23
Results 25
Discussion and Conclusions 34
Acknowledgements 39
References 39

CHAPTER 3. DIATOM SUCCESSION AND VERTICAL EXPORT IN THE CHUKCHI SEA 48
Abstract 48
Introduction 48
Material and Methods 51
Sediment Trap Samples 51
Surface Sediment Samples 51
Diatom Identification and Quantification 52
Environmental Factors 52
Statistical Analysis 54
Results 54
Seasonal Changes in Mooring Samples 54
Composite Mooring Sample 55

Surface Sediment Samples 56
PCA 57
Discussion 59
Conclusions 61
References 62

CHAPTER 4. A DIATOM-BASED QUANTITATIVE SEA ICE PROXY FOR THE BERING AND CHUKCHI SEAS 66
Abstract 66
Introduction 66
Material and Methods 69
Surface Sediment Samples 69
Diatom Slides 70
Sea Ice 70
Statistical Analysis 72
Coring Sites 73
Data Accessibility 74
Results 75
Choosing the diatoms 75
Diatom species 75
Generalized Additive Model 81
Paleo sea ice reconstruction for core 51JPC 81
Paleo sea ice reconstruction for core U1345 82
Discussion 83
Advantages and disadvantages of the model 83
Comparing paleo sea ice reconstructions with previously published records 84
Core 51JPC 84
Core U1345 86
Conclusions 87
References 88

CHAPTER 5. CONCLUSIONS 94

APPENDIX A. CHARACTER DESCRIPTION 97

APPENDIX B. LIST OF DIATOM SPECIES IDENTIFIED IN STUDIED SAMPLES 102

APPENDIX C. TEN SPECIES CONSIDERED FOR THE PROXY 114

APPENDIX D. MODEL CHECKS 117

LIST OF FIGURES

Page

Figure 2.1. Map of the study area showing locations of all samples (gray dots), samples with S. marigela in it (black dots), and the type locality (black star). 24

Figure 2.2. Relative abundance of *Sinerima marigela* plotted against sea ice concentrations for each sample with a local regression line fitted to illustrate the trend. 27

Figure 2.3 LM micrographs of *Sinerima marigela* sp. nov. showing variations in valve shape and size. Figs 3–5. Specimens from slide BM 101 881. Fig. 6. Holotype specimen, slide ANSP GC92687. Figs 7–8. Specimens from slide CANA 127977. Scale bar = 10 μm. 28

Figure 2.4 SEM micrographs of *Sinerima marigela* sp. nov., external valve view. Figs 9–10. Whole valve. Figs 11–13. Valve margin. Note the "extra ribs" separating some of the cribra and marginal fultoportulae. Fig. 14. Central part of a valve. Note the sunken cribra and a hyaline area in the center. Fig. 15. Marginal fultoportula at the inner edge of the pseudoloculate zone with its external tube extending above the smaller reticulate ribs. Fig. 16. Valve face fultoportula with a star-shaped chamber. Fig. 17. Eroded valve face fultoportula showing the openings of the satellite pores. Scale bar = 20 μm (Figs 9–10), 2 μm (Figs 11, 14), 3 μm (Fig. 12), 1 μm (Fig. 13), 500 nm (Figs 15–17)..... 29

Figure 2.5 SEM micrographs of *Sinerima marigela* sp. nov., internal valve view. Fig. 18. Whole valve. Fig. 19. Central part of a valve. Note the raised cribra with rimmed pores and a hyaline area in the center. Figs 20–21. Valve margin. Note the marginal fultoportulae with four satellite pores. Fig. 22. Valve face fultoportula. Note the raised cribra with rimmed pores. Fig. 23. Siliceous knot in the center of a valve. Scale bar = 10 μm (Fig. 18), 2 μm (Fig. 19), 1 μm (Figs 20–21, 23), 500 nm (Fig. 22)..... 30

Figure 2.6 TEM valve view of *Sinerima marigela* sp. nov. Note the lack of a rimoportula and siliceous thickenings around the center. Scale bar = 5 μm. 31

Figure 3.1. Total abundance of diatoms in sediment trap samples. 56

Figure 3.2. Relative abundance of several morphotaxa of *Chaetoceros*. 56

Figure 3.3. Principal Component Analysis (PCA) plot showing the variation among 24 sediment trap samples (in red, numbers are months of collecting with the samples number in parentheses) and 2 sediment samples (in blue), overlaid by species loadings and 95% confidence ellipse. 57

Figure 4.1. Map of the study area. The dots show the location of surface sediment samples; the stars show the location of two sediment cores. The colors represent current sea ice concentration during the spring season (March, April, May, June). 71

Figure 4.2. Relative abundance of the ten species influenced by sea ice plotted against sea ice concentration. 76

Figure 4.3. Reconstruction of sea ice concentration for the core 51JPC. 82

Figure 4.4. Reconstruction of sea ice concentration for the core U1345. 82

Figure 4.5. Relative diatom abundance of the ten species counted by A. Nesterovich (gray areas) and B. Caissie (black lines) plotted against the depth. The only five species presented in both sets of counts are *Chaetoceros* hyaline resting spores, *Paralia sulcata*, *Shionodiscus trifultus*, *Neodenticula seminae*, and *Rhizosolenia hebetata*. The counts show similar patterns for those species. Note that the scale is different for *Chaetoceros* hyaline resting spores, *Shionodiscus trifultus*, and *Rhizosolenia hebetata* due their high relative abundances. 85

Figure 4.6. Relative diatom abundance of the ten species counted in the core U1345. Note that the scale is different for *Chaetoceros* hyaline resting spores and *Paralia sulcata* due their high relative abundances. 86

Figure C.1. LM micrograph of *Sinerima marigela*. 114

Figure C.2. LM micrograph of *Chaetoceros* hyaline resting spore. 114

Figure C.3. LM micrograph of *Ehrenbergiulvia granulosa*. 114

Figure C.4. LM micrograph of *Fossula arctica*. 114

Figure C.5. LM micrograph of *Fragilariopsis reginae-jahniae*. Both vegetative cells and resting spores are visible. 115

Figure C.6. LM micrograph of *Fragilariopsis cylindrus*. 115

Figure C.7. LM micrograph of *Paralia sulcata*. 115

Figure C.8. LM micrograph of *Shionodiscus trifultus*. 115

Figure C.9. LM micrograph of *Rhizosolenia hebetata*. 116

Figure C.10. LM micrograph of *Neodenticula seminae*. 116

Figure C.1. Standard model checks for GAM demonstrating normal distribution of residuals. 117

Figure D.2. Standard model checks for GAM demonstrating independence of error terms. 118

Figure D.3. GAM residuals plotted on a schematic map of the region. 118

LIST OF TABLES

Page

Table 2.1 A matrix of 35 morphological characters observed in 22 species of Thalassiosirales found in our samples along with *S. marigela*. Grey shading indicates characters shared with *S. sinerima*. Boxes are used to highlight similarities between closely related species (see Appendix for character descriptions). 47

Table 3.1. Sediment trap samples from the mooring station. 53

Table 3.2. Changes in relative abundances(%) of the core community species in the sediment trap samples throughout the year. Samples M1–M24 are marked with the month of collection. 58

Table B.1 List of diatom species found in three groups of samples used in this study. The presence of species is indicated by x. Detailed counts for every samples can be downloaded from the Arctic Data Center. 102

ACKNOWLEDGMENTS

I would like to thank my committee members, Dr. Bill Gutowski, Dr. Chris Harding, Dr. Al Wanamaker, and Dr. Yuyu Zhou, for six years of guidance and support. Their mentoring and warm encouragement took me to the next level in my scientific pursues. Special thanks go to my advisor, Dr. Beth Caissie, for not only mentoring me patiently and inspiring when necessary, but also for teaching me that I am not the only procrastinator on the planet and it's ok.

I would like to thank all the faculty, staff, and fellow students for accepting a botanist in their midst and especially Ms. DeAnn Frisk for being able to solve any problem a graduate student might have.

I would have never dreamed of pursuing this degree if not for the three Teachers in my life. I thank:

- Dr. Tatiana Ganf for showing me that languages can be fun, can spark endless conversations, and open doors into unimaginable worlds and books.
- Dr. Aleksandr Pinevich for inspiring me and never once thinking that I couldn't, so that thought never occurred to me either.
- Dr. Tatiana Kozyrenko for making me appreciate biodiversity in a whole new light by going through countless specimens in the algological collection at St. Petersburg State University. And I miss the infamous staircase of the Department of Botany.

This work could not have been accomplished without one special person in my life, to whom I owe my eternal gratitude. My huge thank you goes to my husband, Victor

Andreev, for dropping everything, moving with me to a different country on a different continent, and being a stay at home dad for four years. Thank you. Without you I couldn't have done it.

I am grateful to Dr. Catherine Lalande for giving me an opportunity to work with sediment trap samples. I would also like to acknowledge various sources of funding that supported me in the course of this work: National Science Foundation, Geological Society of America, Phycological Society of America, Joseph Gilman Scholarship Award, and Bowen Departmental Felloship.

ABSTRACT

Dramatic changes in Earth's climate, especially noticeable in the Arctic, require prompt actions and, thus, a better understanding of the processes involved in those changes. Rapidly disappearing sea ice is a vital part of the planet's climate, both affecting the system and being subject to climatic feedbacks. However, to fully understand the effects of sea ice and to incorporate them into climate models, a longer record of sea ice is needed. Proxies for sea ice conditions are the only way to achieve this goal. In this dissertation, I explore the limitations and viability of a proxy based on fossilized diatom communities in marine sediments and present the first quantitative diatom-based proxy for sea ice concentration in Beringia.

Possible sources of alteration must be tested to ensure that diatom communities in marine sediments are a reliable archive and can be used as a proxy. I explore the connection between phytoplankton and taphonomic assemblages, proving sediment records to be representative of phytoplankton and not depleted in sea ice diatoms due to preferential dissolution. I also confirm that diatoms respond to sea ice conditions and that this response is detectable in sediment assemblages. One such diatom that responds to extensive sea ice is *Sinerima marigela*, a new, monotypic genus and species described for the first time in this dissertation. Based on a training set of 104 surface sediment samples from the Bering and Chukchi seas and satellite-derived sea ice concentration, I constructed a proxy for sea ice in Beringia using the Generalized Additive Model fitted to relative abundances of five diatom species: *Neodenticula seminae*, *Paralia sulcata*, *Fragilariopsis cylindrus*, *Fragilariopsis reginae-jahniae*, and *Sinerima marigela*. This proxy is available as a web-based application at http://seaiceproxy.geol.iastate.edu. It

doesn’t require full diatom counts and scrupulous taxonomic work because the model only uses five easily identifiable species. Users can upload their counts to the R Shiny app and download sea ice reconstructions based on the model. The proxy was then applied to two sediment cores, Healy 0202 51JPC and IODP Site U1345, from the Bering Sea, that produced quantitative reconstructions in agreement with previous qualitative estimates.

CHAPTER 1. INTRODUCTION

Motivation

Changes in the planet's climate system have recently become so severe that they are causing concern not only scientific community (IPCC, 2013), but also among the public ("Greta Thunberg nominated for Nobel Peace Prize for climate activism"). There is evidence of increasing air and ocean temperatures, rising sea levels, increasing severity and frequency of natural disasters (IPCC, 2013), and decreasing sea ice extent in both hemispheres (Kwok, 2018; Meehl et al., 2019). These changes make improving our understanding of the climate system, as well as its dynamics and feedbacks, an urgent task. Today, climate is influenced by both natural and human-caused forcings (Meehl et al., 2004). Understanding and mitigating anthropogenic impacts on the system requires knowledge of the natural variability pre-dating anthropogenic forcing. Instrumental measurements, however, do not span into the pre-industrial period, making it difficult to separate the effects of different climate forcings. To overcome this challenge, past climate changes can be studied through natural proxy archives, including ice, marine and freshwater sediments, corals, trees, and mollusks (De Vernal et al., 2013a; Jones et al., 2009). Proxy-based evidence combined with global and/or regional climate models help reveal the response of the climate to new forcings, such as greenhouse gas emissions, introduced into the system.

Variability in Earth's orbit and solar activity control the amount of energy reaching the planet. Small alterations in solar energy absorption can be amplified by climate feedbacks within the system and cause changes as big as transitions between glacial and interglacial periods. The global ocean, due to its large volume, surface area, and high heat capacity of water, plays a particularly important role in regulating climate. An estimated 90% of the

increased stored energy of the planet is accumulated in the ocean (IPCC, 2013). Sea ice is an important part of the planet's energy balance and feedback mechanisms, influencing albedo, ocean mixing and transport (Screen and Simmonds, 2010). Arctic sea ice is rapidly retreating and the Arctic Ocean is predicted to be ice free by summer 2040 (Holland et al., 2006). This dramatic change has prompted many to seek analogs in sediments and to develop sea ice proxies in order to extend the record of sea ice (Justwan and Koç, 2008; Sha et al., 2014). This record would significantly increase our knowledge of past climate changes. A deeper understanding of the past can also help us to predict future changes, already triggered by our activity (De Vernal et al., 2013a).

Arctic Sea Ice

The Arctic has a rich history of sea ice coverage. Such proxies as ice rafted debris and diatom communities have allowed researchers to establish the existence of perennial sea ice cover in the central Arctic Basin since at least 14 Ma during the Miocene (Darby, 2008). The sediments recovered from the Lomonosov Ridge point out the presence of sea ice as far back as the Eocene about 45-47 Ma (Stickley et al., 2009). Since then the Arctic has experienced big fluctuations in ice cover, with episodes ranging from perennial ice over most of the ocean to seasonally ice-free conditions occurred during warmer periods and every state in between (Polyak et al., 2010b).

Because of the unique topography and location, the Bering and Chukchi seas are an ideal place to study Arctic sea ice. Today, the seas have sea ice concentrations ranging from zero to permanent ice, with all intermediate values of seasonal ice (NSIDC). In the past, the region experienced multiple advancements and retreats of sea ice (Polyak et al., 2010a), and its sediment records reflect a rich and dynamic history of sea ice conditions.

The North Pacific region is very important to the human population, being one of the most productive places in the world (Sambrotto et al., 1986; Walsh et al., 1989). The seas are especially important in the light of global climate change, which has undoubtedly affected the Bering Sea and its productivity. For example, the changing climate has already led to a decline in bottom-feeding sea ducks, such as spectacled eiders (*Somatera fuscgeri*), and marine mammals, such as walrus (*Odobenus rosmarus*) and gray whales (*Eschrichtius robustus*), due to a slight shift in bottom water temperatures (Grebmeier, 2012; Grebmeier et al., 2006). Changes in atmospheric circulation and ocean currents intensified cannibalism on juvenile walleye pollock (*Theragra chalcogramma*), affecting the whole Bering Sea food web (Wespestad et al., 2000). Still, little is known of the effects of the changes on phytoplankton community. Some studies suggest that primary productivity will increase (Brown and Arrigo, 2013), while others argue that it will dramatically drop (Hare et al., 2007), yet others believe that no considerable changes may be expected (Sigler et al., 2010). Obviously, the question requires further study, but it is clear that changes in sea ice cover will not only lead to significant changes in phytoplankton assemblages, but will affect the whole polar ecosystems and, possibly, the entire planet.

The exact role of sea ice in supporting biological, chemical, and physical processes is only now starting to be understood (Vancoppenolle et al., 2013), but it is clearly not just an inert substrate for organisms. Diatoms start to colonize sea ice as soon as it forms (Norrman and Andersson, 1994), can be found there at any given time (Horner et al., 1992), and contribute substantially to food webs of their ecosystems (Lee et al., 2008; Lizotte, 2001).

Other ice-covered ecosystems, for example, high latitude lakes in Canada and Europe, show consistent changes in the community composition of diatoms when growing season

increases and the period of ice cover decreases (Douglas et al., 1994; Michelutti et al., 2003a, 2003b; Rühland et al., 2010; Rühland and Smol, 2005). In these environments, warmer conditions often favor small-celled species (Sorvari et al., 2002). In Antarctic waters, a longer growing season and reduced ice extent led to a shift from diatoms to cryptophytes. This shift reduced the abundance of krill, which feeds on diatoms and is in turn an essential food source for fish, whales, seals, and penguins. Instead of krill the waters are becoming dominated by salps and other gelatinous zooplankton (Moline et al., 2004). Even regions far from the poles are affected by current changes. Diatom abundances in the Yellow Sea decreased sharply after 1980, and a less rich warm-water community of diatoms replaced the one that used to live there before the eutrophication and temperature raise (Liu et al., 2008).

In the Bering Sea, the expansion of warm-water dinoflagellates, green algae, and cryptophytes is expected to drive diatoms poleward (Müller-Haeckel et al., 1989), perhaps into the Chukchi Sea. This community shift has resulted in more extensive harmful algal blooms and increased seafood-biotoxins in the Bering Sea (Hallegraeff, 2010). Another consequence of sea ice cover decline is intensified transport of organisms across the Arctic Ocean between the Pacific and Atlantic. Unprecedented trans-Arctic exchanges were first noted in the late 1990s, when a North Pacific diatom species, Neodenticula seminae, was found in the North Atlantic, indicating an exchange characteristic of the mid-Pleistocene, when this species was last recorded in Atlantic waters (Miettinen et al., 2013). The intensification of the trans-Arctic exchanges is further supported by the blooms of Atlantic coccolithophores in the high Arctic (Hegseth and Sundfjord, 2008).

Sea Ice Proxies

There were several attempts to create a proxy for sea ice in the Polar Regions, based on different observations, both physical (Criscitiello et al., 2013; Darby, 2008; Darby et al., 2011; St. John et al., 2015) and biological (Belt et al., 2007; Collins et al., 2013; Cronin et al., 2010; Curran et al., 2003; De Vernal et al., 2013b; Hillaire-Marcel and de Vernal, 2008; Jennings et al., 2002; Sancetta and Robinson, 1983; Vare et al., 2009). The most important limitation of the physical proxies is their ability to point out only the presence of ice. It is even still hard to distinguish between sea ice and iceberg rafted debris. The works on microfeatures and texture of grains can help to differentiate between sea ice and icebergs, especially when used together with information on diatom assemblages, but it is considered impossible right now to infer a quantitative measure of sea ice concentration (Stickley et al., 2009). However, proxies based on ice-rafted debris are especially important in the Arctic, where it was shown to be the main mode of sediment transport (Lisitzin, 2010).

The biological markers in marine sediments present a completely different set of challenges and limitations. First of all, they present a local view and cannot be easily extrapolated over the both Polar Regions. Most of them are indirect indicators of sea ice, like dinoflagellate cysts and foraminifers, and are not present under the permanent ice cover. The processes responsible for formation and sedimentation of chemical biomarkers is not yet entirely clear, which necessitates a cautionary use. Even the best of the biological proxies for sea ice, diatoms, which seem to be related to sea ice directly and which mechanisms of sedimentation and preservation are fairly well understood (Katsuki and Takahashi, 2005), has challenges, including a potential bias due to dissolution and species-related preservation (De Vernal et al., 2013a). Still, even though most of the developed proxies show presence or extent of sea ice, there are some showing some rarely estimated characteristics of the

environment, such as the rate of ice formation (Hillaire-Marcel and de Vernal, 2008). It was already shown (Abrantes et al., 2007) that it is possible to construct a diatom-based proxy allowing to estimate not only the conditions, but also productivity at the time of sedimentation, which is especially important in order to put into context both changes in sea ice extent and their biological consequences. So the biological proxies are very promising and can be used to infer many different factors.

Diatom-based Sea Ice Proxies

A significant share of primary production in the region is made by diatoms (Honjo, 1990; Hunt and Megrey, 2005). Diatoms are widespread and a very diverse group of algae. They are sensitive to environmental conditions and any changes are quickly reflected in their community composition and structure (Pan and Lowe, 1994). Diatoms are not only good indicators of conditions, they can also serve as a proxy, because of silica tests called frustules that often sink to the bottom after a cell died or was eaten. The frustules are preserved in sediments, allowing us to reconstruct sea surface environmental conditions of the past (Harwood and Maruyama, 1992). The wide range of sea ice concentrations and the abundance of diatoms in the region make it possible to correlate the presence of ice and diatom community composition. However, sediments show us a cumulative picture over an extended period of time. On the Bering Sea shelf, the upper 1 cm of sediments is estimated to represent 10 years of sedimentation from phytoplankton communities developing above that spot (Caissie, 2012). In this sense sediments can give us more information, providing data less affected by short, random fluctuations, but they also limit a potential time-resolution of the proxy.

Because diatoms are abundant in the Polar Regions and are good indicators of environmental conditions, including sea ice, it is not surprising that there were quite a few attempts to construct a diatom-based proxy. Most of the them try to correlate sea ice and diatom assemblages by separating diatoms into groups depending on different environmental factors using canonical correspondence analysis (CCA, Jiang et al., 2001), principal component analysis (PCA, Sancetta and Robinson, 1983), or just mapping diatoms alongside with environmental factors (Cremer, 1999). The next step of proxy-building is developing a transfer function based on discovered relationships. A transfer function was developed for the Canadian Arctic, using CCA and weighted averaging with partial least squares transfer function (Sha et al., 2014). The same approach was exploited for the North Atlantic and gave a reasonable reconstruction of past sea ice concentrations (Justwan and Koç, 2008). In those cases, like in many others, the authors tried several models, such as the Imbrie and Kipp transfer function (IKTM), the modern analog technique (MAT), weighted averaging (WA), weighted averaging partial least squares (WAPLS), and the generalized additive model (GAM), before choosing the one that works best with a particular dataset (Esper and Gersonde, 2014a, 2014b; Sha et al., 2014). A recent development led to a more thorough evaluation and comparison of popular models (Ferry et al., 2015), as well as to a re-examination of statistical tools used in proxy-development (Telford and Birks, 2011, 2009).

Diatoms in the Bering Sea have already been applied as important proxies for determining geological ages of marine sediments and reconstructing paleoceanographic conditions (Caissie et al., 2010; Hanna, 1969; Katsuki and Takahashi, 2005; Koizumi, 1973; Sancetta and Robinson, 1983). However, no proxies for ice concentration have been developed and none of the proxies were formalized or made quantitative. They are all

presented as lists of species with their preferred ranges of environmental conditions, without easy-to-apply formulas or indices assigned to each species. In order to achieve a more formalized proxy, I try and compare several models constructed based on 105 sediment samples. The usual approaches that have shown good results in other regions include MAT and WAPLS, which use the whole counts in the process. Not all diatom-based proxies use whole assemblages in predicting sea ice concentrations. It was shown that the relative abundance of only two species can give a good estimate of the conditions (Katsuki et al., 2010; Pike et al., 2009). The GAM also works best with a limited number of species strongly associated with sea ice, rather than with dozens of species associated with different environmental factors (Ferry et al., 2015). Those two possibilities are also explored in this study.

The ultimate goal of this research is to develop a diatom-based proxy for reconstructing the presence and concentration of different types of sea ice and to apply this proxy to previous warm intervals recorded in the Bering and Chukchi seas. The proxy will allow us to make a relatively high resolution reconstruction of sea ice extent in previous geological periods. Such reconstruction would enhance our ability to predict ongoing changes in the Arctic ecosystems and put the rate of the changes into a context. Moreover, a better understanding of the sedimentation processes and the relationship between productivity and sea ice will enhance our ability to reconstruct the actual phytoplankton community based on sediments. With these data we then can contribute to modeling efforts that predict composition and productivity of phytoplankton in the upcoming years. This dissertation explores the connection between diatom communities and sea ice concentrations

in the Bering and Chukchi seas and offers a proxy to reconstruct past ice conditions in the region.

Thesis organization

Chapter 2 ("Taxonomy and ultrastructure of *Sinerima*, a new genus of diatoms (Bacillariophyta), with a description of a new species, *S. marigela*") describes a new diatom monospecific genus that is associated with high concentrations of sea ice. The species is crucial for the proxy, because it's the only species in available samples associated with sea ice concentrations greater than 70%. *Sinerima marigela* appears in 20% of the counted samples, is readily recognizable, and differs from all known fultoportulate diatoms in respect to processes and areolae arrangement. Its unique morphology makes it a good species to use in a proxy. A diatom-based proxy, like any biological proxy relying on organisms, depends on our view of diatom taxonomy and our ability to differentiate between species. Thus, taxonomic analysis sets the stage for using diatoms as a climate archive.

Chapter 3 ("Diatom succession and vertical export in the Chukchi Sea") explores the feasibility of constructing a sea ice proxy based on diatom community composition preserved in marine sediments. This study of diatoms preserved in a sediment trap in the Chukchi Sea over the course of one year lays the foundation for the proxy construction. To reliably infer environmental parameters from diatom assemblages in sediments, it is necessary for the sediments to be representative of phytoplankton growing near the surface. Tsoy and Wong (1999) proposed that ice-associated species are dissolved in the water column preferentially. This hypothesis is based on the fact that core samples corresponding to glaciation events have a very low rate of diatom accumulation. To test this, it is necessary to study sidocoenosis (a term for a sinking assemblage suggested in 1995 by K. Takahashi), which

was last studied in the region 20 years ago. In 1994, K. Takahashi (1995) deployed two sediment traps: in the southern part of the Bering Sea and in the North Pacific, just south of the Aleutian Islands. This work significantly enhanced our knowledge about sidocoenosis, but it didn't answer the question of differential dissolution of ice-associated diatoms, since there are typically not many sea ice species (or sea ice) so far south. Nevertheless, the opinion that species living on ice almost completely dissolve in the water column persists (Katsuki and Takahashi, 2005), though it has never been proved. The investigation in Chapter 3 was, therefore, undertaken in order to explore the possibility of preferential dissolution of sea ice diatoms. My findings suggest no evidence that this is the case, showing that sea ice-related diatoms are present in sediment traps and sediments in similar numbers. Both sets of samples seem to be depleted of large, thin-walled diatoms, but dissolution of fragile valves is expected and was shown previously (Rigual-Hernández et al., 2016).

Chapter 4 ("A diatom-based quantitative sea ice proxy for the Bering and Chukchi seas") builds upon the foundation established in Chapters 2 and 3. The work introduces the first quantitative proxy for reconstructing sea ice concentration in Beringia. I used the Generalized Additive Model (GAM) fitted to 5 species robust enough to withstand dissolution and be preserved in the sediments. Those 5 species were chosen for their regular presence in sediment samples, defined and known preferences of sea ice conditions, and easy identification. In my effort to make the proxy as widely available as possible, I created an open-access R Shiny application that allows any user to upload diatom counts for the five species and download sea ice concentrations predicted by the model. These properties make the model not only quantitative, but biologically meaningful and easy to apply without extensive training in diatom taxonomy or coding.

References

Abrantes, F., Lopes, C., Mix, A.C., Pisias, N., 2007. Diatoms in Southeast Pacific surface sediments reflect environmental properties. Quat. Sci. Rev. 26, 155–169. doi:10.1016/j.quascirev.2006.02.022

BBC,. Greta Thunberg nominated for Nobel Peace Prize for climate activism. BBC News.

Belt, S.T., Massé, G., Rowland, S.J., Poulin, M., Michel, C., LeBlanc, B., 2007. A novel chemical fossil of palaeo sea ice: IP25. Org. Geochem. 38, 16–27. doi:10.1016/j.orggeochem.2006.09.013

Brown, Z.W., Arrigo, K.R., 2013. Sea ice impacts on spring bloom dynamics and net primary production in the Eastern Bering Sea. J. Geophys. Res. Ocean. 118, 43–62. doi:10.1029/2012JC008034

Caissie, B.E., 2012. Diatoms as recorders of sea ice in the Bering ans Chukchi seas: Proxy development and application. University of Massachusetts - Amherst. doi:10.1017/CBO9781107415324.004

Caissie, B.E., Brigham-grette, J., Lawrence, K.T., Herbert, T.D., Cook, M.S., 2010. Last Glacial Maximum to Holocene sea surface conditions at Umnak Plateau , Bering Sea , as inferred from diatom , alkenone , and stable isotope records. Paleoceanography 25, 1–16. doi:10.1029/2008PA001671

Collins, L.G., Allen, C.S., Pike, J., Hodgson, D.A., Weckstrom, K., Massé, G., 2013. Evaluating highly branched isoprenoid (HBI) biomarkers as a novel Antarctic sea-ice proxy in deep ocean glacial age sediments. Quat. Sci. Rev. 79, 87–98. doi:10.1016/j.quascirev.2013.02.004

Cremer, H., 1999. Distribution patterns of diatom surface sediment assemblages in the Laptev Sea (Arctic Ocean). Mar. Micropaleontol. 38, 39–67. doi:10.1016/S0377-8398(99)00037-7

Criscitiello, A.S., Das, S.B., Evans, M.J., Frey, K.E., Conway, H., Joughin, I., Medley, B., Steig, E.J., 2013. Ice sheet record of recent sea-ice behavior and polynya variability in the Amundsen Sea, West Antarctica. J. Geophys. Res. Ocean. 118, 118–130. doi:10.1029/2012JC008077

Cronin, T.M., Gemery, L., Briggs, W.M., Jakobsson, M., Polyak, L., Brouwers, E., 2010. Quaternary Sea-ice history in the Arctic Ocean based on a new Ostracode sea-ice proxy. Quat. Sci. Rev. 29, 3415–3429. doi:10.1016/j.quascirev.2010.05.024

Curran, M.A.J., van Ommen, T.D., Morgan, V.I., Phillips, K.L., Palmer, A.S., 2003. Ice core evidence for Antarctic sea ice decline since the 1950s. Science (80-.). 302, 1203–1206. doi:10.1126/science.1087888

Darby, D.A., 2008. Arctic perennial ice cover over the last 14 million years. Paleoceanography 23, 1–9. doi:10.1029/2007PA001479

Darby, D.A., Myers, W.B., Jakobsson, M., Rigor, I., 2011. Modern dirty sea ice characteristics and sources: The role of anchor ice. J. Geophys. Res. Ocean. 116, 1–18. doi:10.1029/2010JC006675

De Vernal, A., Gersonde, R., Goosse, H., Seidenkrantz, M.-S., Wolff, E.W., 2013a. Sea ice in the paleoclimate system: The challenge of reconstructing sea ice from proxies - an introduction. Quat. Sci. Rev. 79, 1–8. doi:10.1016/j.quascirev.2013.08.009

De Vernal, A., Hillaire-Marcel, C., Rochon, A., Frechette, B., Henry, M., Solignac, S., Bonnet, S., 2013b. Dinocyst-based reconstructions of sea ice cover concentration during the Holocene in the Arctic Ocean, the northern North Atlantic Ocean and its adjacent seas. Quat. Sci. Rev. 79, 111–121. doi:10.1016/j.quascirev.2013.07.006

Douglas, M.S. V., Smol, J.P., Blake, W., 1994. Marked post-18th century environmental change in high-arctic ecosystems. Science (80-.). 266, 416–419. doi:10.1126/science.266.5184.416

Esper, O., Gersonde, R., 2014a. Quaternary surface water temperature estimations: New diatom transfer functions for the Southern Ocean. Palaeogeogr. Palaeoclimatol. Palaeoecol. 414, 1–19. doi:10.1016/j.palaeo.2014.08.008

Esper, O., Gersonde, R., 2014b. New tools for the reconstruction of Pleistocene Antarctic sea ice. Palaeogeogr. Palaeoclimatol. Palaeoecol. 399, 260–283. doi:10.1016/j.palaeo.2014.01.019

Ferry, A.J., Prvan, T., Jersky, B., Crosta, X., Armand, L.K., 2015. Statistical modeling of Southern Ocean marine diatom proxy and winter sea ice data: Model comparison and developments. Prog. Oceanogr. 131, 100–112. doi:10.1016/j.pocean.2014.12.001

Grebmeier, J.M., 2012. Shifting Patterns of Life in the Pacific Arctic and Sub-Arctic Seas. Ann. Rev. Mar. Sci. 4, 63–78. doi:10.1146/annurev-marine-120710-100926

Grebmeier, J.M., Overland, J.E., Moore, S.E., Farley, E. V., Carmack, E.C., Cooper, L.W., Frey, K.E., Helle, J.H., McLaughlin, F.A., McNutt, S.L., 2006. A Major Ecosystem Shift in the Northern Bering Sea. Science (80-.). 311, 1461–1464. doi:10.1126/science.1121365

Hallegraeff, G.M., 2010. Ocean climate change, phytoplankton community responses, and harmful algal blooms: A formidable predictive challenge. J. Phycol. 46, 220–235. doi:10.1111/j.1529-8817.2010.00815.x

Hanna, G.D., 1969. Fossil diatoms from the Pribilof Islands, Bering Sea, Alaska. Proc. Calif. Acad. Sci. 37, 167–234.

Hare, C.E., Leblanc, K., DiTullio, G.R., Kudela, R.M., Zhang, Y., Lee, P.A., Riseman, S., Hutchins, D.A., 2007. Consequences of increased temperature and CO2 for phytoplankton community structure in the Bering Sea. Mar. Ecol. Prog. Ser. 352, 9–16. doi:10.3354/meps07182

Hegseth, E.N., Sundfjord, A., 2008. Intrusion and blooming of Atlantic phytoplankton species in the high Arctic. J. Mar. Syst. 74, 108–119. doi:10.1016/j.jmarsys.2007.11.011

Hillaire-Marcel, C., de Vernal, A., 2008. Stable isotope clue to episodic sea ice formation in the glacial North Atlantic. Earth Planet. Sci. Lett. 268, 143–150. doi:10.1016/j.epsl.2008.01.012

Holland, M.M., Bitz, C.M., Tremblay, B., 2006. Future abrupt reductions in the summer Arctic sea ice. Geophys. Res. Lett. 33, 1–5. doi:10.1029/2006GL028024

Honjo, S., 1990. Particle fluxes and modern sedimentation in the polar oceans, in: Smith Jr., W. (Ed.), Polar Oceanography. Academic Press, San Diego, CA, pp. 687–739.

Horner, R.A., Ackley, S.F., Dieckmann, G.S., Gulliksen, B., Hoshiai, T., Legendre, L., Melnikov, I.A., Reeburgh, W.S., Spindler, M., Sullivan, C.W., 1992. Ecology of sea ice biota. Polar Biol. 12, 429–444. doi:10.1007/BF00243114

Hunt, G.L., Megrey, B.A., 2005. Comparison of the biophysical and trophic characteristics of the Bering and Barents Seas. ICES J. Mar. Sci. 62, 1245–1255.

doi:10.1016/j.icesjms.2005.04.008

Jennings, A.E., Knudsen, K.L., Hald, M., Hansen, V., Andrews, J.T., 2002. A mid-Holocene shift in Arctic sea-ice variability on the East Greenland Shelf. The Holocene 12, 49–58. doi:10.1191/0959683602hl519rp

Jiang, H., Seidenkrantz, M.-S., Knudsen, K.L., Eiríksson, J., 2001. Diatom surface sediment assemblages around Iceland and their relationships to oceanic environmental variables. Mar. Micropaleontol. 41, 73–96. doi:10.1016/S0377-8398(00)00053-0

Jones, P., Briffa, K., Osborn, T., Lough, J.M., van Ommen, T.D., Vinther, B.M., Luterbacher, J., Wahl, E.R., Zwiers, F.W., Mann, M.E., Schmidt, G.A., Ammann, C.M., Buckley, B.M., Cobb, K.M., Esper, J., Goosse, H., Graham, N., Jansen, E., Kiefer, T., Kull, C., Küttel, M., Mosley-Thompson, E., Overpeck, J.T., Riedwyl, N., Schulz, M., Tudhope, A.W., Villalba, R., Wanner, H., Wolff, E., Xoplaki, E., 2009. High-resolution palaeoclimatology of the last millennium: a review of current status and future prospects. The Holocene 1, 3–49. doi:10.1177/0959683608098952

Justwan, A., Koç, N., 2008. A diatom based transfer function for reconstructing sea ice concentrations in the North Atlantic. Mar. Micropaleontol. 66, 264–278. doi:10.1016/j.marmicro.2007.11.001

Katsuki, K., Khim, B.K., Itaki, T., Okazaki, Y., Ikehara, K., Shin, Y., Yoon, H. Il, Kang, C.Y., 2010. Sea-ice distribution and atmospheric pressure patterns in southwestern Okhotsk Sea since the Last Glacial Maximum. Glob. Planet. Change 72, 99–107. doi:10.1016/j.gloplacha.2009.12.005

Katsuki, K., Takahashi, K., 2005. Diatoms as paleoenvironmental proxies for seasonal productivity, sea-ice and surface circulation in the Bering Sea during the late Quaternary. Deep. Res. Part II Top. Stud. Oceanogr. 52, 2110–2130. doi:10.1016/j.dsr2.2005.07.001

Koizumi, I., 1973. The late Cenozoic diatoms of Sites 183–193, Leg 19 Deep Sea Drilling Project. Creager, JS, Sch. DW, al., Init. Repts. DSDP 19, 805–855. doi:10.2973/dsdp.proc.19.130.1973

Kwok, R., 2018. Arctic sea ice thickness, volume, and multiyear ice coverage: losses and coupled variability (1958–2018). Environ. Res. Lett. 13. doi:10.1088/1748-9326/aae3ec

Lee, S.H., Whitledge, T.E., Kang, S.-H., 2008. Spring time production of bottom ice algae in

the landfast sea ice zone at Barrow, Alaska. J. Exp. Mar. Bio. Ecol. 367, 204–212. doi:10.1016/j.jembe.2008.09.018

Lisitzin, A.P., 2010. Marine ice-rafting as a new type of sedimentogenesis in the Arctic and novel approaches to studying sedimentary processes. Russ. Geol. Geophys. 51, 12–47. doi:10.1016/j.rgg.2009.12.002

Liu, D., Sun, J., Zhang, J., Liu, G., 2008. Response of the diatom flora in Jiaozhou Bay, China to environmental changes during the last century. Mar. Micropaleontol. 66, 279–290. doi:10.1016/j.marmicro.2007.10.007

Lizotte, M.P., 2001. The Contributions of Sea Ice Algae to Antarctic Marine Primary Production. Am. Zool. 41, 57–73. doi:10.1668/0003-1569(2001)041[0057:TCOSIA]2.0.CO;2

Meehl, G.A., Arblaster, J.M., Chung, C.T.Y., Holland, M.M., DuVivier, A., Thompson, L., Yang, D., Bitz, C.M., 2016. Sustained ocean changes contributed to sudden Antarctic sea ice retreat in late 2016. Nat. Commun. 10, 1–9. doi:10.1038/s41467-018-07865-9

Meehl, G.A., Washington, W.M., Ammann, C.M., Arblaster, J.M., Wigley, T.M.L., Tebaldi, C., 2004. Combinations of natural and anthropogenic forcings in twentieth-century climate. J. Clim. 17, 3721–3727. doi:10.1175/1520-0442(2004)017<3721:CONAAF>2.0.CO;2

Michelutti, N., Douglas, M.S. V., Smol, J.P., 2003a. Diatom response to recent climatic change in a high arctic lake (Char Lake, Cornwallis Island, Nunavut). Glob. Planet. Change 38, 257–271. doi:10.1016/S0921-8181(02)00260-6

Michelutti, N., Holtham, A.J., Douglas, M.S. V., Smol, J.P., 2003b. Periphytic Diatom Assemblages From Ultra-Oligotrophic and Uv Transparent Lakes and Ponds on Victoria Island and Comparisons With Other Diatom Surveys in the Canadian Arctic 1. J. Phycol. 39, 465–480. doi:10.1046/j.1529-8817.2003.02153.x

Miettinen, A., Koç, N., Husum, K., 2013. Appearance of the Pacific diatom Neodenticula seminae in the northern Nordic Seas - An indication of changes in Arctic sea ice and ocean circulation. Mar. Micropaleontol. 99, 2–7. doi:10.1016/j.marmicro.2012.06.002

Moline, M.A., Claustre, H., Frazer, T.K., Schofield, O., Vernet, M., 2004. Alteration of the food web along the Antarctic Peninsula in response to a regional warming trend. Glob. Chang. Biol. 10, 1973–1980. doi:10.1111/j.1365-2486.2004.00825.x

Norrman, B., Andersson, A., 1994. Development of ice biota in a temperate sea area (Gulf of Bothnia). Polar Biol. 14, 531–537. doi:10.1007/BF00238222

Pan, Y., Lowe, R.L., 1994. Independent and interactive effects of nutrients and grazers on benthic algal community structure. Hydrobiologia 291, 201–209.

Pike, J., Crosta, X., Maddison, E.J., Stickley, C.E., Denis, D., Barbara, L., Renssen, H., 2009. Observations on the relationship between the Antarctic coastal diatoms *Thalassiosira antarctica* Comber and *Porosira glacialis* (Grunow) Jorgensen and sea ice concentrations during the late Quaternary. Mar. Micropaleontol. 73, 14–25. doi:10.1016/j.marmicro.2009.06.005

Polyak, L., Alley, R.B., Andrews, J.T., Brigham-grette, J., Cronin, T.M., Darby, D.A., Dyke, A.S., Fitzpatrick, J.J., Funder, S., Holland, M., Jennings, A.E., Miller, G.H., Regan, M.O., Savelle, J., Serreze, M., St, K., White, J.W.C., Wolff, E., 2010a. History of sea ice in the Arctic. Quat. Sci. Rev. 29, 1757–1778. doi:10.1016/j.quascirev.2010.02.010

Polyak, L., Alley, R.B., Andrews, J.T., Brigham-Grette, J., Cronin, T.M., Darby, D.A., Dyke, A.S., Fitzpatrick, J.J., Funder, S., Holland, M.M., Jennings, A.E., Miller, G.H., O'Regan, M., Savelle, J., Serreze, M., St. John, K., White, J.W.C., Wolff, E.W., 2010b. History of sea ice in the Arctic. Quat. Sci. Rev. 29, 1757–1778. doi:10.1016/j.quascirev.2010.02.010

Rigual-Hernández, A.S., Trull, T.W., Bray, S.G., Armand, L.K., 2016. The fate of diatom valves in the Subantarctic and Polar Frontal Zones of the Southern Ocean: Sediment trap versus surface sediment assemblages. Palaeogeogr. Palaeoclimatol. Palaeoecol. 457, 129–143. doi:10.1016/j.palaeo.2016.06.004

Rühland, K.M., Paterson, A.M., Hargan, K., Jenkin, A., Clark, B.J., Smol, J.P., 2010. Reorganization of algal communities in the Lake of the Woods (Ontario, Canada) in response to turn-of-the-century damming and recent warming. Limnol. Oceanogr. 55, 2433–2451. doi:10.4319/lo.2010.55.6.2433

Rühland, K.M., Smol, J.P., 2005. Diatom shifts as evidence for recent Subarctic warming in a remote tundra lake, NWT, Canada. Palaeogeogr. Palaeoclimatol. Palaeoecol. 226, 1–16. doi:10.1016/j.palaeo.2005.05.001

Sambrotto, R.N., Niebauer, H.J., Goering, J.J., Iverson, R.L., 1986. Relationships among vertical mixing, nitrate uptake, and phytoplankton growth during the spring bloom in the southeast Bering Sea middle shelf. Cont. Shelf Res. 5, 161–198. doi:10.1016/0278-4343(86)90014-2

Sancetta, C., Robinson, S.W., 1983. Diatom evidence on Wisconsin and Holocene events in the Bering Sea. Quat. Res. 20, 232–245. doi:10.1016/0033-5894(83)90079-0

Screen, J.A., Simmonds, I., 2010. The central role of diminishing sea ice in recent Arctic temperature amplification. Nature 464, 1334–1337. doi:10.1038/nature09051

Sha, L., Jiang, H., Seidenkrantz, M.-S., Knudsen, K.L., Olsen, J., Kuijpers, A., Liu, Y., 2014. A diatom-based sea-ice reconstruction for the Vaigat Strait (Disko Bugt, West Greenland) over the last 5000yr. Palaeogeogr. Palaeoclimatol. Palaeoecol. 403, 66–79. doi:10.1016/j.palaeo.2014.03.028

Sigler, M.F., Harvey, H.R., Ashjian, C.J., Lomas, M.W., Napp, J.M., Stabeno, P.J., Van Pelt, T.I., 2010. How does climate change affect the Bering Sea ecosystem? Eos, Trans. Am. Geophys. Union 91, 457–458. doi:10.1029/2010EO480001

Sorvari, S., Korhola, A., Thompson, R., 2002. Lake diatom response to recent Arctic warming in Finnish Lapland. Glob. Chang. Biol. 8, 171–181. doi:10.1046/j.1365-2486.2002.00463.x

St. John, K., Passchier, S., Tantillo, B., Darby, D.A., Kearns, L.E., 2015. Microfeatures of modern sea-ice-rafted sediment and implications for paleo-sea-ice reconstructions. Ann. Glaciol. 56, 83–93. doi:10.3189/2015AoG69A586

Stickley, C.E., St. John, K., Koç, N., Jordan, R.W., Passchier, S., Pearce, R.B., Kearns, L.E., 2009. Evidence for middle Eocene Arctic sea ice from diatoms and ice-rafted debris. Nature 460, 376–379. doi:10.1038/nature08163

Stocker, T.F., D. Qin, G.-K. Plattner, M. Tignor, S.K. Allen, J. Boschung, A. Nauels, Y. Xia, V.B. and P.M.M. (eds. ., 2013. IPCC, 2013: Climate Change 2013: The Physical Science Basis. Contribution of Working Group I to the Fifth Assessment Report of the Intergovernmental Panel on Climate Change. Cambridge, United Kingdom and New York, NY, USA.

Telford, R.J., Birks, H.J.B., 2011. A novel method for assessing the statistical significance of quantitative reconstructions inferred from biotic assemblages. Quat. Sci. Rev. 30, 1272–1278. doi:10.1016/j.quascirev.2011.03.002

Telford, R.J., Birks, H.J.B., 2009. Evaluation of transfer functions in spatially structured environments. Quat. Sci. Rev. 28, 1309–1316. doi:10.1016/j.quascirev.2008.12.020

Tsoy, I.B., Wong, C.S., 1999. Diatom fluxes and preservation in the deep Northwest Pacific Ocean., in: Idei, M., Koizumi, I. (Eds.), 14th Diatom Symposium. Koeltz Scientific Books, Koenigstein, pp. 521–549.

Vancoppenolle, M., Meiners, K.M., Michel, C., Bopp, L., Brabant, F., Carnat, G., Delille, B., Lannuzel, D., Madec, G., Moreau, S., Tison, J.-L., van der Merwe, P., 2013. Role of sea ice in global biogeochemical cycles: Emerging views and challenges. Quat. Sci. Rev. 79, 207–230. doi:10.1016/j.quascirev.2013.04.011

Vare, L.L., Massé, G., Gregory, T.R., Smart, C.W., Belt, S.T., 2009. Sea ice variations in the central Canadian Arctic Archipelago during the Holocene. Quat. Sci. Rev. 28, 1354–1366. doi:10.1016/j.quascirev.2009.01.013

Walsh, J.J., McRoy, C.P., Coachman, L.K., Goering, J.J., Nihoul, J.J., Whitledge, T.E., Blackburn, T.H., Parker, P.L., Wirick, C.D., Shuert, P.G., Grebmeier, J.M., Springer, A.M., Tripp, R.D., Hansell, D.A., Djenidi, S., Deleersnijder, E., Henriksen, K., Lund, B.A., Andersen, P., Müller-Karger, F.E., Dean, K., 1989. Carbon and nitrogen cycling within the Bering/Chukchi Seas: Source regions for organic matter effecting AOU demands of the Arctic Ocean. Prog. Oceanogr. 22, 277–359. doi:10.1016/0079-6611(89)90006-2

Wespestad, V.G., Fritz, L.W., Ingraham, W.J., Megrey, B.A., 2000. On relationships between cannibalism, climate variability, physical transport, and recruitment success of Bering Sea walleye pollock (*Theragra chalcogramma*). ICES J. Mar. Sci. 57, 272–278. doi:10.1006/jmsc.2000.0640

CHAPTER 2. TAXONOMY AND ULTRASTRUCTURE OF *SINERIMA*, A NEW GENUS OF DIATOMS (BACILLARIOPHYTA), WITH A DESCRIPTION OF A NEW SPECIES, *S. MARIGELA*

Modified from version published in Phytotaxa, June, 2018

Nesterovich, Anna and Beth E. Caissie (2018) Taxonomy and ultrastructure of Sinerima, a new genus of diatoms (Bacillariophyta), with a description of a new species, S. marigela. Phytotaxa, 351 (3): 197-209. DOI: http://dx.doi.org/10.11646/phytotaxa.351.3.1

Abstract

Based on light, scanning and transmission electron microscopy observations, a detailed description of a new marine fultoportulate diatom *Sinerima marigela* gen. et sp. nov. is presented. This new taxon is rare (<3% of the thanatocoenosis) in surface sediments in the Bering and Chukchi seas, but appears to have an association with high spring sea ice concentrations. The new monotypic genus is distinct due to its 1) lack of rimoportulae, 2) one-layer valves with marginal pseudoloculi, 3) characteristic velum composed of a cluster of short tubes, and 4) central part without either central fultoportulae or an annulus. This set of characters, especially the lack of rimoportulae, makes *S. marigela* unique and easily distinguishable from other fultoportulate diatoms.

Keywords: Sinerima, taxonomy, surface sediments; Chukchi Sea, Bering Sea, Thalassiosirales

Introduction

The diatoms of the Arctic Ocean have been studied extensively over the past century. The first accounts were published by Ehrenberg (1853), O'Meara (1860), and Cleve (1873, 1867) and included almost two hundred diatom names. Since then hundreds of samples have

been collected in the Arctic from all possible biotopes such as phytoplankton, sediments, periphyton, cryophyton, and so on. It was noted early on that the diatom communities in Arctic waters depend on sea ice conditions in many respects. Cleve (1873) mentions that among others he examined ice samples, and Gran (1904) found a rich epontic (under ice) diatom community in samples from March in the Karajak Fjord of West Greenland. The prevalence of under-ice development of diatoms was confirmed recently by an analysis of satellite-derived data on phytoplankton blooms in the Chukchi Sea (Arrigo et al., 2014). In many regions of the Arctic a massive bloom occurs as soon as the ice retreats, leaving behind nutrient and silica-rich, cold, stratified water ideal for mass development of diatoms (Vancoppenolle et al., 2013). These marginal ice blooms can contain the same species that live attached to the bottom of the ice earlier in the season (Gran 1904) or a different set of species (Ligowski et al., 1992). Despite this long taxonomic history of sea ice diatoms, new and interesting diatoms are still regularly described from Arctic waters (Percopo et al., 2016; Poulin and Cardinal, 1982; Syvertsen and Hasle, 1984).

As was observed from the beginning of diatom studies in the Arctic (Gran, 1897; Østrup, 1895), Arctic waters are especially rich in diatoms belonging to the genera *Chaetoceros* Ehrenberg (1844: 198), *Bacterosira* Gran (1900: 114), *Melosira* C. Agardh (1824: 8), *Fragilariopsis* Hustedt in Schmidt (1913: pl. 299), and *Thalassiosira* Cleve (1873: 6). Thalassiosiroid diatoms are a very successful group of diatoms, abundant in both marine and freshwater, with the genus *Thalassiosira* accounting for the majority of species diversity in the order. Fourtanier and Kociolek (2011) list 381 taxa in the genus, accounting for approximately 65% of all species belonging to Thalassiosirales Glezer et Makarova and 75% of Thalassiosiraceae Lebour. The genus description is very vague and allows room for

interpretation. It was first described by Cleve (1873), who pointed out its frustule shape similar to *Coscinodiscus* Ehrenberg (1838: 128) only with a much finer structure and its submarginal spines as in *Stephanopyxis* (Ehrenberg, 1844b: 85) Ehrenberg (1845: 28). He singled out the type of colony formation as the main feature of the genus, since the cells are connected into long chains by "mucus threads" without touching by their "spines." After scanning electron microscope studies flourished and enriched diatomology, it became apparent that all those species also possess fultoportulae, specialized structures now characteristic of the order (Round et al., 1990). The genus description was emended by Lebour (1930) and Hasle (1973) to include fultoportulate diatoms with one or more rimoportulae and colonies joined by threads extruded from the central process(es). It was shown that the colony formation is not a reliable taxonomic feature, because it tends to change according to environmental conditions or for no apparent reason (Kaczmarska et al., 2005; Schöne, 1972; Smayda and Boleyn, 1965). It also is not always possible to observe colonies, because this requires observations of live material. Consequently, the type of colony formation is unknown for a number of described species of *Thalassiosira*.

In recent years, a number of genera, such as *Shionodiscus* Alverson, Kang et Theriot (Alverson et al., 2006: 258) and *Conticribra* Stachura-Suchoples et Williams (Stachura-Suchoples and Williams, 2009), were separated from *Thalassiosira*, but the genus still remains a heap of species belonging to Thalassiosiraceae, but not belonging to any of the smaller, clearly defined genera in the family. Even though phylogenetic relationships within the group were extensively studied (Fryxell and Hasle, 1977; Kaczmarska et al., 2005; Makarova, 1994; Medlin et al., 1996; Theriot et al., 1987; Theriot and Serieyssol, 1994), nomenclature revisions are lagging behind. Right now, the genus includes a wide variety of

diatoms, regardless of colony types, with one or multiple rimoportulae, operculate fultuportulae forming at least one marginal ring, with or without central fultoportulae, and a staggering diversity of areolation patterns (Makarova, 1988) and cingulum structure (Fryxell et al., 1981).

This paper describes a new genus *Sinerima* with a single species *S. marigela* belonging to the family Thalassiosiraceae. It has been found in sediments from the Chukchi and Bering seas, mostly in samples under waters with nearly permanent ice cover conditions. We argue that, while *S. marigela* has a marginal ring of operculate fultoportulae, it is unique among the described Thalassiosirales and requires a new genus to be erected to accommodate it.

Material and Methods

Samples

The main material for this paper was represented by sediment samples from the Bering and Chukchi seas (Fig. 2.1). To collect sediments, the top 1 cm was taken from a Van Veen grab aboard the USCGC Healy in the Bering Sea and aboard the R/V Norseman II in the Chukchi Sea. Although the undisturbed sediments from a small multi-corer are often considered preferable to sediments from a Van Veen grab, care was taken to remove the most top sediments before opening the Van Veen grab. Additionally, Pirtle-Levy and co-authors showed no significant difference between samples retrieved from the sediment water interface preserved in Haps cores and the top sediments from a Van Veen grab (Pirtle-Levy et al., 2009). These samples were bagged and refrigerated until analysis. Subsamples were treated with hydrogen peroxide, centrifuged several times with water or with water and then alcohol, and stored in water or alcohol.

Microscopy

For light microscope (LM) studies, diatom slides were prepared according to the method described by Scherer (1994) or Battarbee (1986). Cover slips were mounted on cleaned microscope slides using Hyrax® or Naphrax®. Diatoms were identified using a Nikon ECLIPSE Ni transmitted light microscope at a magnification of 1000x equipped with a Nikon DS-Fi2 camera. For the scanning electron microscopy (SEM), cleaned subsamples stored in alcohol were air-dried on cover slips or silica chips, mounted on carbon stubs with carbon glue, coated with 5 nm of iridium, using a Quorum Q150T S sputter coater, and studied under a FEI Quanta 250 FE-SEM set to high vacuum and voltage of 8–10 kV. For the transmission electron microscopy (TEM), cleaned subsamples stored in alcohol were air-dried on coated grids and studied under a 200kV JEOL 2100 scanning/transmission electron microscope (STEM).

Statistical Analysis

Sea ice concentrations were obtained from the National Snow and Ice Data Center (NSIDC dataset 0051) and derived from the Defense Meteorological Satellite Program (DMSP) –F11 and –F13 Special Sensor Microwave/Imagers (SSM/I) (Cavalieri et al., n.d.). The surface sediments included only the 1 top cm, which in Beringia represents approximately 10 years of sedimentation (Caissie, 2012), so the corresponding sea ice concentrations were averaged over the 10 years preceding the sampling. Because the major blooms happen in the Arctic in the spring, starting right before or immediately after the ice retreat, March, April, May, June (MAMJ) sea ice concentration for 1998–2007 was interpolated for each station and spring averages were calculated using ArcGIS software. The selection of morphological characters considered in the comparison of the new species with other fultoportulate species in the region was based on the lists of characters deemed

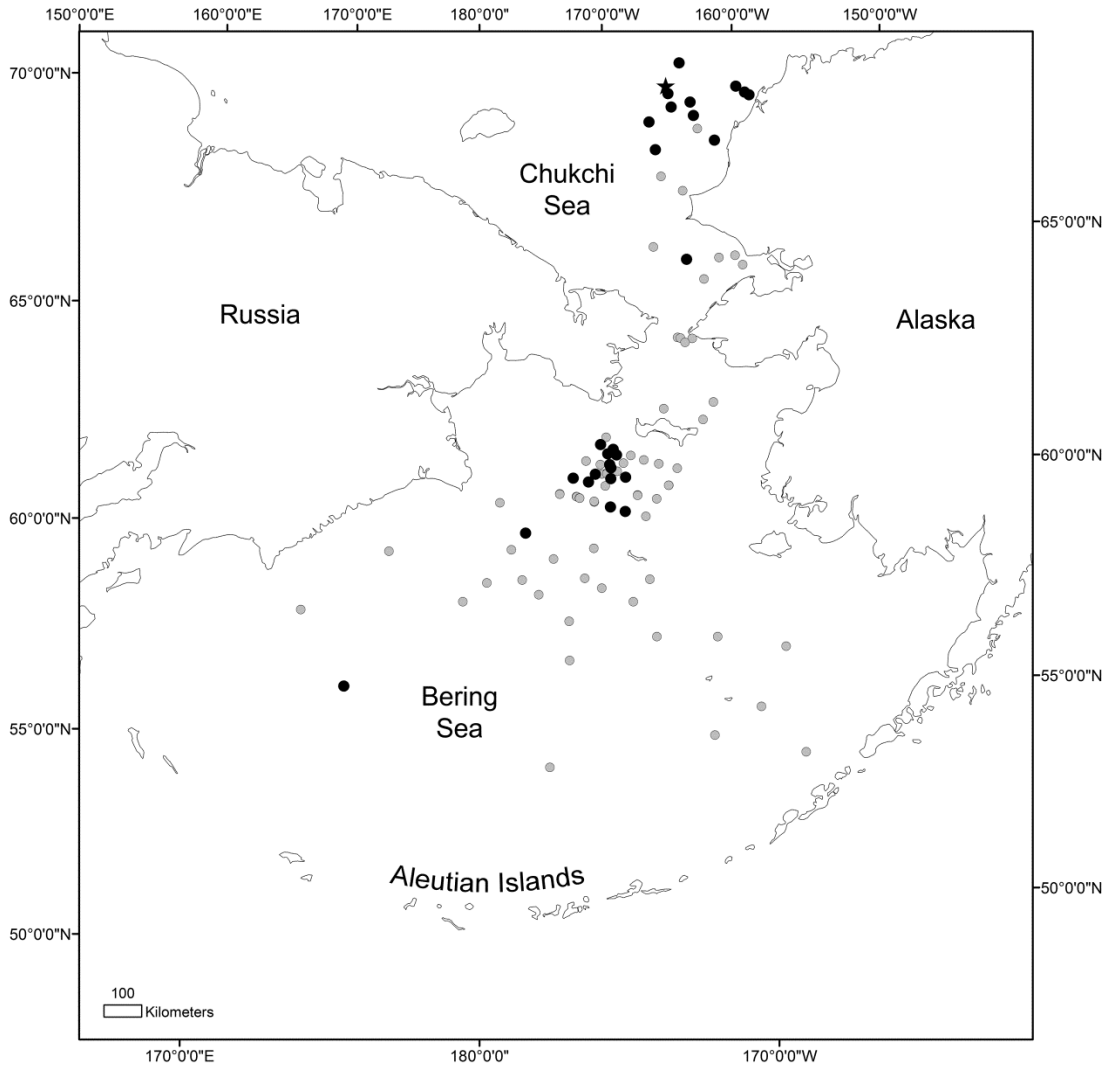

Figure 2.1. *Map of the study area showing locations of all samples (gray dots), samples with S. marigela in it (black dots), and the type locality (black star).*

important for Thalassiosirales (Julius and Tanimura, 2001; Theriot and Serieyssol, 1994). Only characters referring to the valve, and not the girdle bands, were used in the analysis due to the lack of information on girdle band morphology for many species, including *S. marigela*. The states of the characters were observed, when possible, on our own SEM micrographs, representing specimens found in the Bering and Chukchi seas. Otherwise, the information was gathered from figures in published articles, with the preference given to

papers where the species were described (Fryxell and Hasle, 1980, 1977, 1972, Hasle, 1983, 1979, 1973; Hasle et al., 1971; Julius and Tanimura, 2001; Makarova, 1988; Park et al., 2016; Syvertsen and Hasle, 1984, 1982).

Results

Order: Thalassiosirales Glezer et Makarova 1986

Family: Thalassiosiraceae Lebour 1930

Genus monotypic

Sinerima Nesterovich & Caissie gen. nov.

Description

The valves are circular, structurally differentiated into the valve face and the mantle. The valve face consists of the basal layer perforated by pores arranged in individual or continuous (row-long) cribra in radial rows, separated by radial ribs. The mantle is areolated. Marginal fultoportulae are in one or several more or less regular rings; some fultoportulae are scattered on the valve face. No occluded processes, no central fultoportulae, no rimoportulae.

Generitype

Sinerima marigela Nesterovich & Caissie sp. nov.

Etymology

The word *Sinerima* is composed of a Latin preposition *sine* meaning without and a Latin word for a fissure, *rima*, implying that those organisms have no rimoportulae.

Sinerima marigela Nesterovich & Caissie sp. nov.

Description

The valves are circular, 21–75 µm in diameter (n = 50), very delicate, concave, with shallow mantle. Fine anastomosing ribs (costae sensu Hasle 1973) radiate from the centre,

vaguely (not apparent in some specimen) arranged in four or more (up to 15) fascicules; pores penetrate the basal layer between the costae, arranged in individual cribra or in continuous rows. Around the circumference only, anastomosing ribs are extended externally, producing an areolate structure represented by pseudoloculi. Pseudoloculi on the margin of the valve face, visible in LM, around 10–22 in 10 µm, cover less than a third of the diameter. Toward the centre pseudoloculi come to naught and only cribra arranged in uniserial rows between the bifurcate radial ribs are visible, 9 to 16 rows of cribra in 10 µm. The central area of the valve is structureless or has siliceous thickenings. Around the circumference numerous fultoportulae are arranged in several ranks; 4–5 in 10 µm in the outmost ring, one or two pseudoloculi away from the valve edge. A few fultoportulae also occur scattered on the valve face. The processes are not visible in LM. The fultoportulae lack developed external tubes, presenting as chambers with short tubes flush with the valve surface (marginal zone) or raised slightly above it (central zone). Internally the fultoportulae are small, with four, rarely three, satellite pores. No rimoportula is found.

Etymology

The word *marigela* is derived from the Latin words *marituma,* which means related to the sea, and *gelo,* which means frozen, and refers to the presence of the species in the North Pacific and its apparent association with sea ice.

Type locality

Chukchi Sea (71.599°N, 166.0053°E).

Holotype

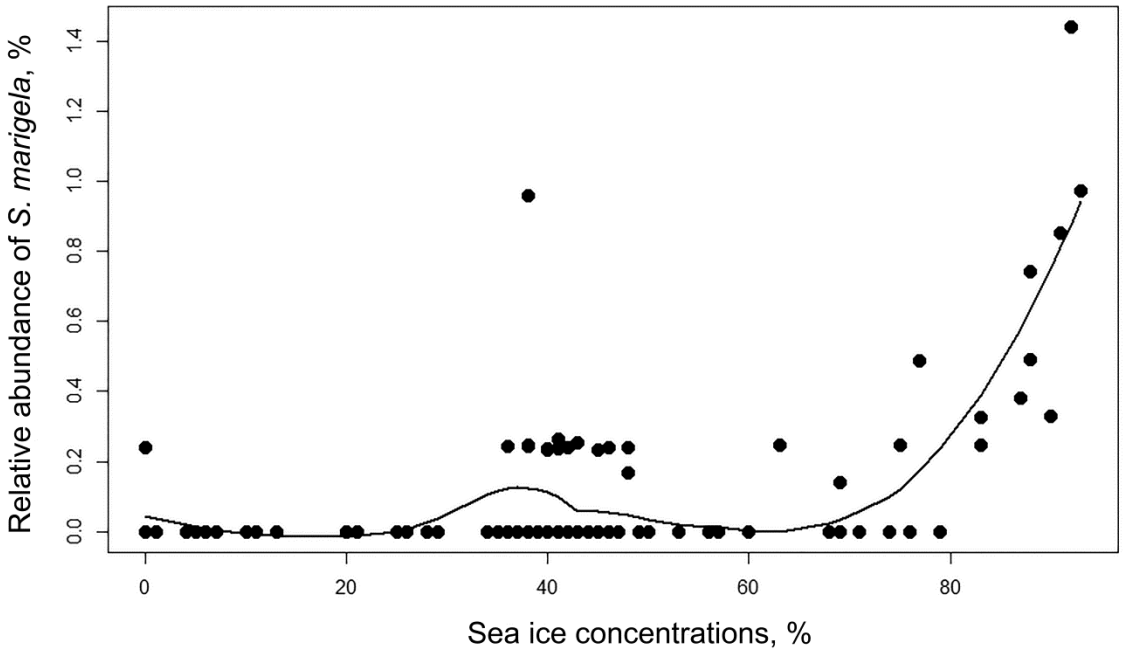

Figure 2.2. *Relative abundance of Sinerima marigela plotted against sea ice concentrations for each sample with a local regression line fitted to illustrate the trend.*

Specimen with coordinates 17.2:11 (Sterrenburg et al., 2012) on slide ANSP GC92687 (Academy of Natural Sciences of Philadelphia, Fig. 2.6 shows the holotype).

Isotypes

Slides BM 101 881 and BM 101 882 (Natural History Museum, London), CANA 127977 (Canadian Museum of Nature, Ottawa), MSL-ISC 453227 (Marine Sediments Laboratory, Iowa State University, Ames).

Type material

ANSP sample GCM85002 (Academy of Natural Sciences of Philadelphia) collected as sample LB 6.5 by Dr. Caissie in 2008 in the Chukchi Sea.

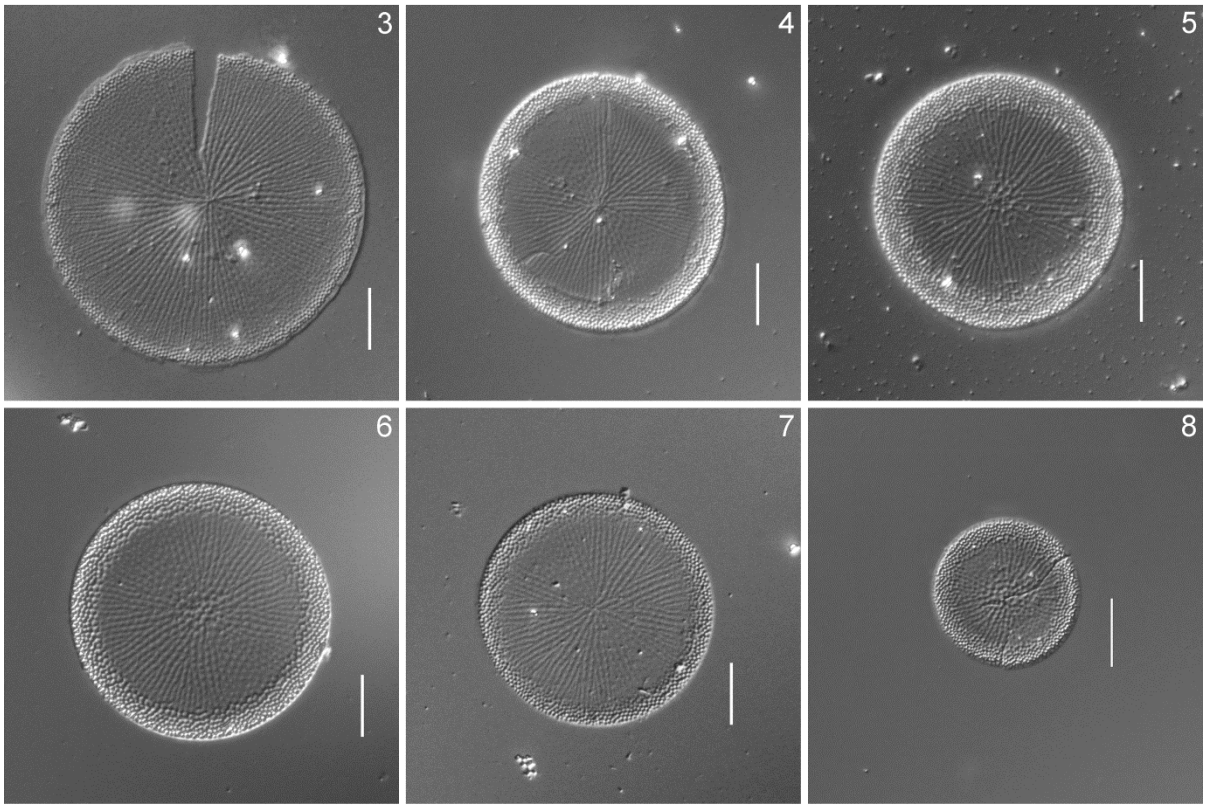

Figure 2.3 *LM micrographs of Sinerima marigela sp. nov. showing variations in valve shape and size. Figs 3–5. Specimens from slide BM 101 881. Fig. 6. Holotype specimen, slide ANSP GC92687. Figs 7–8. Specimens from slide CANA 127977. Scale bar = 10 μm.*

Habitat

The species is described from sediment samples and thus the environmental preferences of the species are very hard to discern. However, since all the samples *S. marigela* was found in were collected in a seasonally ice covered region, it seems reasonable to assume that the species is cold-water. The relative abundance of the species in our samples shows a positive relationship with sea ice concentrations, with a probable optimum at about 90% sea ice during spring season (Fig. 2.2).

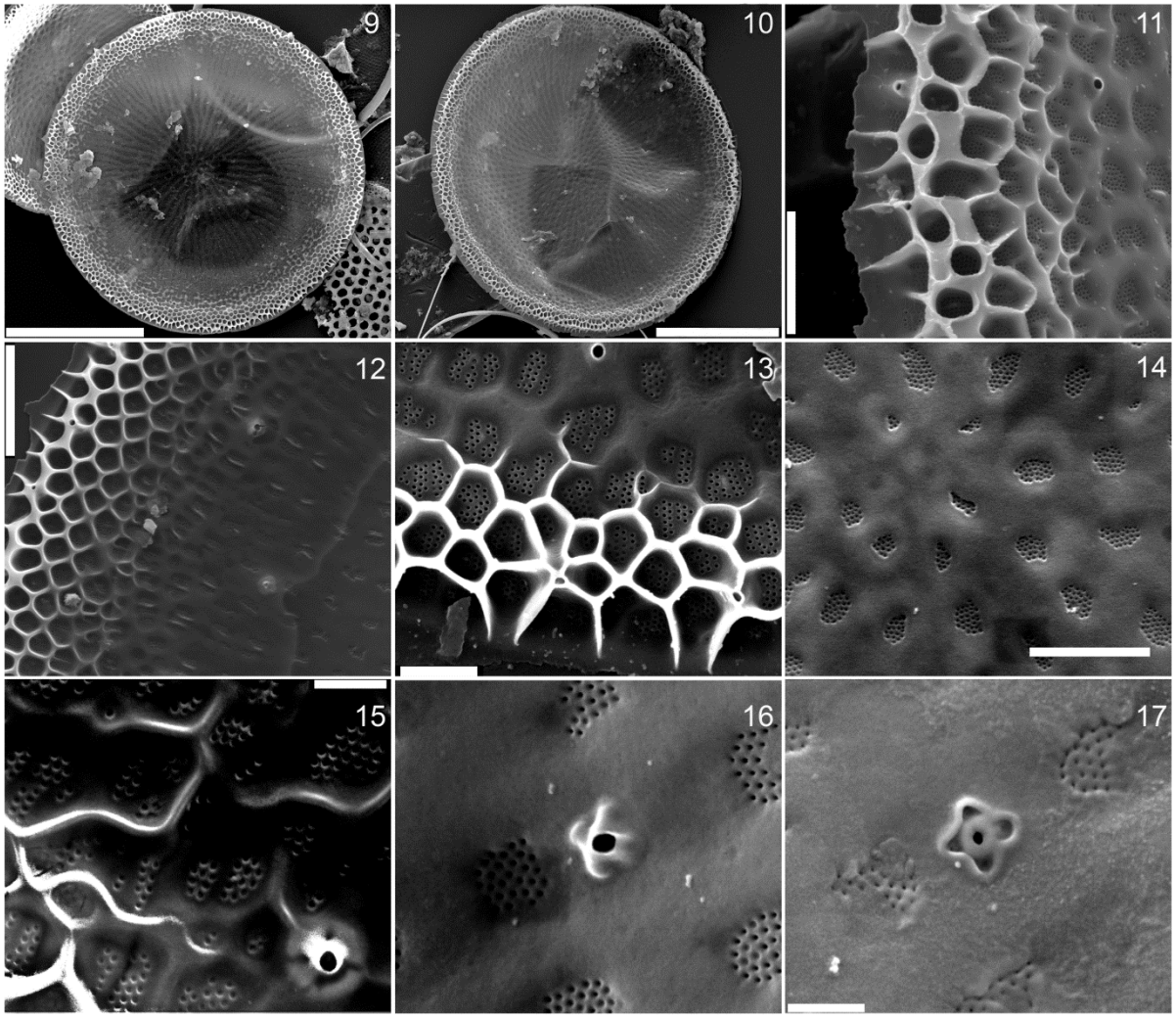

Figure 2.4 *SEM micrographs of Sinerima marigela sp. nov., external valve view. Figs 9–10. Whole valve. Figs 11–13. Valve margin. Note the "extra ribs" separating some of the cribra and marginal fultoportulae. Fig. 14. Central part of a valve. Note the sunken cribra and a hyaline area in the center. Fig. 15. Marginal fultoportula at the inner edge of the pseudoloculate zone with its external tube extending above the smaller reticulate ribs. Fig. 16. Valve face fultoportula with a star-shaped chamber. Fig. 17. Eroded valve face fultoportula showing the openings of the satellite pores. Scale bar = 20 μm (Figs 9–10), 2 μm (Figs 11, 14), 3 μm (Fig. 12), 1 μm (Fig. 13), 500 nm (Figs 15–17).*

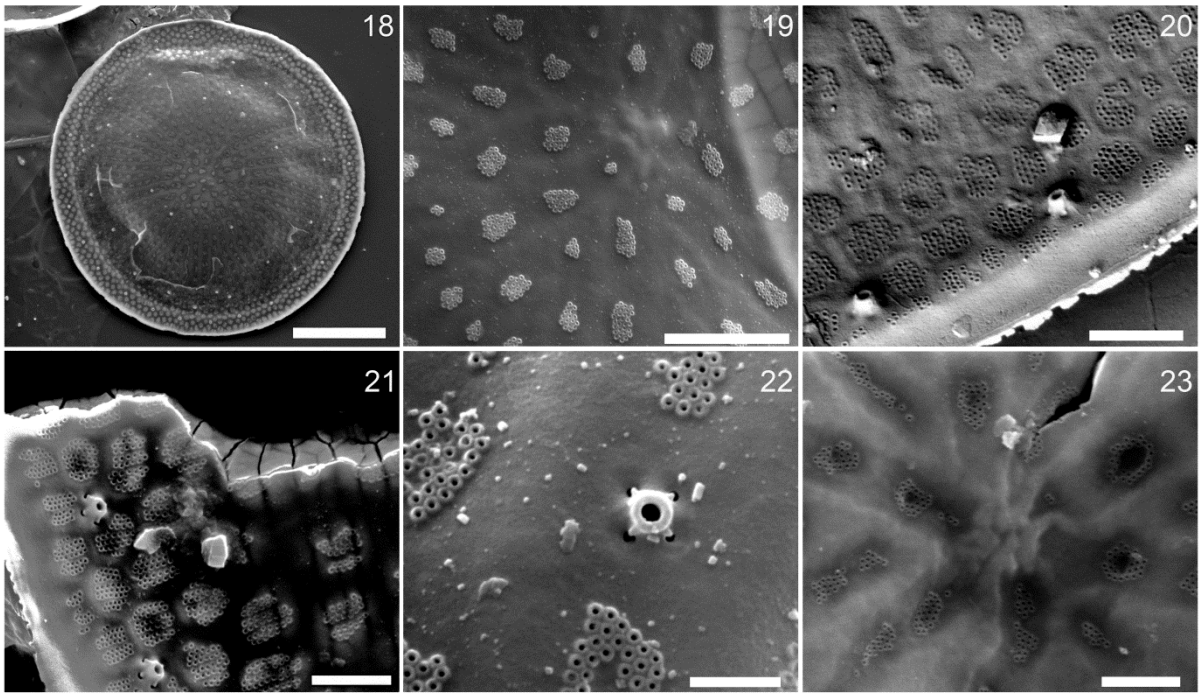

Figure 2.5 *SEM micrographs of Sinerima marigela sp. nov., internal valve view. Fig. 18. Whole valve. Fig. 19. Central part of a valve. Note the raised cribra with rimmed pores and a hyaline area in the center. Figs 20–21. Valve margin. Note the marginal fultoportulae with four satellite pores. Fig. 22. Valve face fultoportula. Note the raised cribra with rimmed pores. Fig. 23. Siliceous knot in the center of a valve. Scale bar = 10 µm (Fig. 18), 2 µm (Fig. 19), 1 µm (Figs 20–21, 23), 500 nm (Fig. 22).*

LM observations

The valves appear flat or crumpled when flattened with a clearly distinct pseudoloculate marginal zone and the valve face with radial ribs and rows of perforations. No processes are visible in LM (Figs. 2.3.3–8).

SEM and TEM observations

External surface (Figs. 2.4.9–17). The marginal zone is covered by pseudoloculi formed by expansion of the distal parts of reticulate ribs (Figs. 2.4.9–11). Often, there are also "extra ribs" that don't reach as high and seem to split a cribrum into sections (Fig.

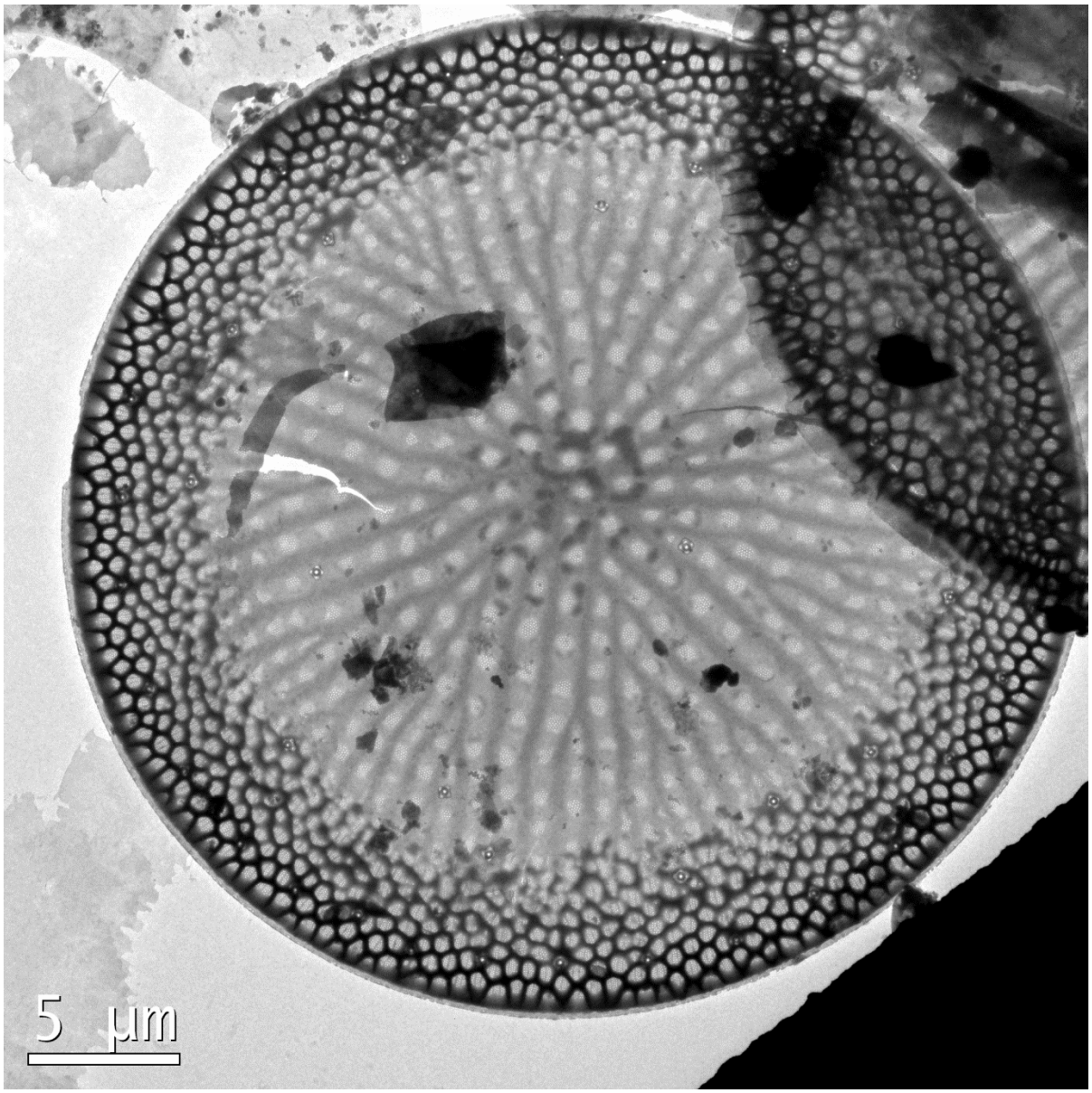

Figure 2.6 *TEM valve view of Sinerima marigela sp. nov. Note the lack of a rimoportula and siliceous thickenings around the center. Scale bar = 5 µm.*

2.4.12). Marginal fultoportulae are placed between areolae, positioned at the junctions of ribs. The distal parts of the fultoportulae are wide at the base, the size of an areola, and narrow towards the end. The distal tubes don't rise above the pseudoloculi (Fig. 2.4.13). The central part doesn't have outward expansions of the ribs; the surface is level with the

exception of slightly sunken cribra (Fig. 2.4.14). The transition between the marginal and the central parts is gradual; the walls of pseudoloculi become lower and disappear over a distance of two to three areolae (Fig. 2.4.15). The fultoportulae in the central part are smaller; the chamber is star-shaped with radii corresponding to satellite pores, as wide at the base as an areola, but soon narrowing into a small opening that doesn't extend into a tube (Fig. 2.4.16–17).

Internal surface (Figs. 2.5.18–23). In most specimens, areolae are visible as individual cribra (sometimes they are merged to form a continuous cribrum), which are flat, but appear raised because each pore in a cribrum consists of a small tube and looks rimmed (Figs. 2.5.19–20). On the mantle of some specimens the pores are not rimmed and the cribra are flush with the surface (Fig. 2.5.21). There are 10–22 cribral pores in 1 μm. On the mantle the areolae are arranged in a honeycomb structure, between the reticulate ribs (Fig. 2.5.20–21). The marginal ring of fultoportulae is two to three areolae from the edge. Each fultoportula has four, rarely three, satellite pores (Fig. 2.5.22). The proximal tubes are short, the covers are triangular flaps of silica, and there is no cowling. On the valve the cribra are arranged in rows toward the centre. Several fultoportulae are scattered on the valve face, sometimes forming a second, less regular ring three to four areolae from the first (Fig. 2.5.18). The structure of the valve face fultoportulae is the same as that of marginal fultoportulae (Figs. 2.5.20–22). The centre of the valve is either hyaline, has an amorphous or spiral siliceous knot formed by meeting of the ribs (Fig. 2.5.23), or has several plaques (Fig. 2.6); there is never a process there. The areolation may be less dense toward the centre.

Differentiating diagnosis

The main feature uniting the genus *Thalassiosira* is the ability to form colonies held together by long threads, however, we don't know what type of colonies, if any, *Sinerima marigela* makes. The new genus differs from *Thalassiosira* in lacking the characteristic areolae with cribra on the inside and foramena on the outside, since there are no loculate areolae in the species. It also has fultoportulae with short distal tubes, though this character appears in some *Thalassiosira* species, especially in the group with eccentric rows of areolae, and lacks rimoportulae, which all species in the *Thalassiosira* genus possess. It should be noted that some of the *Thalassiosira* species don't possess the loculate areolae and have only the poroid basal layer with ribs on the valve face, obligatory as in *Thalassiosira oceanica* Hasle (Hasle, 1983: 220) or occasionally as was documented for *T. eccentrica* (Ehrenberg, 1841: 146) Cleve (1904: 216) (Fryxell and Hasle, 1972), *T. antarctica* Comber (1896: 491), and many others (Makarova 1988).The latest diagnosis of the genus *Thalassiosira* probably should be either emended (or split) to properly accommodate those species. *Sinerima* still differs from all those species by not having a process in the centre, which most of *Thalassiosira* species have, having short proximal and distal fultoportulae tubes, and no rimoportula.

Though *Sinerima* may at first glance look similar to *Lauderia* Cleve (1873: 8), bescause both genera have radiating ribs on the valve face with poroid basal layer between them, a pseudoloculate structure around the circumference, and fultoportulae in rings on the circumference and scattered on the valve face, there are significant differences that don't allow *Sinerima* to be placed into the family Lauderiaceae (Schütt) Lemmermann. The description of the family Lauderiaceae includes fultoportulae with long external tubes and

occluded processes (Round *et al.* 1990) or, in the very least, a central annulus (Kaczmarska et al., 2005), all of which *Sinerima* lacks. Besides, all members of the family Lauderiaceae so far possess a fultoportula.

There is also a certain similarity in areolation with *Bacterosira*. The valve of a *Bacterosira* vegetative cell consists of the poroid basal layer with ribs that become reticulate and extend to form a pseudoloculate structure around the circumference. However, both species of *Bacterosira* have a cluster of fultoportulae in the centre surrounded by a hyaline area and no fultoportulae scattered on the valve face. *Sinerima*, on the other hand, never has processes in the centre, only the scattered fultoportulae. Moreover, the structure of the valve face fultoportulae is different: in *Bacterosira* they open externally as rimmed pores or short tubes without visible chambers (see Figs. 2.23–2.27 and 40 in Park *et al.* (2016)), while *Sinerima*'s valve face fultoportulae have a developed chamber that opens as a short tube (Fig. 2.4.16).

Discussion and Conclusions

Fultoportula-bearing diatoms cluster together on a phylogenetic tree and appear to be a monophyletic group (Kaczmarska *et al.* 2005). All of them are characterized by the presence of fibril-secreting organelles, fultoportulae, which are often involved in colony formation. Two orders of diatoms contain species with fultoportulae, Stephanodiscales Nikolaev et Harwood and Thalassiosirales Glezer et Makarova. The order Stephanodiscales comprises mostly freshwater diatoms, often with alveolae and with only marginal and central fultoportulae. The order Thalassiosirales circumscribes marine and freshwater diatoms with fultoportulae scattered on the valve face. It contains three families: Thalassiosiraceae Lebour,

Skeletonemataceae Lebour emend. Round et Crawford, and Lauderiaceae (Schütt) Lemmermann emend. Round et Crawford (Nikolaev and Harwood, 2002).

The two smaller families are well defined. Lauderiaceae includes a single genus *Lauderia* (occasionally, *Porosira* Jørgensen (1905: 97), which also possesses an annulus, is also included in Lauderiaceae), characterized by particular shape of fultoportulae, long occluded processes, and an annulus. Skeletonemataceae, also with only one extant genus *Skeletonema* Greville (1865: 43), includes species with long distal tubes of fultoportulae used in colony formation. Thalassiosiraceae, on the other hand, includes everything else that doesn't fit in more defined groups, including a number of small, well-defined genera with up to 20 species, such as *Shionodiscus.* The genus *Thalassiosira,* however, has approximately 175– 300 species by different estimates (Fourtanier and Kociolek, 2011; Guiry and Guiry, 2017; Round et al., 1990), and is apparently used as a "go to" genus, where every diatom with fultoportulae, but without any other striking features is placed. The genus is defined by the colony formation (cells are connected by threads some distance apart from each other), by areolae with cribra on the inside and foramena on the outside, and by operculate fultoportulae. However, not every species within the genus concur with even this vague set of features. For example, *T. livingstoniorum* Prasad, Hargraves et Nienow (2011): 3) wasn't observed forming colonies (Prasad *et al.* 2011), *T. fragilis* Fryxell (2007: 147) forms gelatinous colonies (Fryxell et al., 2007), and *T. oceanica* doesn't have loculate areolae (Hasle 1983). At least all of them have operculate fultoportulae, but this character is not restricted to the genus and is shared by *Bacterosira*, *Cyclotella* (Kützing, 1833: 535) Brébisson (1838: 19), etc. Moreover, none of the defining features of the genus is a synapomorphy, since other groups in the order share them all in different combinations.

Since *Sinerima* lacks the synapomorphies that characterize other families within the order, it belongs to Thalassiosiraceae. However, we consider *Sinerima* to be different enough to be placed in a separate genus within the family. One of the striking features of *Sinerima* is the lack of rimoportulae, which is not an apomorphy in and of itself, but still sets the genus apart from every other member of the family.

The second important feature is *Sinerima's* one-layer valves. It can't be considered an apomorphy for the genus, because several other genera, such as *Lauderia* and vegetative cells of *Bacterosira*, and even some *Thalassiosira* species display the same feature. In species such as *T. oceanica*, one layer valves are obligatory, while a group of *Thalassiosira* species, including *T. symmetrica* Fryxell et Hasle (1972: 312), *T. eccentrica*, and *T. tumida* (Janisch in Schmidt (1878: pl. 59) Hasle (1971: 326), is pleomorphic, forming alternatively lightly and heavily silicified valves. Lightly silicified valves often have only the basal layer. However, even lightly silicified valves of those species have cross-bars separating areolae from each other in a row, and *S. marigela* doesn't have them. In *Sinerima* one-layer valves seem obligatory, which makes the genus similar to *Lauderia, Bacterosira,* and some *Thalassiosira* species. The latter, however, tend to be much smaller than *S. marigela* (Hasle, 1983).

It could be possible that *S. marigela* represents an underdeveloped stage of some other diatom, in which the silicification process stopped before the second layer started to form. However, in that case we would expect transitional forms to be observed in the samples, like in populations of other pleomorphic species (Fryxell and Hasle, 1972). The hypothesis that *S. marigela* is not a collection of underdeveloped valves is supported by the fact that we didn't find any valves that can be called transitional or any species with the same

arrangement of fultoportulae in our samples from the Bering and Chukchi seas. Another possibility would be a resting spore of some fultoportulate diatom, which could explain the lack of rimoportulae. However, resting spores of this group of diatoms tend to be heavily-silicified and more robust than vegetative cells and have two layers of silica even in species represented by one-layer valves in the vegetative stage, as can be seen in *Thalassiosira antarctica*, *Bacterosira constricta* (Gaarder, 1938: 64) J.S.Park & J.H.Lee (2016: 11), and other species (Heimdal, 1971; Makarova, 1988). Besides, while we would expect that some resting spores may be missing a rimoportula, the consistent lack of it would be unusual. No trace of a rimoportula or a rimoportula-like slit was found on any of the investigated valves of *S. marigela*. The complete lack of a rimoportula, combined with thin, lightly silicified, one-layer valves, make it unlikely that *S. marigela* is a resting stage of another fultoportulate diatom.

An analysis of morphological characters that included all species of Thalassiosirales found in our samples along with *S. marigela* showed that it is most similar to *Lauderia annulata* Cleve (1873a: 8) and *Porosira glacialis* (Grunow, 1884: 108) Jørgensen (1905: 97). The analysis included 22 species of fultoportulate diatoms (see Table 2.1) and 35 discrete morphological characters (see Appendix A). The species in the table are arranged by the number of characters shared with *S. marigela* (grey highlighting), with the exception of *T. hyalina* (Grunow in Cleve & Grunow 1880: 113) Gran (1897: 4), which was placed near *T. gravida* Cleve (1896: 12) due to the number of characters they share with each other. It is only a morphological analysis and doesn't represent phylogenetic relationships within the group, due to the limited number of species included in the analysis. The table is meant to demonstrate the striking difference between *S. marigela* and all other fultoportulate diatoms

living in the same region, supporting the hypothesis that the new species is not a transitional, underdeveloped, or resting stage of any known diatom from the North Pacific. Nevertheless, it also shows that genera *Shionodiscus* and *Bacterosira* are defined and separated from the rest of the group by the number of character states they share with each other, but not other members of the group. The same can be said about small groups formed by *L. annulata* and *P. glacialis*, *T. gravida* and *T. hyalina*, and *T. eccentrica* and *T. symmentrica*, while other species of *Thalassiosira* are scattered among other representatives of the group and don't form a monolithic cluster. A phylogenetic analysis would be desirable to place *S. marigela* on the phylogenetic tree of diatoms, but it is currently impossible, since there is no genetic material available.

The third feature of the new genus is the special type of cribra, with rimmed pores. We consider it an apomorphy for the genus. The typical cribra of Thalassiosiraceae are raised flat sieves with 20–40 pores in 10 μm. In *Sinerima*, on the other hand, the cribra are coarser and appear not as perforated flaps of silica, but as clusters of individually rimmed pores, 10–22 in 10 μm. Moreover, because they are not strictly speaking "plates with pores", they can't be called cribra, but should be considered some other type of vela, probably tubular vela (Nikolaev and Harwood, 2002). We didn't see a similar structure of the cribra in any other genus in the order. There is, however, a very similar looking cribra in the genus *Auliscus* Ehrenberg (1843: 271). In particular, *Auliscus pruinosus* Bailey (1854: 8), lacking both fultoportulae and rimoportulae, exhibits the same structure of cribra (Sullivan, 1987). However, the lack of fultoportulae in *Auliscus* suggests that it's not closely related to *Sinerima*.

It appears that *Sinerima marigela* is a unique diatom that probably went unnoticed and undescribed because of its rarity. Even in the sample with the highest abundance of the species we found, it constitutes less than 3% of the total diatom assemblage. Rare species though can be the most valuable in assessing the environmental conditions, since widespread species with a wide range of tolerance can hardly be reliable indicators (Noss, 1990). In this sense the search for rare species associated with particular environmental factors can be extremely fruitful. Since *S. marigela* appears to be associated with high concentrations of sea ice in Beringia, this species is a good candidate for a diatom-based proxy to reconstruct past sea ice conditions in the region.

Acknowledgements

This work was supported by the NSF under Ocean Sciences Research Initiation Grant OCE-RIG 1524784 and by the GSA under a Graduate Student Research Grant awarded to Anna Nesterovich in 2015. We thank the captain and crew of the F/V Norseman II and Dr. Jacqueline Grebmeier for inviting us to collect samples from the Chukchi Sea during the Norseman II's 2008 cruise.

References

Agardh, C.A., 1824. Systema Algarum. Literis Berlingianis [Berling], Lundae [Lund].

Alverson, A.J., Kang, S.-H., Theriot, E.C., 2006. Cell wall morphology and systematic importance of *Thalassiosira ritscheri* (Hustedt) Hasle , with a description of Shionodiscus gen. nov. Diatom Res. 21, 251–262. doi:10.1080/0269249X.2006.9705667

Arrigo, K.R., Perovich, D.K., Pickart, R.S., Brown, Z.W., van Dijken, G.L., Lowry, K.E., Mills, M.M., Palmer, M.A., Balch, W.M., Bates, N.R., Benitez-Nelson, C.R., Brownlee, E., Frey, K.E., Laney, S.R., Mathis, J., Matsuoka, A., Greg Mitchell, B., Moore,

G.W.K., Reynolds, R.A., Sosik, H.M., Swift, J.H., 2014. Phytoplankton blooms beneath the sea ice in the Chukchi sea. Deep. Res. Part II Top. Stud. Oceanogr. 105, 1–16. doi:10.1016/j.dsr2.2014.03.018

Bailey, J.W., 1854. Notes on new species and localities of microscopical organisms. Smithsonian Institution.

Battarbee, R.W., 1986. Diatom analysis, in: Berglund, B.E. (Ed.), Handbook of Holocene Palaeoecology and Palaeohydrology. J. Wiley, New York, pp. 527–570.

Caissie, B.E., 2012. Diatoms as recorders of sea ice in the Bering ans Chukchi seas: Proxy development and application. University of Massachusetts - Amherst. doi:10.1017/CBO9781107415324.004

Cavalieri, D., Parkinson, C., Gloersen, P., Zwally, H.J., n.d. Sea Ice Concentrations from Nimbus-7 SMMR and DMSP SSM/I-SSMIS Passive Microwave Data, Version 1. [1996-2008]. Boulder, Colorado USA: NASA DAAC at the National Snow and Ice Data Center [WWW Document]. doi:http://dx.doi.org/10.5067/8GQ8LZQVL0VL

Cleve, P.T., 1904. Plankton table for the North Sea. Cons. Perm. Int. pour l'Exploration la Mér 1903-1904 216.

Cleve, P.T., 1896. Diatoms from Baffins Bay and Davis Strait. Bih. till K. Sven. Vetenskapsakademiens Handl. 22, III, 1–22.

Cleve, P.T., 1873. On diatoms from the Arctic Sea. Bih. till Kongliga Sven. Vetenskaps-Akademiens Handl. 1, 1–28.

Cleve, P.T., 1867. Diatomaceer från Spetsbergen. Öfversigt af Kongliga Sven. Vetenskaps-Akademiens Förhandlingar 24, 661–670.

Cleve, P.T., Grunow, A., 1880. Beiträge zur Kenntniss der arctischen Diatomeen. Kongliga Sven. Vetenskaps-Akademiens Handl. 17, 1–121.

Comber, T., 1896. On the occurrence of endocysts in the genus *Thalassiosira*. J. R. Microsc. Soc. 489–491.

de Brébisson, L.A., 1838. Considerations sur les diatomées et essai d'une classification des

genres et des espèces appartenant à celle famille. Brée l'Ainé Imprimeur-Libraire, Falaise.

Ehrenberg, C.G., 1853. Über neue Anschauungen des kleinesten nördlichen Polarlebens. Bericht über die zur Bekanntmachung geeigneten Verhandlungen der Königlich-Preussischen Akad. der Wissenschaften zu Berlin 522–533.

Ehrenberg, C.G., 1845. Neue Untersuchungen über das kleinste Leben als geologisches Moment. ericht über die zur Bekanntmachung geeigneten Verhandlungen der Königlich-Preussischen Akad. der Wissenschaften zu Berlin 53–87.

Ehrenberg, C.G., 1844a. Mittheilung über 2 neue Lager von Gebirgsmassen aus Infusorien als Meeres-Absatz in Nord-Amerika und eine Vergleichung derselben mit den organischen Kreide-Gebilden in Europa und Afrik. Bericht über die zur Bekanntmachung Geeigneten Verhandlungen der Königl. Preuss. Akad. Der Wissenschaften zu Berlin 57–97.

Ehrenberg, C.G., 1844b. Einige vorläufige Resultate seiner Untersuchungen der ihm von der Südpolreise des Captain Ross, so wie von den Herren Schayer und Darwin zugekommenen Materialien über das Verhalten des kleinsten Lebens in den Oceanen und den grössten bisher zugänglichen T. Bericht über die zur Bekanntmachung Geeigneten Verhandlungen Der Königl. Preuss. Akad. Der Wissenschaften zu Berlin 182–207.

Ehrenberg, C.G., 1841. Über noch jetzt zahlreich lebende Thierarten der Kreidebildung und den Organismus der Polythalamien. Abhandlungen der Königlichen Akad. der Wissenschaften zu Berlin 81–174.

Ehrenberg, C.G., 1838. Über die Bildung der Kreidefelsen und des Kreidemergels durch unsichtbare Organismen. Abhandlungen der Königlichen Preußischen Akad. der Wissenschaften zu Berlin 59–147.

Fourtanier, E., Kociolek, J.P., n.d. Catalogue of Diatom Names, California Academy of Sciences, On-line Version updated 19 Sep 2011. [WWW Document]. URL http://research.calacademy.org/research/diatoms/names/index.asp

Fryxell, G.A., Gould Jr., R.W., Watkins, T.P., 2007. Gelatinous colonies of the diatom Thalassiosira in Gulf Stream Warm Core Rings including *T. fragilis* , sp. nov. Br. Phycol. J. 19, 141–156. doi:10.1080/00071618400650151

Fryxell, G.A., Hasle, G.R., 1980. The marine diatom *Thalassiosira oestrupii*: Structure, taxonomy and distribution. Am. J. Bot. 67, 804–814.

Fryxell, G.A., Hasle, G.R., 1977. The genus *Thalassiosira*: some species with a modified ring of central strutted processes. Nov. Hedwigia Beih. 54, 67–98.

Fryxell, G.A., Hasle, G.R., 1972. *Thalassiosira eccentrica* (Ehrenb.) Cleve, *T. symmetrica* sp. nov., and some related centric diatoms. J. Phycol. 8, 297–317.

Fryxell, G.A., Hubbard, G.F., Villareal, T.A., 1981. The genus *Thalassiosira*: Variations of the cingulum. Bacillaria 4, 41–63.

Gaarder, K.R., 1938. Phytoplancton studies from the Tromsø district 1930–31. Tromsø Museums Arsh. Naturhistorisk Adv. Nr. 11 55, 1–159.

Gran, H.H., 1904. Diatomaceae from the ice-floes and plankton of the Arctic Ocean. Nor. North-Polar Exped. 1893-1896, Sci. Results IV, 1–74. doi:10.1017/CBO9781107415324.004

Gran, H.H., 1900. Bemerkungen über einige Planktondiatomeen. Nytt Mag. naturvidenskapene 38, 102–128.

Gran, H.H., 1897. Bacillariaceen vom Kleinen Karajakfjord. Bibl. Bot. 42, 1–24.

Greville, R.K., 1865. Descriptions of new and rare diatoms. Series XVI. Trans. Microsc. Soc. New Ser. London 13, 43–57.

Grunow, A., 1884. Die Diatomeen von Franz Josefs-Land. Denkschriften der Kais. Akad. der Wissenschaften. Math. Cl. 48, 53–112.

Guiry, M.D., Guiry, G.M., 2017. AlgaeBase. World-wide electronic publication, National University of Ireland, Galway. http://www.algaebase.org; searched on 21 March 2017 [WWW Document]. AlgaeBase. World-wide Electron. Publ. Natl. Univ. Ireland, Galway. http//www.algaebase.org; searched 21 March 2017. URL http://algaebase.org/about/

Hasle, G.R., 1983. The marine, planktonic diatoms *Thalassiosira oceanica* sp. nov. and *T. partheneia*. J. Phycol. 19, 220–229. doi:10.1111/j.0022-3646.1983.00220.x

Hasle, G.R., 1979. *Thalassiosira decipiens* (Grun.) Jorg. (Bacillariophyceae). Bacillaria 2, 85–107.

Hasle, G.R., 1973. Thalassiosiraceae, a new diatom family. Nor. J. Bot. 20, 67–69.

Hasle, G.R., Heimdal, B.R., Fryxell, G.A., 1971. Morphologic variability in fasciculated diatoms as exemplified by *Thalassiosira tumida* (Janisch) Hasle, comb. nov., in: Llano, G.A., Wallen, I.E. (Eds.), Biology of Antarctic Seas IV. American Geophysical Union, Washington, D.C., pp. 313–333.

Heimdal, B.R., 1971. Vegetative cells and resting spores of *Thalassiosira constricta* Gaarder (Bacillariophyceae). Nor. J. Bot. 18, 153–159.

Hustedt, F., 1913. Atlas der Diatomaceen-kunde. O. R. Reisland, Leipzig.

Jørgensen, E.G., 1905. Remarks on the plankton, in: Nordgaard, O. (Ed.), Hydrographical and Biological Investigations in Norwegian Fiords. Bergens Museum Skrift, John Grieg, Bergen, pp. 87–157.

Julius, M.L., Tanimura, Y., 2001. Cladistic analysis of plicated *Thalassiosira* (Bacillariophyceae). Phycologia 40, 11–122.

Kaczmarska, I., Beaton, M., Benoit, A.C., Medlin, L.K., 2005. Molecular phylogeny of selected members of the order Thalassiosirales (Bacillariophyta) and evolution of the fultoportula. J. Phycol. 138, 121–138. doi:10.1111/j.1529-8817.2005.00161.x

Kützing, F.T., 1833. Synopsis Diatomacearum oder Versuch einer systematischen Zusammenstellung der Diatomeen. Linnaea 8, 529–620.

Lebour, M.V., 1930. The planktonic diatoms of northern seas. Ray Society Publications. London., Issue: no. 116.

Ligowski, R., Godlewski, M., Łukowski, A., 1992. Sea ice diatoms and ice edge planktonic diatoms at the nothern limit of the Weddell Sea pack ice, in: Proc. NIPR Symp. Polar Biol. pp. 9–20.

Makarova, I. V., 1994. The morphology of marine genera of the family Thalassiosiraceae Lebour emend Hasle, in: Kociolek, J.P. (Ed.), Proceeding of the 11th International

Diatom Symposium. California Academy of Sciences, San Francisco, Califormia, pp. 103–111.

Makarova, I. V., 1988. Diatoms of the USSR seas: genus Thalassiosira Cleve. Nauka, Leningrad.

Medlin, L.K., Kooistra, W.H.C.F., Gersonde, R., Welbrock, U., 1996. Evolution of the diatoms (Bacillariophyta): III. Molecular evidence for the origin of the Thalassiosirales. Nov. Hedwigia, Beih. 112, 221–234.

Nikolaev, V.A., Harwood, D.M., 2002. Morphology, taxonomy and system classification of centric diatoms. Nauka, St. Petersburg.

Noss, R.F., 1990. Indicators for monitoring biodiversity: a hierarchical approach. Conversat. Biol. 4, 355–364.

O'Meara, E., 1860. On some diatomaceous forms from the Arctic Regions, collected during the late voyage of the Fox. J. R. Dublin Soc. III, 59–60.

Østrup, E., 1895. Marine diatomeer fra Østgrønland. Meddelelser om Grønland, Kjøbenhavn 18, 397–476.

Park, J.S., Alverson, A.J., Lee, J.H., 2016. A phylogenetic re-definition of the diatom genus *Bacterosira* (Thalassiosirales, Bacillariophyta), with the transfer of *Thalassiosira constricta* based on morphological and molecular characters. Phytotaxa 245, 1–16. doi:10.11646/phytotaxa.245.1.1

Percopo, I., Ruggiero, M.V., Balzano, S., Gourvil, P., Lundholm, N., Siano, R., Tammilehto, A., Vaulot, D., Sarno, D., 2016. *Pseudo-nitzschia arctica* sp. nov., a new cold-water cryptic Pseudo-nitzschia species within the P. pseudodelicatissima complex. J. Phycol. 52, 184–199. doi:10.1111/jpy.12395

Pirtle-Levy, R., Grebmeier, J.M., Cooper, L.W., Larsen, I.L., 2009. Chlorophyll a in Arctic sediments implies long persistence of algal pigments. Deep. Res. Part II Top. Stud. Oceanogr. 56, 1326–1338. doi:10.1016/j.dsr2.2008.10.022

Poulin, M., Cardinal, A., 1982. Sea ice diatoms from Manitounuk Sound, southeastern Hudson Bay (Quebec, Canada). I. Family Naviculaceae. Can. J. Bot. 60, 1263–1278. doi:10.1139/b82-160

Prasad, A.K.S.K., Nienow, J.A., Hargraves, P., 2011. Plicate Species of the Diatom Genus *Thalassiosira* (Bacillariophyta) from the Atlantic and Gulf Coasts of Southeastern United States, with the Description of T. livingstoniorum sp. nov. Proc. Acad. Nat. Sci. Philadelphia 161, 1–34. doi:10.1635/053.161.0101

Round, F.E., Crawford, R.M., Mann, D.G., 1990. The Diatoms: Biology & morphology of the genera. Cambridge University Press, Cambridge.

Scherer, R.P., 1994. A new method for the determination of absolute abundance of diatoms and other silt-sized sedimentary particles. J. Paleolimnol. 12, 171–179. doi:10.1007/BF00678093

Schmidt, A., 1878. Atlas der Diatomaceen-kunde.

Schöne, H.K., 1972. Experimentelle Untersuchungen zur Ökologie der marinen Kieselalge Thalassiosira rotula. I. Temperatur und Licht. Mar. Biol. 13, 284–291.

Smayda, T.J., Boleyn, B.J., 1965. Experimental observations on the flotation of marine diatoms. I. *Thalassiosira* cf. *nana, Thalassiosira rotula* and *Nitzschia seriata*. Limnol. Oceanogr. 10, 499–509.

Stachura-Suchoples, K., Williams, D.M., 2009. Description of *Conticribra tricircularis*, a new genus and species of Thalassiosirales, with a discussion on its relationship to other continuius cribra species of *Thalassiosira* Cleve (Bacillariophyta) and its freshwater origin. Eur. J. Phycol. 44, 477–486. doi:10.1080/09670260903225431

Sterrenburg, F.A.S., Hamilton, P.B., Williams, D.M., 2012. Universal coordinate method for locating light-microscope specimens. Diatom Res. 27, 91–94. doi:10.1080/0269249x.2012.688493

Sullivan, M.J., 1987. A light- and scanning electron microscope study of the marine diatom *Aulicus pruinosus* Bailey (Eupodiscaceae). Br. Phycol. J. 22, 33–42. doi:10.1080/00071618700650041

Syvertsen, E.E., Hasle, G.R., 1984. *Thalassiosira bulbosa* Syvertsen, sp. nov., an arctic marine diatom. Polar Biol. 3, 167–172. doi:10.1007/BF00442648

Syvertsen, E.E., Hasle, G.R., 1982. The marine planktonic diatom *Lauderia annulata* Cleve, with particular reference to the processes. Bacillaria 5, 243–256.

Theriot, E.C., Serieyssol, K., 1994. Phylogenetic systematics as a guide to understanding features and potential morphological characters of the centric diatom family Thalassiosiraceae. Diatom Res. 9, 429–450. doi:10.1080/0269249X.1994.9705318

Theriot, E.C., Stoermer, E.F., Håkansson, H., 1987. Taxonomic interpretation of the rimoportula of freshwater genera in the centric diatom family Thalassiosiraceae. Diatom Res. 2, 251–265. doi:10.1080/0269249X.1987.9705003

Vancoppenolle, M., Meiners, K.M., Michel, C., Bopp, L., Brabant, F., Carnat, G., Delille, B., Lannuzel, D., Madec, G., Moreau, S., Tison, J.-L., van der Merwe, P., 2013. Role of sea ice in global biogeochemical cycles: Emerging views and challenges. Quat. Sci. Rev. 79, 207–230. doi:10.1016/j.quascirev.2013.04.011

Table 2.1 *A matrix of 35 morphological characters observed in 22 species of Thalassiosirales found in our samples along with S. marigela. Grey shading indicates characters shared with S. sinerima. Boxes are used to highlight similarities between closely related species (see Appendix for character descriptions).*

	Rimoportula					Central fultoportulae								Marginal fultoporulae								Other pr.			Areolae				Other						
Species/Character	01	02	03	04	05	06	07	08	09	10	11	12	13	14	15	16	17	18	19	20	21	22	23	24	25	26	27	28	29	30	31	32	33	34	35
S. marigela	-	-	-	-	-	0	-	-	-	-	-	-	-	4	1	1	0	2	1	1	2	0	0	0	0	3	0	2	0	4	1	1	0	0	1
L. annulata	1	1	1	1	3	0	-	-	-	-	-	-	-	5	3	1	1	1	3	1	2	0	1	0	0	0	0	2	0	1	1	1	0	0	1
P. glacialis	1	1	2	2	3	0	-	-	-	-	-	-	-	3	2	1	1	0	3	1	2	0	0	0	0	0	3	2	0	0	0	0	0	0	1
T. oceanica	1	2	1	3	1	5	3	2	1	0	2	0	2	4	2	1	0	2	1	0	2	1	0	0	0	1	0	2	0	1	1	1	0	0	0
T. gravida	1	1	1	1	3	3	4	1	1	1	0	0	2	4	1	1	0	0	2	0	2	0	0	0	0	1	0	1	0	0	1	0	0	0	1
T. hyalina	1	1	1	2	2	3	4	1	1	1	0	0	2	4	1	1	0	0	1	0	2	1	0	0	0	1	1	1	0	0	0	0	0	1	0
T. antarctica	1	1	2	4	3	3	3	2	1	0	2	0	1	4	2	1	0	2	2	1	2	0	1	0	0	1	0	3	0	0	1	0	1	0	1
B. constricta	1	2	2	3	1	3	4	3	1	1	0	0	2	4	3	1	1	0	1	0	2	1	0	0	0	0	0	2	0	1	1	0	0	0	0
B. bathyomphala	1	2	1	3	1	4	4	3	1	1	1	0	1	4	3	1	1	1	1	0	1	1	0	0	0	0	0	2	0	1	1	0	0	0	0
T. hyperborea	1	1	2	2	1	5	4	2	1	0	2	0	1	4	2	1	0	2	1	0	2	1	0	0	0	0	2	1	0	5	0	0	0	0	0
T. decipiens	1	1	1	2	1	1	4	1	1	0	1	0	0	4	1	1	0	1	1	0	2	1	0	0	0	1	2	1	3	0	0	0	0	1	1
T. tumida	4	1	2	2	1	5	4	2	1	0	0	0	1	4	2	1	0	0	1	0	1	0	0	0	0	1	2	2	3	1	0	0	0	1	1
T. pacifica	1	2	2	1	2	1	4	1	1	0	2	1	1	4	1	1	0	2	1	0	3	1	0	0	0	1	1	1	2	0	0	0	0	1	0
T. nordenskioeldii	1	1	1	1	1	1	4	2	1	0	2	1	2	4	2	1	0	2	1	0	3	1	0	0	0	1	1	1	0	1	0	0	0	1	0
T. eccentrica	1	1	2	1	3	5	4	1	1	0	0	0	0	4	1	1	0	0	1	1	1	1	0	1	0	1	2	1	3	0	0	0	0	1	0
T. symmetrica	2	1	2	2	3	6	4	?	1	0	0	0	0	4	?	1	0	0	1	1	1	0	0	1	0	1	2	1	3	0	0	0	0	1	0
T. bulbosa	1	2	1	2	1	1	3	0	1	2	0	1	2	3	0	1	2	0	1	0	3	1	0	0	2	0	1	2	0	0	1	0	0	0	0
Sh. poroseriatus	1	3	2	3	3	2	3	3	2	1	2	0	0	3	3	2	1	2	1	0	0	1	0	0	0	1	2	1	3	1	0	0	0	1	1
Sh. trifultus	1	3	2	3	3	2	3	3	2	1	2	0	0	3	3	2	1	2	1	0	0	1	0	0	0	1	2	1	3	0	0	0	0	1	1
Sh. oestrupii	1	3	2	3	3	5	3	3	2	2	0	0	0	3	3	2	1	0	1	0	0	1	0	0	0	1	2	1	3	3	0	0	0	3	1
T.anguste-lineata	1	2	1	1	1	5	4	?	1	?	?	1	1	4	?	1	?	?	1	0	1	1	0	0	0	1	2	1	3	0	0	0	0	1	0
T. punctigera	1	2	2	1	3	1	4	0	1	2	1	0	2	4	0	1	2	1	1	0	3	1	1	0	2	0	1	1	1	0	0	0	0	1	0

CHAPTER 3. DIATOM SUCCESSION AND VERTICAL EXPORT IN THE CHUKCHI SEA

In preparation for publication

Abstract

Fossil diatom assemblages preserved in sediments are widely used as proxies for paleo reconstructions, including Arctic sea ice. However, the sedimentation processes leading to formation of taphonomic assemblages are not well understood. We analyzed a consecutive series of 24 samples collected by a sediment trap on the shelf of the Chukchi Sea from August 2015 to August 2016 and compared diatom communities in these samples with two surface sediment samples collected nearby. We found that species composition and relative abundance in sediment trap and surface sediment samples are very similar. Species associated with sea ice are present in both sets of samples at the same levels of abundance, which suggests that there is no preferential species-specific dissolution in the lower part of the water column or at the bottom. The seasonal succession in sediment trap samples indicates that sediments reflect changes in phytoplankton communities in the photic zone and can be used as a reliable archive for paleoreconstructions.

Introduction

Sea ice in the polar regions strongly affects both the planet's climate system and its biota (Serreze and Barry, 2011). The current dramatic decline in Arctic sea ice extent (Stroeve et al., 2007; Yongqi et al., 2015) surpasses predicted ice loss (Stroeve et al., 2007) and requires a better understanding of the repercussions of these changes. Modelling the climate system, including sea ice impacts and feedbacks, however, is impeded by insufficient

and short-term monitoring data. Proxy archives can be compared to and calibrated with instrumental series allowing for sea ice records to be extended many millennia and beyond (Abram et al., 2013).

Fossil diatom assemblages preserved in sediments are widely used as proxies for paleo reconstructions, including Arctic sea ice. Diatoms are unicellular organisms producing a hard silica frustule that is often well preserved in underlying sediments. The group is very diverse, with representatives preferring different environmental conditions. The species composition of a diatom community provides information on all aspects of the environment it inhabited (Round et al., 1990). However, the paths and mechanisms of diatom sedimentation are not fully studied. Sediment traps, especially deployed for extended periods of time and collecting samples year-round, can provide many insights into sedimentation processes.

Most of the sediment traps that have been deployed in the Arctic have collected data only during spring and summer, which limits their applicability to processes only occurring during part of the year. They do, however, indicate higher productivity during spring (Lomas et al., 2012), the prevalence of diatoms at the marginal ice zone (Lomas et al., 2012), and increased grazing after the retreat of ice (Lalande et al., 2007). It was also shown that about 10–20% of primary productivity is exported below 50 m unconsumed (Lepore et al., 2007), implying that sediments are representative of surface waters. There are, however, species-specific sedimentation rates that are further complicated by changes of rates from season to season that can lead to selective sedimentation. It is important to note that many species have different sedimentation rates during and after a bloom, as well as later in the season (Passow, 1991); and short-term traps cannot capture those changes. Year-long traps that were set under

permanent ice in the Arctic showed a pattern unique to the Polar Regions, with only one bloom per year, instead of two blooms in more temperate waters. *Melosira arctica* dominated in all samples in terms of both number and biomass throughout the period (Nöthig et al., 2015). Those differences make the knowledge gleaned from year-long traps under permanent ice impossible to extrapolate into regions with variable ice conditions.

In the Southern Ocean, a set of multi-decadal sediment traps deployed in a latitudinal transect allowed a deeper understanding of the sedimentation processes in Antarctic ice-influenced waters. It was shown that seasonal flux patterns at different depths mirrored seasonal water column changes, increasing in spring along with light levels, but ahead of temperature increases (Rigual-Hernández et al., 2016). These changes in sedimentation reflected community composition changes at the surface (Wilks et al., 2017). Studies on these traps also showed strong dissolution in the sediment/water interface in the sediments below, pointing out selective sedimentation of more robust diatoms and dissolution of the weakly silicified species that were responsible for the bulk of the spring bloom (Rigual-Hernández et al., 2016, 2015). Sedimentation rates in Antarctic waters also vary with species and season (Closset et al., 2015).

Longer and more detailed records are often available from sediment traps in lakes, where it was shown that a bloom is not necessarily followed by a sedimentation event, with sedimentation depending also on aggregating factors, such as meteorological conditions, water chemistry and grazing (Fuchs et al., 2016).

Thus, as with other sea ice proxies (Cronin et al., 2010; De Vernal et al., 2013a), diatom-based proxies raise several concerns. Primarily, it is necessary to test if sediments are representative of the phytoplankton communities found in the surface waters above them and

if the full range of species present in the water column is preserved in the sediments. This study addresses some of these concerns by testing the second hypothesis. To do this, I investigated diatom succession in a year-long record from a sediment trap deployed in the Chukchi Sea and compare it with two sediment samples collected nearby. This study provides valuable insight into temporal trends in diatom assemblages at a site with variable sea ice coverage and vertical transfer of diatom valves from the surface waters to the sediments. We aim to improve interpretability of diatom-based sea ice proxies and validate diatoms as a good archive for sea ice reconstructions.

Material and Methods

Sediment Trap Samples

We analyzed a consecutive series of 24 samples collected by a sediment trap deployed on the Chukchi Sea shelf from August 2015 to August 2016. The trap was a part of the NE Chukchi Sea Moored Ecosystem Observatory project (71.6° N, 161.5° W). Each sediment trap was open for a period of 1 to 4 weeks, depending on the time of year (TABLE 3.1). The last bottle was still open during the recovery, and the counts from this sample were treated with caution. In order to compare with sediment samples, which consist of sediments accumulated over several years, we created a composite mooring sample by combining the counts from all 24 samples and calculating relative percent abundances of species from the total number of valves.

Surface Sediment Samples

Two surface sediment samples were collected as part of the Distributed Biological Observatory project from the top of a 0.1 m^2 single Van Veen grab before it was opened. The two samples, S-2/HLY1702 (71.4823 N 161.513 W) and DBO4.4N/HLY1801 (71.4805 N

161.5048 W) were within 13 km of the mooring location, and were collected in 2017 and 2018, respectively (Pickart and Grebmeier, 2017, 2018).

Diatom Identification and Quantification

Quantitative diatom slides were prepared according to the modified method described in Scherer (1994). From each sample, 1 mL was used in the analysis. Cover slips were mounted on cleaned microscope slides using Naphrax® (refractive index 1.73). At least 400 diatom valves in at least 3 random transects across each slide were identified using a Nikon ECLIPSE Ni transmitted light microscope at a magnification of 1000x equipped with differential interference contrast and a Nikon DS-Fi2 camera. The transects were measured using a stage micrometer. Partial valves were counted according to the methods of Schrader and Gersonde (1978). All diatoms were identified to the species level when possible following published taxonomic descriptions and images (Medlin and Priddle, 1990; Witkowski et al., 2000). For resting spores of *Chaetoceros* the classification made by Suto (2006, 2005, 2004a, 2004b, 2004c) has been used.

Environmental Factors

Sea ice concentrations have been derived using brightness temperatures from the Special Sensor Microwave/Imager (SSM/I) passive microwave satellite data (Cavalieri et al., 1996). The daily sea ice concentrations were obtained for the duration of the sediment trap deployment. The duration of daylight was calculated using Duration of Daylight/Darkness Table for One Year web application (https://aa.usno.navy.mil/data/docs/Dur_OneYear.php).

Table 3.1. *Sediment trap samples from the mooring station.*

Sample #	Date opened	Date close	# days open	Abundance, valves/mL	Flux, valves/m^2 day
1	08/16/2015	09/01/2015	16	$1.714 \cdot 10^5$	$32.559 \cdot 10^8$
2	09/01/2015	09/16/2015	15	$1.291 \cdot 10^5$	$24.523 \cdot 10^8$
3	09/16/2015	10/01/2015	15	$9.297 \cdot 10^4$	$17.664 \cdot 10^8$
4	10/01/2015	10/16/2015	15	$1.031 \cdot 10^5$	$19.587 \cdot 10^8$
5	10/16/2015	11/01/2015	16	$9.634 \cdot 10^4$	$18.304 \cdot 10^8$
6	11/01/2015	11/16/2015	15	$4.251 \cdot 10^4$	$8.076 \cdot 10^8$
7	11/16/2015	12/012015	15	$5.805 \cdot 10^4$	$11.030 \cdot 10^8$
8	12/01/2015	01/01/2016	31	$3.299 \cdot 10^4$	$6.268 \cdot 10^8$
9	01/01/2016	02/01/2016	31	$5.445 \cdot 10^4$	$10.345 \cdot 10^8$
10	02/01/2016	03/01/2016	29	$3.119 \cdot 10^4$	$5.926 \cdot 10^8$
11	03/01/2016	03/16/2016	15	$4.009 \cdot 10^4$	$7.618 \cdot 10^8$
12	03/16/2016	04/01/2016	16	$8.328 \cdot 10^3$	$1.582 \cdot 10^8$
13	04/01/2016	04/16/2016	15	$6.950 \cdot 10^4$	$13.204 \cdot 10^8$
14	04/16/2016	05/01/016	15	$1.729 \cdot 10^4$	$3.285 \cdot 10^8$
15	05/01/2016	05/16/2016	15	$2.872 \cdot 10^4$	$5.457 \cdot 10^8$
16	05/16/2016	05/23/2016	7	$1.645 \cdot 10^4$	$3.125 \cdot 10^8$
17	05/23/2016	06/01/2016	9	$4.087 \cdot 10^4$	$7.765 \cdot 10^8$
18	06/01/2016	06/08/2016	7	$6.657 \cdot 10^4$	$12.648 \cdot 10^8$
19	06/08/016	06/16/2016	8	$7.222 \cdot 10^4$	$13.722 \cdot 10^8$
20	06/16/2016	06/23/2016	7	$1.661 \cdot 10^5$	$31.563 \cdot 10^8$
21	06/23/2016	07/01/2016	8	$3.740 \cdot 10^5$	$71.066 \cdot 10^8$
22	07/01/2016	07/16/2016	15	$3.922 \cdot 10^5$	$74.522 \cdot 10^8$
23	07/16/2016	08/01/2016	16	$5.476 \cdot 10^4$	$10.404 \cdot 10^8$
24	08/01/2016	08/10/2016	9	$3.029 \cdot 10^4$	$5.755 \cdot 10^8$

Statistical Analysis

For the analysis, both relative abundances of diatom species and absolute number of settled valves were calculated. Relative abundances in the composite sample were calculated after the counts were added together. The Principal Component Analysis (PCA) and its visualization were performed using R 3.5.2 and R Studio 1.1.463 software with several additional packages (*ggplot2* and *ggfortify).*

Results

Seasonal Changes in Mooring Samples

A total of 138 diatom species have been identified in the sediment trap samples (see Appendix B). The community of diatoms can be divided into several groups. The first group consists of species present in all 24 samples, the core community at this location consisting of 13 taxa: *Chaetoceros* hyaline resting spores, Dispinodiscus, Vallodiscus, Xanthioisthmus, *Bacterosira bathyomphala* resting spores, *Paralia sulcata, Thalassiosira antarctica, Thallassiosira nordenskioldii, Porosira glacialis, Fossula arctica, Fragilariopsis cylindrus, Fragilariopsis oceanica*, *Fragilariopsis reginae-jahniae.* Relative abundances of the core community species are stable from sample to sample with the exception of the massive marginal ice bloom of *F. arctica* (Table 3.2).

The second group is represented by species achieving dominance at one particular time during the year and almost disappearing in all other samples. These blooming species paint a pattern of seasonal succession. The summer open waters are dominated by *Nitzschia longissima*, which is replaced by *Proboscia* spp. in autumn. Species of *Proboscia* are present in sediment trap samples until the start of the polar night, at which point only continually present species appear in the samples. After the return of the sun and before the melt,

diversity increases dramatically and a number of sea ice diatoms reach high abundances: *Fragilariopsis cylindrus*, *Nitzschia frigida*, and *Synedropsis hyperborea*. During the fast retreat of sea ice the sediment traps were filled with *Fossula arctica.* It reached very high abundances and constituted almost 70% of the diatom community. The bloom of *F. arctica* at the marginal ice zone was the biggest bloom recorded this year in our samples (Fig. 3.1). In spring samples immediately following the start of spring ice melt, *Fragilariopsis oceanica*, accompanied by *Fragilariopsis reginae-jahniae*, *Pauliella taeniata*, and *Fragilariopsis cylindrus*, become the most abundant diatoms. *Chaetoceros* resting spores constituted the bulk of the community setting during the winter. Their relative abundance was stable for most of the year, with the exception of spring, when the relative abundance of two main *Chaetoceros* morphotaxa—hyaline resting spores and Vallodiscus—dropped during the sea ice melt and stayed low until the water was open (Fig. 3.2), coeval with this drop, the abundance of vegetative cells increased slightly.

Composite Mooring Sample

The counts from 24 sediment trap samples were added together in order to create a theoretical sediment sample and compare it with real surface sediment samples, since they represent a longer period of sedimentation. In the composite sample the pronounced bloom of *F. arctica* is less noticeable; its relative abundance reaching only 21.5% of the entire community accumulated throughout the year.

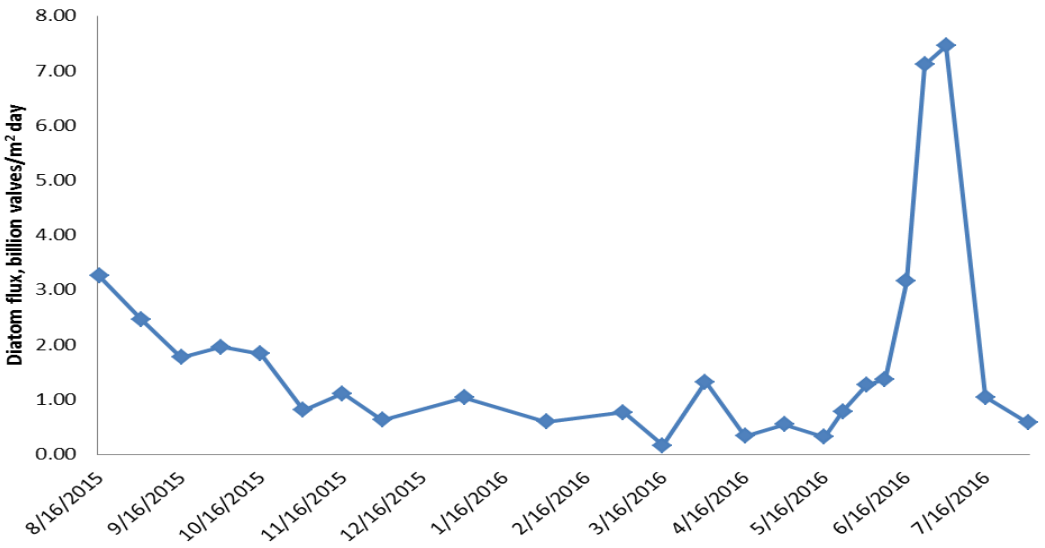

Figure 3.1. *Total abundance of diatoms in sediment trap samples.*

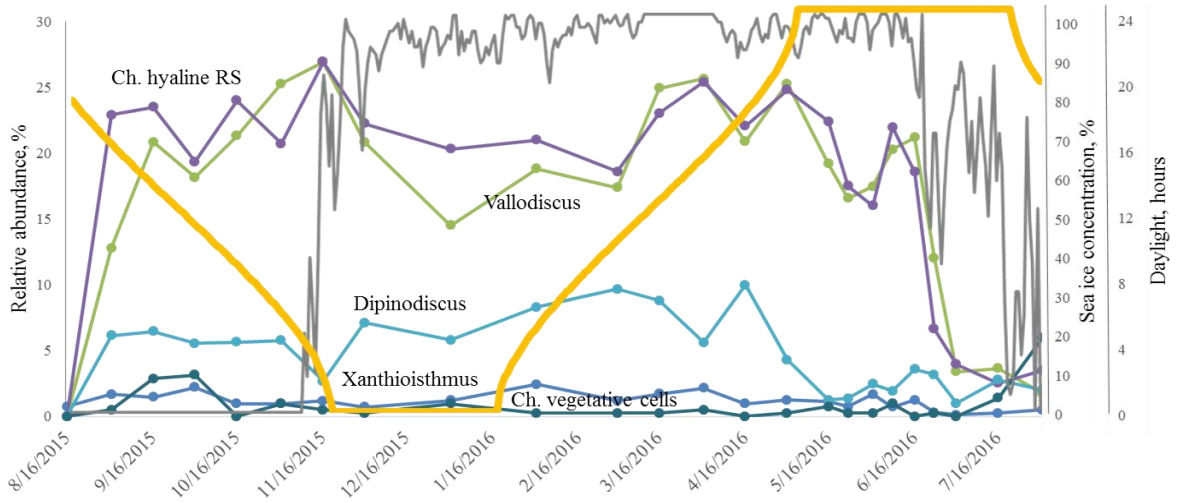

Figure 3.2. *Relative abundance of several morphotaxa of Chaetoceros.*

Surface Sediment Samples

The total number of species identified in two surface sediment samples is 54, with sample S-2 containing 44 species and sample DBO4.4N, 38. The diversity is not lower than in sediment trap samples, where the average number of species is 45.8 and the maximum number of species found in one sample is 56. The two sediment samples are dominated by

Chaetoceros Vallodiscus and hyaline *Chaetoceros* resting spores, with maximum relative abundances of 23.9% and 21.7%, respectively. *F. arctica* in the sediment samples has abundances of 5.3% and 8.2%. The only taxa reaching abundances above 10% are hyaline *Chaetoceros* RS, Dispinodiscus, *Fossula arctica*, and Vallodiscus. The highest relative abundance for any one taxon in the sediment samples is 23.9% (Vallodiscus in DBO4.4N), while in sediment trap samples *F. arctica* reaches 67.1%. However, the average maximum abundance in sediment trap samples is only 26.3%, including the sample dominated by *F. arctica*.

PCA

Principal Component Analysis (PCA) was performed to summarize the abundance data of the large number of identified species and to visualize the differences between the

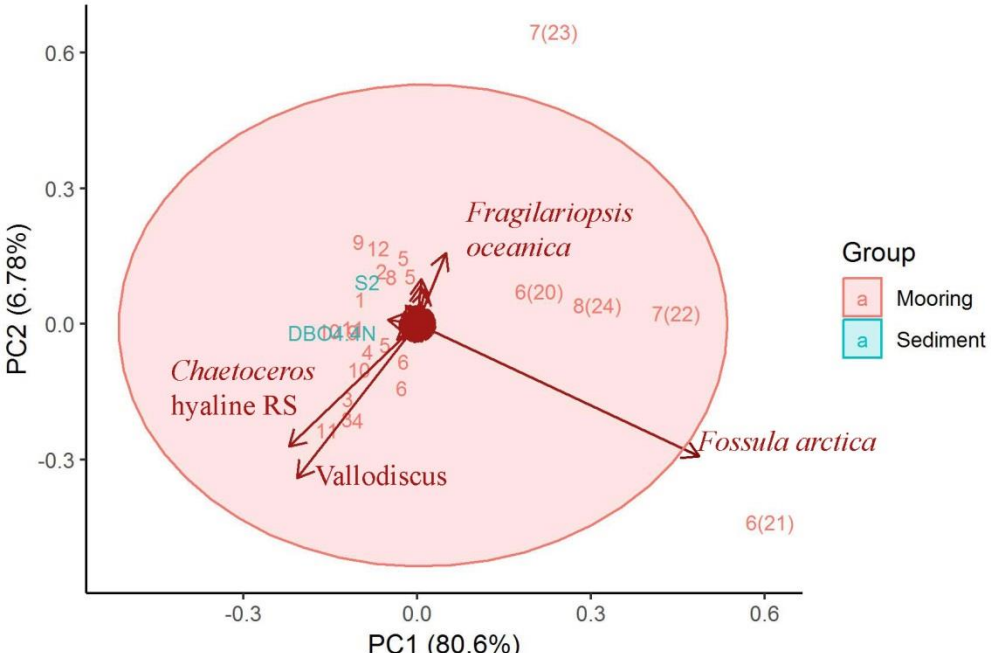

Figure 3.1. *Principal Component Analysis (PCA) plot showing the variation among 24 sediment trap samples (in red, numbers are months of collecting with the samples number in parentheses) and 2 sediment samples (in blue), overlaid by species loadings and 95% confidence ellipse.*

Table 3.2. *Changes in relative abundances(%) of the core community species in the sediment trap samples throughout the year. Samples M1–M24 are marked with the month of collection.*

Species	Relative abundance, %, in each of the 24 samples																							
	8	9		10		11		12	1	2	3		4		5			6				7		8
	M1	M2	M3	M4	M5	M6	M7	M8	M9	M10	M11	M12	M13	M14	M15	M16	M17	M18	M19	M20	M21	M22	M23	M24
Ch. hyaline RS	22.9	23.5	19.4	24.0	20.7	26.9	22.3	20.3	21.0	18.6	23.0	25.4	22.1	24.8	22.4	17.5	16.0	22.0	18.6	6.6	4.0	2.5	3.5	7.1
Dispinodiscus	6.2	6.5	5.6	5.6	5.8	2.7	7.1	5.8	8.3	9.7	8.8	5.6	10.0	4.3	1.2	1.4	2.5	1.9	3.6	3.2	1.0	2.8	2.0	4.4
Vallodiscus	12.8	20.9	18.2	21.3	25.3	26.9	20.9	14.5	18.8	17.4	24.9	25.7	20.9	25.3	19.2	16.6	17.5	20.3	21.2	12.0	3.4	3.7	1.7	7.5
Xanthioisthmus	0.7	1.7	1.5	2.2	1.0	1.0	1.2	0.7	1.2	2.4	1.2	1.7	2.1	1.0	1.2	1.2	0.7	1.7	0.7	1.2	0.3	0.1	0.2	0.5
B. bathyomphala RS	1.0	1.2	1.0	3.2	3.6	1.2	1.7	3.9	3.2	1.4	2.1	2.7	2.4	1.7	1.7	1.4	3.0	2.2	2.6	1.2	0.6	0.6	1.7	1.0
P. sulcata	3.2	3.6	3.6	3.9	4.1	4.1	4.0	4.4	4.6	2.9	5.2	3.7	3.3	2.9	3.7	3.2	2.5	4.6	3.6	2.9	0.9	0.6	0.5	1.2
Th. antarctica	4.2	0.7	2.9	3.7	1.2	2.2	1.9	4.6	4.2	5.8	2.1	2.0	2.6	3.6	1.7	2.5	2.0	3.6	2.6	1.2	1.2	2.3	2.0	0.5
Th. nordenskioldii	0.7	1.7	1.0	2.7	1.9	1.0	1.2	1.5	0.5	2.4	2.1	2.0	2.9	2.4	1.7	0.2	2.7	0.7	0.7	1.5	1.0	2.3	2.7	0.7
P. glacialis	1.2	1.0	1.2	0.7	1.4	0.5	0.7	0.7	1.0	0.7	1.0	0.7	0.7	0.5	0.5	0.5	0.7	1.0	1.7	0.2	0.2	0.3	0.7	1.0
F. arctica	11.6	8.2	6.3	9.8	4.6	7.0	7.6	8.7	7.8	9.9	9.0	9.5	10.5	11.0	11.8	11.3	12.8	15.5	14.5	29.5	67.1	48.9	25.2	38.4
F. cylindrus	3.4	2.6	3.4	2.7	3.1	2.2	5.2	2.9	0.2	3.4	3.3	2.9	2.6	5.3	3.9	6.5	6.9	5.1	1.9	3.2	3.0	2.5	4.2	1.9
F. oceanica	2.0	1.2	2.4	1.0	1.7	2.9	2.4	2.4	1.0	2.2	0.7	2.9	1.9	2.9	2.2	4.6	3.0	2.7	2.1	2.0	2.9	7.8	12.2	6.8
F. reginae-jahniae	1.7	1.4	1.5	0.2	1.2	1.9	2.1	2.2	3.7	3.4	1.2	0.7	1.0	1.9	1.7	0.2	0.5	0.2	1.4	1.5	0.4	2.4	5.2	2.9

samples. The analysis was performed using the covariance matrix to eliminate effects of rare species occasionally found in samples. Sediment trap and surface sediment samples plotted together revealed no clustering of those two types of samples (Fig. 3.3). The two surface sediment samples are very similar to most of the mooring samples. The differences in community composition are mostly driven by relative abundances of four taxa: *Fossula arctica*, *Fragilariopsis oceanica*, *Chaetoceros* hyaline RS, and Vallodiscus. Sediment trap samples collected at the end of summer, during and right after the ice melt are the most unique, dominated by *Fossula arctica*, later replaced by *Fragilariopsis oceanica*.

Discussion

Sediment traps are often used to study sedimentation processes. Diatom communities in traps, however, are necessarily different from both phytoplankton at the surface and taphonomic records in the sediments. The advantage of the traps lies in the fact that content of a sediment trap is representative of the sinking particles (Coppola et al., 2002), which gives us a diatom community after it was changed at the surface and before it was changed at the bottom, which allows for easy comparisons. Sediments could, however, be heavily changed by strong currents. Average ocean current speeds near the trap during the deployment were 11 cm/s. Although episodes of higher velocities occurred regularly, the average value is below the threshold of 12-15 cm/s above which currents have significant hydrodynamic effects on trap collections (Baker et al., 1988; Gardner, 1989).

The assumption that the sediment trap samples correspond with phytoplankton events in surface waters is supported by changes in diatom communities' composition from sample to sample. Particularly, the appearance of open water species, such as *Thalassiosira hyperborean*, *Stauronella arctica* and *Nitzschia longissima*, coincides with the period of open

water. On the other hand, some species continue to settle throughout the year without significant changes in the amount of settling valves: *Chaetoceros* hyaline RS, Vallodiscus, and *Paralia sulcata* are the more noticeable of those taxa. It must be noted that confirmed producers of IP_{25} (such as *Pleurosigma*, *Navicula*, and *Haslea*) are present in samples in low abundances from December (100% ice cover, no light) to August (open water, constant light), but were not detected during the formation of sea ice in the autumn and do not show any increase in abundance after the spring melt, when they are thought to be released from ice and deposited in sediments (Limoges et al., 2018). The fact that abundance of IP_{25} producers does not seem to depend on sea ice concentration directly may suggest that IP_{25} is a more complex indicator and cannot be used to reconstruct sea ice concentration without careful interpretation.

The sediment samples do not have lower diversity. We saw no evidence of preferential dissolution of sea ice diatoms at the sediment-water interface, suggested in previous research (Tsoy and Wong, 1999). The differences in species composition can be explained by the composite nature of sediment samples. Species that are rare in phytoplankton and do not develop in noticeable numbers every year, become even more rare in sediments, quickly falling below the detection level, which is at least one valve out of every 400, or .25%. That number translates into a species that has an abundance of at least 1% (from the total diatom biomass throughout a year, not just during a bloom) in phytoplankton at least once every 4 years. Anything rarer than that cannot be reliably counted in sediment samples.

The marginal ice bloom is represented by *Fossula arctica* in the sediment trap samples, but the species does not display the same level of dominance in sediment samples

below. Either the marginal ice bloom is not the ‘saving account’ for sediments (Grebmeier and Barry 2007), or the almost mono-specific bloom at this location this year was exceptional. If different species bloom each year, then sediments would not be dominated by only one species, since each sediment sample is an aggregate of several years. It was shown for Arctic lakes (Maier et al., 2018) that in different years different diatoms bloom, depending on conditions and, most importantly, the timing of environmental events, so sediments traps indicate a large year-to-year variability of diatom succession and abundance patterns.

Conclusions

Sediment trap samples resemble sediments and do not significantly differ from them on a PCA plot. The total diversity and community structure are also very similar in those two sets of samples, demonstrating that diatom community composition is not dramatically altered during sedimentation at the interface between water and sea bottom. Surprisingly, diatom valves continue to settle all year long, even during winter, when nothing can possibly bloom under sea ice due to total darkness. The species settling during the winter at the mooring site belong to the “core community”, a group of 13 species whose relative abundances change very little throughout the year. Those are either resting spores or robust valves of species forming resting spores morphologically indistinguishable from vegetative cells. Most species, however, demonstrate seasonal changes in their abundances. For example, open water species like *Nitzschia longissima* can be found in sediment traps in September, during the open water season and minimum ice extent; low light tolerant species of *Proboscia* appear in traps in late autumn; and relative abundance of a number of marginal sea ice diatoms (*Fragilariospsis cylindrus, F. oceanica, F. reginae-jahniae, Nitzschia frigida,*

Pauliella taeniata, Synedropsis hyperborea) increase at the onset of spring, in May, when light availability increases. Diversity in sediment trap samples increases immediately after the first light appears in spring.

This study is based on sediment trap samples representing one full year of sedimentation in the Chukchi Sea. To fully understand sedimentation processes in the Arctic, data from more year-long or multi-year sediment traps should be analyzed. During 2015–2016 the most prominent bloom at the site was a marginal ice bloom of *Fossula arctica*. Surface sediment samples, on the other hand, represent several years of sedimentation. Thus, diatom communities in sediments are smoothed and a large bloom of a single species may not be visible if it doesn't happen every year. This decreases the resolution, but also decreases random fluctuations not relevant to sea ice reconstructions.

References

Abram, N.J., Wolff, E.W., Curran, M.A.J., 2013. A review of sea ice proxy information from polar ice cores. Quat. Sci. Rev. 79, 168–183. doi:10.1016/j.quascirev.2013.01.011

Baker, E.T., Milburn, H.B., Tennant, D.A., 1988. Field assessment of sediment trap efficiency under varying flow conditions. J. Mar. Res. 46, 573–592.

Closset, I., Cardinal, D., Bray, S.G., Thil, F., Djouraev, I., Rigual-hernández, A.S., Trull, T.W., 2015. Seasonal variations, origin, and fate of settling diatoms in the Southern Ocean tracked by silicon isotope records in deep sediment traps. Global Biogeochem. Cycles 1495–1510. doi:10.1002/2015GB005180

Coppola, L., Roy-Barman, M., Wassmann, P., Mulsow, S., Jeandel, C., 2002. Calibration of sediment traps and particulate organic carbon export using 234Th in the Barents Sea. Mar. Chem. 80, 11–26. doi:10.1016/S0304-4203(02)00071-3

Cronin, T.M., Gemery, L., Briggs, W.M., Jakobsson, M., Polyak, L., Brouwers, E., 2010. Quaternary Sea-ice history in the Arctic Ocean based on a new Ostracode sea-ice proxy. Quat. Sci. Rev. 29, 3415–3429. doi:10.1016/j.quascirev.2010.05.024

De Vernal, A., Gersonde, R., Goosse, H., Seidenkrantz, M.-S., Wolff, E.W., 2013. Sea ice in the paleoclimate system: The challenge of reconstructing sea ice from proxies - an introduction. Quat. Sci. Rev. 79, 1–8. doi:10.1016/j.quascirev.2013.08.009

Fuchs, A., Selmeczy, G.B., Kasprzak, P., Padisák, J., Casper, P., 2016. Coincidence of sedimentation peaks with diatom blooms, wind, and calcite precipitation measured in high resolution by a multi-trap. Hydrobiologia 763, 329–344. doi:10.1007/s10750-015-2388-9

Gardner, W.D., 1989. Baltimore Canyon as a modern conduit of sediment to the deep sea. Deep Sea Res. Part A. Oceanogr. Res. Pap. 36, 323–358. doi:10.1016/0198-0149(89)90041-1

Lalande, C., Lepore, K., Cooper, L.W., Grebmeier, J.M., Moran, S.B., 2007. Export fluxes of particulate organic carbon in the Chukchi Sea: A comparative study using 234Th/238U disequilibria and drifting sediment traps. Mar. Chem. 103, 185–196. doi:10.1016/j.marchem.2006.07.004

Lepore, K., Moran, S.B., Grebmeier, J.M., Cooper, L.W., Lalande, C., Maslowski, W., Hill, V., Bates, N.R., Hansell, D.A., Mathis, J.T., Kelly, R.P., 2007. Seasonal and interannual changes in particulate organic carbon export and deposition in the Chukchi Sea. J. Geophys. Res. 112, 1–14. doi:10.1029/2006JC003555

Limoges, A., Ribeiro, S., Weckström, K., Heikkilä, M., Zamelczyk, K., Andersen, T.J., Tallberg, P., Massé, G., Rysgaard, S., Nørgaard-Pedersen, N., Seidenkrantz, M.S., 2018. Linking the Modern Distribution of Biogenic Proxies in High Arctic Greenland Shelf Sediments to Sea Ice, Primary Production, and Arctic-Atlantic Inflow. J. Geophys. Res. Biogeosciences 760–786. doi:10.1002/2017JG003840

Lomas, M.W., Moran, S.B., Casey, J.R., Bell, D.W., Tiahlo, M., Whitefield, J., Kelly, R.P., Mathis, J.T., Cokelet, E.D., 2012. Spatial and seasonal variability of primary production on the Eastern Bering Sea shelf. Deep. Res. Part II Top. Stud. Oceanogr. 65–70, 126–140. doi:10.1016/j.dsr2.2012.02.010

Maier, D.B., Galman, V., Renberg, I., Bigler, C., 2018. Using a decadal diatom sediment trap record to unravel seasonal processes important for the formation of the sedimentary diatom signal. J. Paleolimnol. 60, 133–152. doi:10.1007/s10933-018-0020-5

Medlin, L.K., Priddle, J., 1990. Polar marine diatoms. British Antarctic Survey, Cambridge.

Nöthig, E.-M., Bauerfeind, E., Lalande, C., Shevshenko, V., Zernova, V., 2015. Vertical diatom flux observed in sediment traps in the Arctic Ocean with special emphasis on Melosira arctica, in: 9th Central European Diatom Meeting, Bremerhaven, Germany, 10 March 2015 - 13 March 2015. doi:10013/epic.45264

Passow, U., 1991. Species-specific sedimentation and sinking velocities of diatoms. Mar. Biol. 108, 449–455. doi:https://doi.org/10.1007/BF01313655

Pickart, R.S., Grebmeier, J.M., 2017. Distributed Biological Observatory – Northern Chukchi Integrated Study Healy 1702 Cruise Report.

Rigual-Hernández, A.S., Trull, T.W., Bray, S.G., Armand, L.K., 2016. The fate of diatom valves in the Subantarctic and Polar Frontal Zones of the Southern Ocean: Sediment trap versus surface sediment assemblages. Palaeogeogr. Palaeoclimatol. Palaeoecol. 457, 129–143. doi:10.1016/j.palaeo.2016.06.004

Rigual-Hernández, A.S., Trull, T.W., Bray, S.G., Cortina, A., Armand, L.K., 2015. Latitudinal and temporal distributions of diatom populations in the pelagic waters of the Subantarctic and Polar Frontal zones of the Southern Ocean and their role in the biological pump. Biogeosciences 12, 5309–5337. doi:10.5194/bg-12-5309-2015

Round, F.E., Crawford, R.M., Mann, D.G., 1990. The Diatoms: Biology & morphology of the genera. Cambridge University Press, Cambridge.

Schrader, H.-J., Gersonde, R., 1978. Diatoms and silicoflagellates. In: A. Zachariasse, et al. (Eds), Micropaleontological counting methods and techniques — An exercise on an eight meters section of the Lower Pliocene of Capo Rossello, Sicily. Utr. Micropaleontol. Bull. 17, 129–176.

Serreze, M.C., Barry, R.G., 2011. Processes and impacts of Arctic amplification: A research synthesis. Glob. Planet. Change 77, 85–96. doi:10.1016/j.gloplacha.2011.03.004

Stroeve, J., Holland, M.M., Meier, W., Scambos, T., Serreze, M., 2007. Arctic sea ice decline: Faster than forecast. Geophys. Res. Lett. 34, 1–5. doi:10.1029/2007GL029703

Suto, I., 2006. Taxonomy of the fossil marine diatom resting spore norpho-genera Xanthioisthmus Suto gen. nov. and Quadrocistella Suto gen. nov. in the North Pacific and Norwegian Sea. J. Micropalaeontology 25, 3–22. doi:10.1144/jm.25.1.3

Suto, I., 2005. Vallodiscus gen. nov., a new fossil resting spore morpho-genus related to the marine diatom genus Chaetoceros (Bacillariophyceae). Phycol. Res. 53, 11–29. doi:10.1111/j.1440-183.2005.00369.x

Suto, I., 2004a. Fossil marine diatom resting spore morpho-genus Gemellodiscus gen. nov. in the North Pacific and Norwegian Sea. Paleontol. Res. 8, 255–282. doi:10.2517/prpsj.8.255

Suto, I., 2004b. Dispinodiscus gen. nov., a new diatom resting spore genus from the North Pacific and Norwegian Sea. Diatom 20, 79–94. doi:10.11464/diatom1985.20.0_79

Suto, I., 2004c. Coronodiscus gen. nov., a new diatom resting spore genus from the North Pacific and Norwegian Sea. Diatom 20, 95–104. doi:10.11464/diatom1985.20.0_95

Tsoy, I.B., Wong, C.S., 1999. Diatom fluxes and preservation in the deep Northwest Pacific Ocean., in: Idei, M., Koizumi, I. (Eds.), 14th Diatom Symposium. Koeltz Scientific Books, Koenigstein, pp. 521–549.

Wilks, J. V., Rigual-Hernández, A.S., Trull, T.W., Bray, S.G., Flores, J.-A., Armand, L.K., 2017. Biogeochemical flux and phytoplankton succession: A year-long sediment trap record in the Australian sector of the Subantarctic Zone. Deep. Res. Part I 121, 143–159. doi:10.1016/j.dsr.2017.01.001

Witkowski, A., Lange-Bertalot, H., Metzeltin, D., 2000. Diatom flora of marine coasts I. Iconographia Diatomologica 7. ARG Gantner Verlag KG, Ruggell.

Yongqi, G., Jianqi, S., Fei, L., Shengping, H., Sandven, S., Qing, Y. an, Zhongshi, Z., Lohmann, K., Keenlyside, N., Furevik, T., Lingling, S., 2015. Arctic Sea Ice and Eurasian Climate : A Review. Adv. Atmospheic Sci. 32, 92–114. doi:10.1007/s00376-014-0009-6.1.

CHAPTER 4. A DIATOM-BASED QUANTITATIVE SEA ICE PROXY FOR THE BERING AND CHUKCHI SEAS

In preparation for publication

Abstract

Sea ice is an important component of Earth's climate system, affecting it on both regional and global scales. Its incorporation into climate models is a necessary step to achieve more accurate predictions of the future climate. However, instrumental records of sea ice concentration do not extend far into the past. In an effort to extend this record, we constructed a proxy using the Generalized Additive Model based on relative abundances of five diatom species found in sediment samples across the Bering and Chukchi seas. This study contributes to the cause of paleo sea ice reconstruction and presents the first quantitative diatom-based sea ice proxy developed for Beringia. The developed proxy has been applied to two sediment cores in the Bering Sea, ages ranging from 0 to 23.4 ka and 369 to 430 ka. The obtained reconstruction of sea ice concentration is in agreement with qualitative records. The proxy is publicly available as an R Shiny app and can be applied to any diatom counts from marine sediments of the region.

Introduction

Sea ice in the Polar Regions supports unique and productive ecosystems (Selz et al., 2018), but the current dramatic decline in Arctic sea ice extent (Serreze et al., 2007; Yongqi et al., 2015), which surpasses predicted changes (Stroeve et al., 2007), prompts questions about a previous sea ice decline and the response of ice related ecosystems. Decline in sea ice is predicted to affect the ecosystem, but there is ambiguity in the predictions. Previous estimates of the post-sea ice era's primary productivity ranged from a drastic decrease (Hare

et al., 2007) to no change at all (Sigler et al., 2010) to an increase in productivity (Brown and Arrigo, 2013). Ongoing observations, however, demonstrated a 22% drop in annual ice algal net primary production for the central Chukchi Sea between 1980 and 2015 (Selz et al., 2018). According to Grebmeier and Barry (1991), the sea ice bloom is the largest bloom of the year, which would mean a drop in productivity associated with the decrease of ice algal productivity. It is therefore paramount to understand the polar ecosystems, especially the North Pacific region because it supports half of the US fishery industry (NOAA Fisheries of the United States 2017 report). Reconstructions of past sea ice conditions and associated ecosystems are necessary for predicting future productivity in the changing world. However, since satellite data only extends back to 1978, the study of sea ice before this time requires a proxy.

A number of proxies have been developed to reconstruct environmental conditions of the past, including sea ice in the Polar Regions. These proxies are primarily based on one or several archives that can be biological, such as diatoms (Ferry et al., 2015; Justwan and Koç, 2008; Sha et al., 2014), dinoflagellate cysts (De Vernal et al., 2013c), ostracods (Cronin et al., 2010), or foraminifera (Jennings et al., 2002); biochemical, such as oxygen isotopes in foraminifera (Hillaire-Marcel and de Vernal, 2008), highly branched isoprenoids (such as IP_{25}) secreted by some diatom species in presence of ice (Belt et al., 2007; Collins et al., 2013; Müller et al., 2011), methanesulfonic acid (Curran et al., 2003), or a combination of proxies (Vare et al., 2009); or physical, such as sea salt in glaciers (Criscitiello et al., 2013) grain size (Darby, 2008), sediment provenance (Darby et al., 2011), or microfeatures of ice rafted quartz grains (St. John et al., 2015). There is no “ultimate” proxy; all of them have

advantages and limitations. A multy-proxy approach might be best, but in order to achieve this step, individual, complementary proxies must be carefully developed and validated.

Sea ice, floating on the surface of the ocean, leaves several lines of evidence in sediments. One of the strongest indications are drop stones and sand grains transported by ice. It is even possible, though difficult (Immonen, 2013), to distinguish between grains transported by sea ice and by icebergs. However, grains are deposited sporadically and there are many scenarios in which sea ice doesn't leave any sand grains behind, such as when ice forms far from the shore and doesn't accumulate sediments as fast ice forming in shallow water would. Biochemical proxies, on the other hand, are tied to their biological producers and therefore can be only interpreted in light of biological processes responsible. Geochemical biomarkers, such as IP_{25}, are considered ubiquitous and stable in marine sediments (Brown et al., 2014), but they depend on a few non-dominant diatom species that may not be present in all types of sea ice. There is also indication that biomarkers may not be as stable as necessary for a robust proxy reconstruction, degrading depending on physical conditions (Rontani et al., 2019).

A biological proxy based on organisms specifically associated with sea ice may be the most useful in reconstructing past sea ice conditions. This is especially true in the North Pacific, which is one of the most productive and diatom-dominated regions in the world (Sambrotto et al. 1986; McRoy 1987; Walsh et al. 1989). High diatom abundances make their silica valves an ideal material for environmental reconstructions in the region. For these reasons, we chose diatom assemblages as the basis for the quantitative proxy described here. Together, the Bering and Chukchi seas have a range of sea ice concentrations (NSIDC) from almost 100% coverage in spring to permanent open water. The geographical range of our

proxy makes it applicable in as many situations as possible for a regional proxy. We apply this first quantitative, diatom-based sea ice proxy to two cores in the Bering Sea and document sea ice decline since the Last Glacial Maximum at the Umnak Plateau, and fluctuating, seasonal sea ice present throughout Marine Isotope Stage 11 farther north in the Bering Sea.

Material and Methods

Surface Sediment Samples

Sediment samples were collected on board the US Coast Guard Cutter Healy icebreaker in 2006 and 2007 (HLY0601 and HLY0702), as well as on board the Norseman II in 2008 (Shell08), and were bagged and refrigerated until analysis. Most surface samples were taken from HAPS cores. A HAPS corer is a specially designed gravity multicorer that preserves the sediment-water interface. In the case of sandy sediments, however, it wasn't possible to retrieve HAPS cores, so the top 1 cm was scooped out of Van Veen grabs that were not overloaded with sediment. Research has shown that there is no discernable difference between Bering Sea shelf sediments collected via the two methods (Pirtle-Levy et al., 2009). Samples were classified according to their grain-size. Although, relatively fine grained, poorly sorted samples, where the sediments were not reworked or redeposited, were prioritized for analysis, some relatively sandy samples were used when necessary. Since the goal of the study was to develop a sea ice proxy, care was taken to include in the analysis at least one sample for every 5% change in sea ice concentration along the gradient from open water to permanent cover. In some cases, this required us to include less desirable, slightly more sorted samples. Additional archived diatom smear slides made from sediments collected in 1969 (Sancetta, 1981) have been included in the analysis to represent areas in the

study region not currently affected by sea ice (there is no information on grain size distribution in these samples). A total of 104 surface sediment samples have been analyzed (Fig. 4.1).

Diatom Slides

Quantitative diatom slides were prepared according to the method described in Scherer (1994). Cover slips were mounted on cleaned microscope slides using Hyrax® or Naphrax® in toluene (refractive index is 1.71 and 1.73, respectively). At least 400 diatom valves in at least 3 random transects across the slide were identified using a Nikon ECLIPSE Ni transmitted light microscope at a magnification of 1000x equipped with differential interference contrast and a Nikon DS-Fi2 camera. The transects were measured using a stage micrometer. Partial valves were counted according to the methods of Schrader and Gersonde (1978). All diatoms were identified to the species level when possible following published taxonomic descriptions and images (Medlin and Priddle 1990; Witkowski et al. 2000). For resting spores of *Chaetoceros* the classification made by Suto (2004, 2006) has been used. A total of 473 species have been identified. Diatom counts were transformed into relative percent abundances.

Sea Ice

The diatom assemblages were compared to satellite-derived sea ice data. Sea ice concentrations have been derived using brightness temperatures from the Special Sensor Microwave/Imager (SSM/I) passive microwave satellite data (Cavalieri et al., 1996). Since on the Bering Sea shelf the upper 1 cm of sediments is estimated to represent 10 years of neritic sedimentation from phytoplankton communities developing above that spot (Caissie, 2012), the monthly sea ice concentrations for the spring growing season (March, April, May,

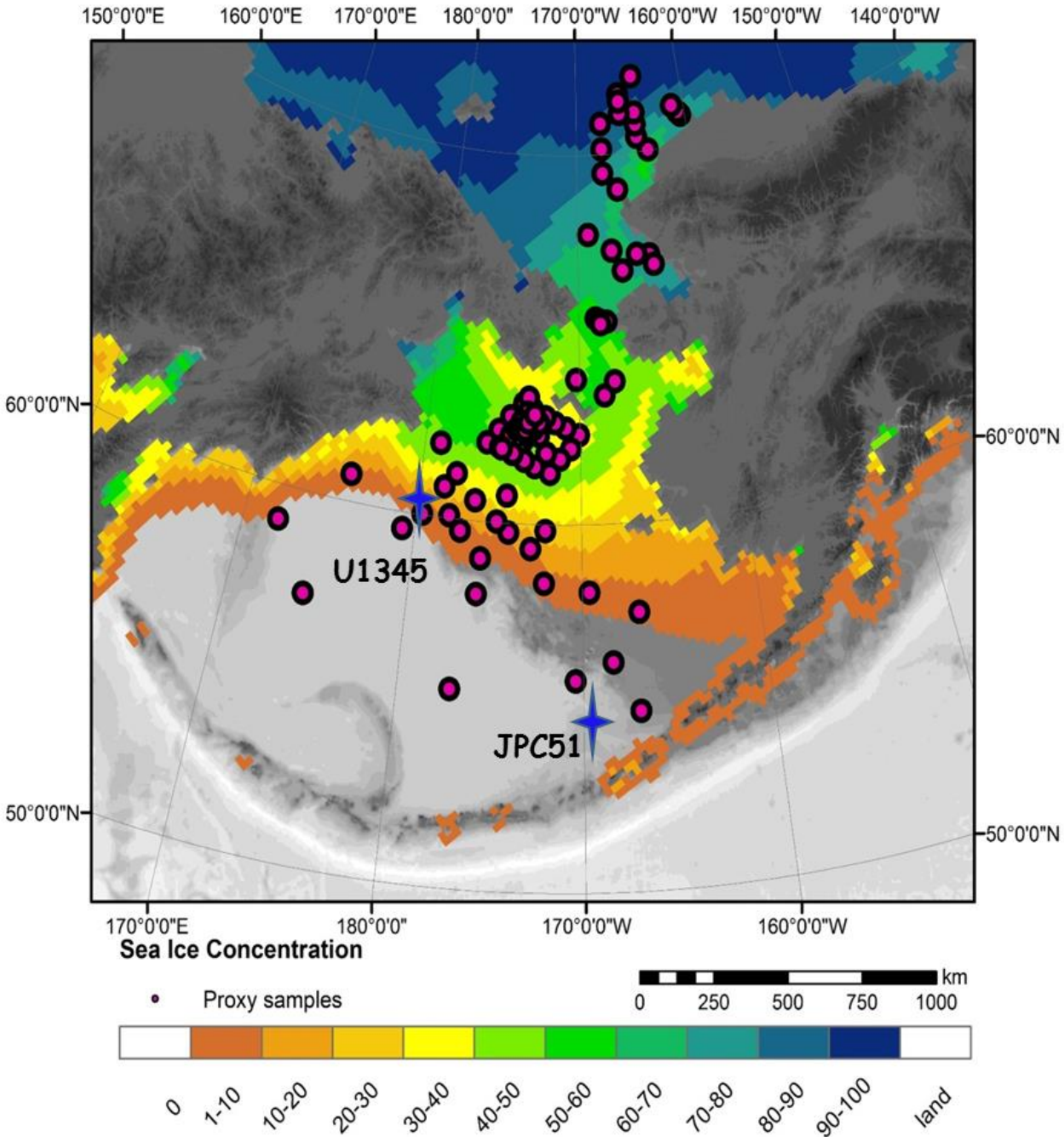

Figure 4.1. *Map of the study area. The dots show the location of surface sediment samples; the stars show the location of two sediment cores. The colors represent current sea ice concentration during the spring season (March, April, May, June).*

June) were averaged over 10 years.

Statistical Analysis

Statistical analysis and data visualization were performed using R 3.5.2 and R Studio 1.1.463 software with several additional packages (*dplyr, extrafont, GAM, ggplot2, glm, RandomForests, Shiny*, *stringdist,* and *tidyr*). The resulting quantitative proxy was obtained by fitting the Generalized Additive Model subsequently called the GAM, (Hastle and Tibshirani 1990; Wood 2006) to the data. GAM is a semi-parametric regression technique, which instead of imposing a function on data, is data driven, allowing a smooth spline to explore the relationship between a covariate and a response. The GAM is less restrictive in assumptions about data distribution and functional relationships than parametric methods; covariates are assumed to affect the response as an additive sum of smooth functions. We chose this method over other traditionally used in diatom-based reconstructions (such as the modern analog technique, the Imbrie and Kipp transfer function, or weighted averaging partial least squares) based on three reasons: 1) its data driven nature; 2) its use of only a few species that can be chosen based on their ecological preferences, which minimizes responses to other environmental factors in the model; and 3) it was shown to perform better than other models on a similar data set of Antarctic sea ice diatoms (Ferry 2015).

The species for the GAM model were chosen based on the output of the Random Forests (RF) model fitted to all species in all available sediment samples (Genuer et al., 2010). In situations with a large number of variables (species in this case) in a smaller number of samples, Random Forests is an increasingly popular approach for variable selection. The method has several advantages, which include its non-parametric nature and ability to handle interactions between variables, to work with high dimensional data, to

robustly identify informative variables, and to produce variable importance measures that are sensitive to correlations. The RF method also has good prediction strength, but since its process of model development is not transparent, this feature was not used in our study (Hapfelmeier and Ulm, 2013). After fitting the RF, the 10 species with the highest relative contribution among variables were selected as the potential basis of the proxy. Five species were eliminated based on ecological data and the GAM model was fitted to the remaining 5 species.

Since the prediction of the GAM is not restricted by anything other than data, sometimes the model predicts negative or exceeding 100% concentrations of sea ice. In all cases when we applied the model the deviations from a meaningful range of concentrations were small (less than 10%), but since those numbers do not make physical sense, we implemented a trimming function on the results. In previous studies the same problem was solved by implementing a logit function (Ferry 2015, 2017), which forces the results into the interval between 0 and 100% sea ice concentration, but introduces new problems. The logit function is not defined at 0 and 100, requiring an arbitrary number to substitute for them, and it also scales the values differently, stretching out the ends of the interval. Instead, we decided that if the model predicts a value slightly less than 0% (more than 100%), it effectively predicts that there was no ice (permanent ice). Thus, those values can be 'trimmed' and substituted with 0% (100%).

Coring Sites

The proxy was applied to two sediment cores collected in the Bering Sea – 51JPC and U1345 (Fig. 4.1). Core 51JPC (54.55° N, 168.67° W; at the water depth of 1467 m) spans 1986 cm and was collected on the USCGC Healy ice breaker in 2002 (Caissie et al., 2010). The samples were taken every 5 cm from 0 to 570 cm, which corresponds with a range from

recent sediments to 23.4 ka (Pelto et al., 2018). Diatom species on the slides were counted in the same way as the surface sediment samples, but only 10 species that were candidates for the proxy were identified, while all other valves were counted as "other" to the total of at least 400 valves. Core U1345 (60.15° N, 179.47° W; at the water depth of ~1008 m) was collected by the Integrated Ocean Drilling Program's Expedition 323 on the JOIDES Resolution in 2009, it provided the bottom age of 0.5 Ma at 150 m below sea floor (Cook et al., 2016). A total of 57 samples from 132.92 m CCSF (430 ka) to 112.97 m CCSF (369 ka) were analyzed. Diatom species from Marine Isotope Stage 11 were previously published (Caissie et al., 2016); however, one of the species used in the model was combined with another, similar species at the time of counting, so we substituted with the sum of abundance of the two species in the model (*Fragilariopsis oceanica* and *Fragilariopsis reginae-jahniae* instead of just *F. reginae-jahniae*), and applied a modified version of the proxy to this core.

Data Accessibility

As the vast majority of proxies constructed over the years, especially any diatom-based transfer functions, require their training set and the full statistical procedure in order to recreate and apply to a new set of data, most of them are unavailable for application. To make this proxy reproducible and applicable to new data sets, all the data, code, and instructions are archived and accessible. To achieve this, we have archived our full counts, counts of only 10 species used in the proxy, and the R code at the Arctic Data Center (doi pending). The proxy is also easily available as an R Shiny App at http://seaiceproxy.geol.iastate.edu, where any user can upload their counts and receive predictions of sea ice concentrations. However, we caution users that it is likely only appropriate to upload counts of diatoms from the Bering and Chukchi seas.

Results

Choosing the diatoms

The first step in creating a diatom-based proxy for sea ice concentration was to select the species to be included in the model. We used the variable selection feature of the Random Forests procedure to choose diatom species affected primarily by sea ice concentration in our samples. Out of 467 taxa identified in the sediment surface samples, the top 10 influenced by sea ice concentration are *Sinerima marigela* Nesterovich & Caissie 2018, hyaline *Chaetoceros* resting spores (Suto, pers. comm.), *Ehrenbergiulva granulosa* (Grunow) Witkowski, Lange-Bertalot & Metzeltin in Witkowski & Bertalot 2004, *Fossula arctica* Hasle, Syvertsen & von Quillfeldt 1996, *Fragilariopsis reginae-jahniae* Witkowski, Lange-Bertalot & Metzeltin 2000, *Fragilariopsis cylindrus* (Grunow ex Cleve) Helmcke & Krieger 1954, *Paralia sulcata* (Ehrenberg) Cleve 1873, *Shionodiscus trifultus* (Fryxell) Alverson, Kang & Theriot 2006, *Neodenticula seminae* (Simonsen & Kanaya) Akiba & Yanagisawa 1986, and *Rhizosolenia hebetata* Bailey 1856. Each of the species has a unique association with sea ice, with optimal conditions occurring at different concentrations of ice (Fig. 4.2). As such a large data set is bound to have some statistically significant associations by pure chance, and other variables, such as light availability or latitude, are highly correlated with sea ice concentration, we looked carefully into what is known about the ecological preferences of these 10 species. We only included species whose known preferences supported the possibility of their preferential responses to sea ice.

Diatom species

Sinerima marigela (Fig. C.1) is a rare fultoportulate diatom belonging to the family Thalassiosiraceae. It can be easily recognized by the differentiation between the central one-layered part and the marginal pseudoloculate zone and by the lack of portulae in the center of

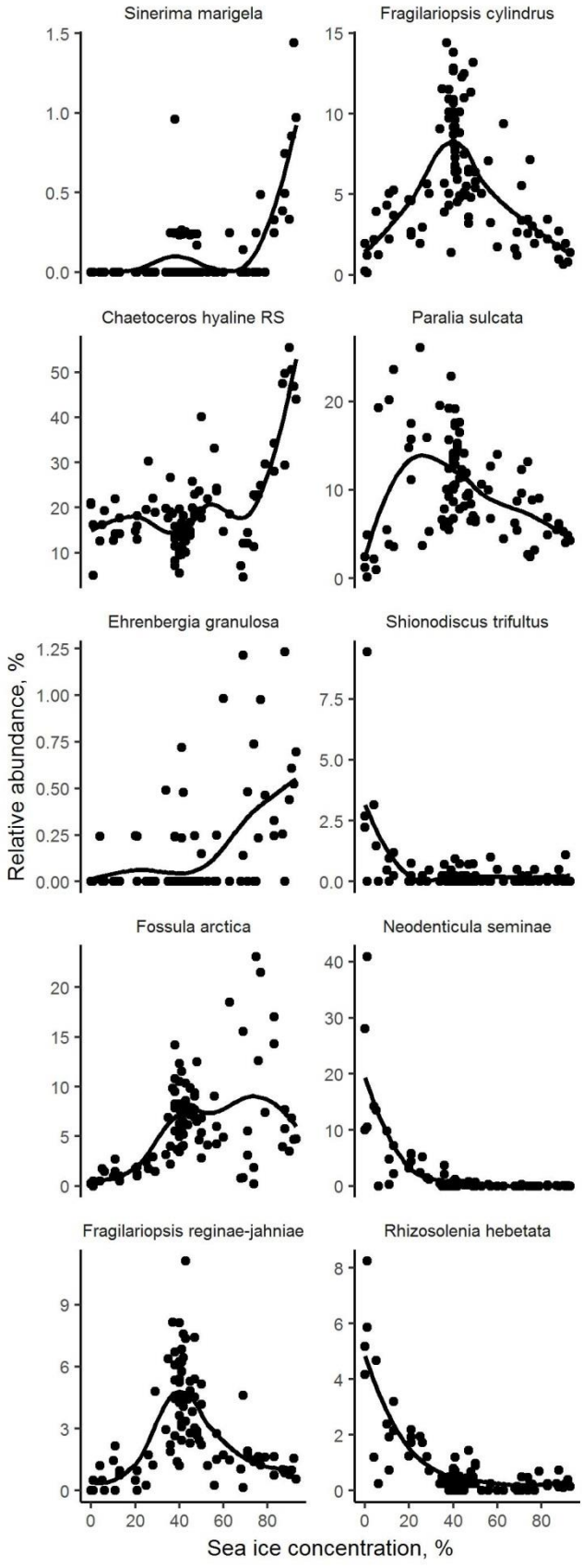

the valve. Similar taxa include species of *Porosira* Jørgensen 1905, *Lauderia* Cleve 1873, and *Bacterosira* Gran 1900, from which it differs by lacking either fultoportulae or an annulus in the center. The records so far indicate that it has a strong association with sea ice, preferring concentrations of about 90% (Nesterovich and Caissie 2018).

Chaetoceros hyaline resting spores (Fig. C.2) are resting spores most likely belonging to the genus *Chaetoceros* Ehrenberg 1844 (family Chaetoceroceae), and lacking any identifiable characteristics, such as spines, chaeta, or any other ornamentation. It is easily identified, as it looks like a small oval diatom without any features; it can also be very abundant, sometimes constituting more than 50% of a diatom taphonomic community. However,

Figure 4.2. *Relative abundance of the ten species influenced by sea ice plotted against sea ice concentration.*

it is likely that several species of *Chaetoceros*, as well as possibly representatives of other genera, produce those spores, so it cannot be identified to the species level. It is even possible that the majority of these sea ice-indicative hyaline spores belong to *Attheya* West 1860, a widespread spring genus in the Northern Hemisphere (Crawford et al., 1994; Edler, 1975), which was thought not to produce any spores (Crawford et al., 1994), but recent observations showed that it likely does (Tsukazaki, pers. comm.). Thus, despite its easy identification, the unknown taxonomy makes hyaline resting spores a less desirable candidate for the model.

Ehrenbergiulva granulosa (Fig. C.3) is a fultoportulate diatom from the family Thalassiosiracea described in 1880 from benthic communities of the Kara Sea. Round or slightly oval valves of this species have a narrow, delicately striped margin and a large central area covered with scattered fultoportulae. The information regarding distribution of the species is scarce, but it seems to be a cold-water diatom associated with high concentrations of sea ice and, possibly, shallow waters (Lange-Bertalot & Metzeltin 2000). Because of the limited knowledge on ecology of *E. granulosa* we consider it a poor choice for the proxy.

Fossula arctica (Fig. C.4) is a pennate araphid diatom from the family Fragilariaceae. It was described from Arctic waters influenced by sea ice (Hasle et al., 1996) and is often associated with the sea ice melt bloom (von Quillfeldt, 2000). It can be distinguished from species of *Fragilariopsis* Hustedt 1913 by the lack of a raphe and a presence of a sternum. It may be more difficult to distinguish from *Fragilaria*-like species, since the main identifying features—chloroplasts, cingulum structure, and rows of larger openings on cell apices—are not usually visible under a light microscope. The features that make the species identifiable under a light microscope are capitate ends (that can be absent in smaller cells) and uniseriate

striae (12-19 in 10 μm), which are narrower than the interstriae. Unlike any other diatom in the region, *F. arctica* has striae that seem sunken into the valve due to the grooves that areolae are located in. Nevertheless, due to the possible problems with identification and its ubiquitous distribution in the Arctic waters, we decided not to include *F. arctica* in the model.

Fragilariopsis reginae-jahniae (Fig. C.5) is a pennate diatom from the family Bacillariaceae. It can be distinguished from other canal-raphe bearing diatoms by bi-seriate striae between ribs on the valve face, corresponding in number with fibulae of the highly eccentric, keel-less raphe canal. It can be distinguished from other species of the genus *Fragilariopsis* by longer and thinner valves (length to width ratio is ~8.7 vs ~3.5) with parallel sides and attenuate ends. *F. reginae-jahniae* is a known sea ice species, described from clay in ice off East Greenland and, apparently, associated with seasonal ice (Lundholm and Hasle, 2010)

Fragilariopsis cylindrus (Fig. C.6) is a pennate diatom from the family Bacillariaceae commonly associated with cold waters rather than sea ice (Von Quillfeldt, 2004). It was described from Arctic waters near Greenland and prefers to live attached to sea ice, though can develop in the plankton. It is often reported in the spring bloom and Hasle (1965) characterized *F. cylindrus* as a bipolar cold-water species. It is easily distinguished from all other species in the region by a characteristic cylindrical shape. The only other diatom in the North Pacific with valve margins parallel throughout the valve is *Fragialriopsis nana* (Steemann Nielsen) Paasche 1961, which is smaller: 4.4–15.5 μm in length and 1.4–2.4 μm in width as opposed to 4.5–74 and 2.4–4 μm, respectively, for *F. cylindrus* (Lundholm and Hasle, 2008). It could also be confused with longer specimens of *F. cylindroformis* (Hasle

and Booth 1984), but this species has narrower valves and closer spaced fibulae (16–20 in 10 μm vs 13–18).

Paralia sulcata (Ehrenberg) Cleve 1873 (Fig. C.7) is a diatom commonly found in both plankton and benthos in a wide range of coastal environments. While the genus is easily recognized by its robust cells with radial markings, the identification of a species can be more challenging. The matter is further complicated by the heterovalvy of the diatom; cameo, intaglio, and separation valves all look very different (MacGillivary and Kaczmarska, 2013). Despite those difficulties, we feel that *P. sulcata* is distinct enough so it can be easily recognized after a short study. The only other diatom in the region that can be confused with *Paralia* Heiberg 1863 is *Ellerbeckia sol* (Ehrenberg) Crawford & Sims 2006, but its radial ridges extend all the way to the marginal area. Additionally, *P. sulcata* was shown to be a good indicator of environmental conditions, increasing in abundance in vertically mixed waters, while highly stratified waters after a spring ice melt have lower abundances (McQuoid and Nordberg, 2003).

Shionodiscus trifultus (Fig. C.8) is a fultoportulate diatom that belongs to the family Thalassiosiraceae, the genus being separated from *Thalassiosira* Cleve 1873 due to their unusual trifultate fultoportulae and the rimoportula located on the valve face. *Sh. trifultus* is distinguishable by 1 to 4 (up to 8) fultoportulae in the center in 1, sometimes 2 rows; a rimoportula on the valve face (though it can be difficult to see); and a wide ribbed margin, reminiscent of *T. nordenskioldii* Cleve 1873 and *T. antarctica* Comber 1896 resting spores. It was described as a cold-water species, associated with the dicothermal layer (Sancetta 1983). In our samples its distribution is associated with cold water not covered in ice. However, high morphological plasticity of *Sh. trifultus* and general difficulties in identification of

species in *Shionodiscus* Alverson, Kang & Theriot 2006 and *Thalassiosira* make *Sh. trifultus* not the best choice for the model.

Neodenticula seminae (Fig. C.9) is a canal raphe bearing diatom from the family Bacillariaceae. Its unique appearance—a costa with prominent ridges and foramina—allows for an easy identification (Shimada et al., 2003). There are no extant diatoms in the region that can be confused with *N. seminae*. Though the species is believed to be a cold water diatom, the morphological variability in the Bering Sea is significantly lower than in the North Pacific (Shimada et al. 2003), which probably indicates suboptimal conditions in the northern part of the species range (Eckert et al., 2008). The appearance of this species in the North Atlantic is considered to be the result of declining sea ice in the Arctic and changing ocean circulation (Miettinen et al., 2013; Reid et al., 2007). The aversion to sea ice and the easily recognizable appearance make *N. seminae* an ideal candidate for the proxy.

Rhizosolenia hebetata (Fig. C.10) is a cylindrically shaped representative of the family Rhizosoleniaceae with a single rimoportula without otaria at the top of each valve. Though it seems to be strongly associated with cold, but ice-free waters, a reliable identification presents a problem. The genus *Rhizolenia* Brightwell 1858 is very diverse, with a number of species "almost indistinguishable" from *Rh. hebetata*, complicated further by the heterovalvy of the species (Sundström, 1986). Those difficulties make *Rh. hebetata* a less optimal choice for including in the proxy than *N. seminae* with a similar distribution.

Based on the known ecological preferences and the ease of identification, the following five species are included in our final model for the Bering and Chukchi seas: *Sinerima marigela, Fragilariopsis reginae-jahniae, Fragilariopsis cylindrus, Paralia sulcata*, and *Neodenticula seminae*.

Generalized Additive Model

The GAM is based on the distribution of the five species in the surface sediment samples across the Bering and Chukchi seas. Our application used Gaussian (identity) link function and default tuning parameters. It was tested to check that it satisfied the assumptions underlying the model. The assumptions of normal distribution and independence of the GAM residuals appear to be satisfied (Figs. D.1–2). The residuals, however, have a strong spatial autocorrelation (Fig. D.3) that would not have been noticed if we had only run standard model checks. The residuals show that the model consistently overpredicts sea ice concentration in the Bering Sea and under-predicts in the Chukchi Sea. We tried to solve this distribution by including latitude and longitude as predictors to the model, but the spatial pattern persisted. We concluded that the two seas differ in more ways than sea ice concentration, and their ecosystems could be responding differently to similar ice conditions. A similar conclusion was previously reached regarding dinoflagellates and their distribution in the Bering Sea and Arctic Ocean (Radi et al. 2001). Since neither sea has a full range of sea ice concentrations to serve as a training data set for a proxy, we decided to keep the full training set from both seas in the model and accept the spatial autocorrelation.

Paleo sea ice reconstruction for core 51JPC

We applied the GAM to 51JPC and found that it predicted sea ice concentrations ranging from 0 to 88.3%. From 23.4 to 12.8 ka the average predicted sea ice concentration was 74.6%. At 12.5 ka the concentration declined to 47.3% and stayed relatively stable until 8.5 ka with the average of 44.6% The sample at 8.0 ka is the oldest samples with predicted sea ice concentration above 15%; the average sea ice concentration between 8.0 and 1.0 ka was 5.3% (Fig. 4.3).

Paleo sea ice reconstruction for core U1345

The section of the core we applied our model to falls almost entirely during Marine Isotope Stage 11 (MIS11). The application of the model on the fossil diatom record from the U1345 core produced fluctuations of spring sea ice concentrations around 50%, with an excursion towards unconsolidated ice and even ice-free conditions between 410 and 393 ka (Fig. 4.4). The estimates for the oldest samples at the bottom of the core (from 430.4 to 409.3 ka) indicated relatively high ice cover with an average of 60.2%. This period is followed by a drop in concentrations culminating in open water conditions at 403.9–401.9 ka, after which ice expands slowly back to the pre interglacial levels.

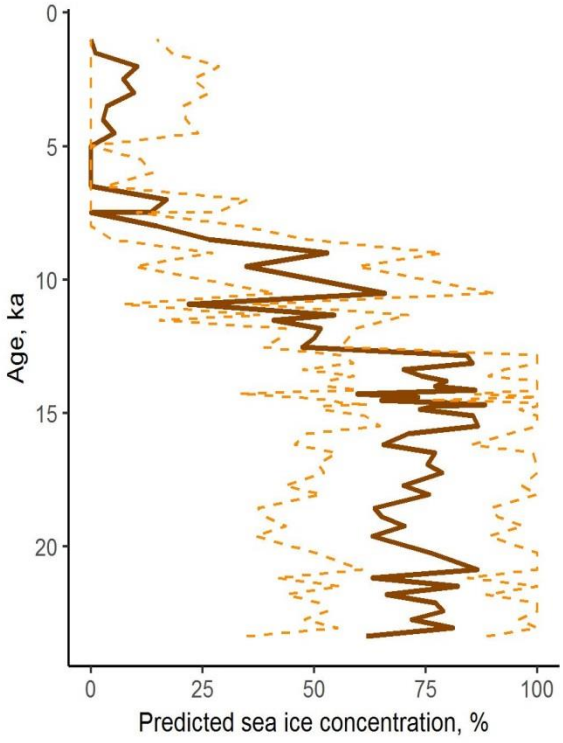

Figure 4.3. *Reconstruction of sea ice concentration for the core 51JPC.*

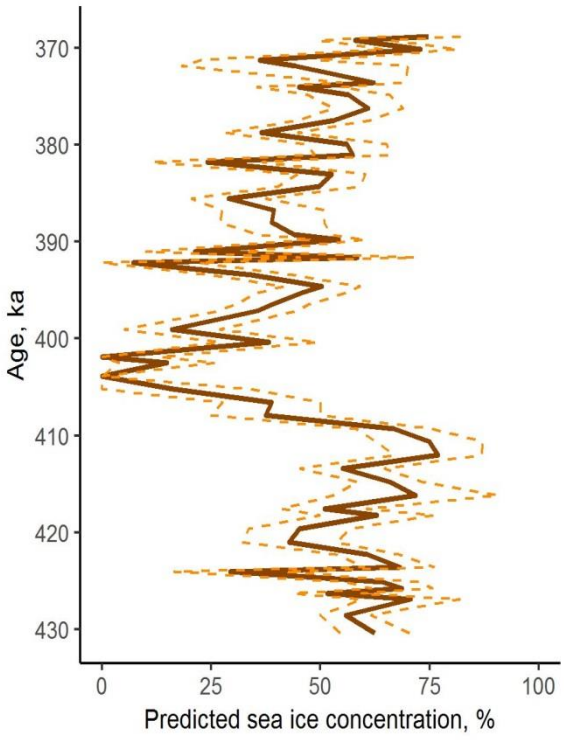

Figure 4.4. *Reconstruction of sea ice concentration for the core U1345.*

Discussion

Advantages and disadvantages of the model

Previous studies in the Polar Regions demonstrated that the Generalized Additive Model (GAM) is one of the best choices for proxy construction (Ferry et al., 2015). It has the advantage of using only several species instead of the whole assemblage, thus including only sea ice-associated species and minimizing the noise created by species responding to other environmental factors, which can be very difficult to disentangle (Anderson et al., 2006). Using only a few, five in our case, species makes the model more transparent and easy to interpret because we have control of selecting only species known for their association with sea ice. While the similar proxy for the Southern Ocean uses only ice-dependent species, we also included one that has a negative response to sea ice to better resolve ice free periods in the records. Thus, we achieve both a quantitative model, and a biologically meaningful interpretation of sea ice estimates because the model is based on our current knowledge of diatom ecology.

The limitations of the model include high spatial autocorrelation of the residuals. To incorporate the whole range of sea ice concentrations into the model we had to use samples from two different seas belonging to two different oceans. We tried to address this issue by including a spatial variable into the model, but neither the resulting predictions, nor the spatial pattern of residuals changed in the expanded model. As of now, we cannot address this issue, and it's possible that it cannot be solved, because unlike chemical or physical archives, biological proxies are limited by ranges and preferences of species used in them. This leads us to a second limitation of the model: It cannot be applied outside the region it was developed. The model is trained on species found in the North Pacific region. Although all five species in the model probably have a circumpolar distribution and have been recorded

in the North Atlantic, it is possible that inter-species interactions in different communities may affect their response to sea ice concentration.

Comparing paleo sea ice reconstructions with previously published records

Core 51JPC

51JPC was previously studied by Caissie et al. (2010). They performed diatom counts on the same slides (Fig. 4.5) and made a qualitative reconstruction of sea ice concentrations. Their prediction was based on different diatom species than the ones used in the proxy: *Thalassiosira antarctica* and abundant pennate taxa were considered indicators of high sea ice cover; those ice-related species were replaced by *Chaetoceros* resting spores (all morphotaxa) when seasonal sea ice was present. Later, *Neodenticula seminae*, an ice free species, dominated the assemblage and sea ice was considered absent. The age model for this core was improved since this first study (Pelto, 2017), so in comparing the results we present both sets of ages and depths rather than just calendar ages. According to Caissie et al. (2010), diatom assemblages in this core shift from permanent to seasonal sea ice at 15.1 ka (14.52 ka according to the new model, 222 cm) and to warmer water species dominated at 11.3 ka (11.3 ka, 138 cm).

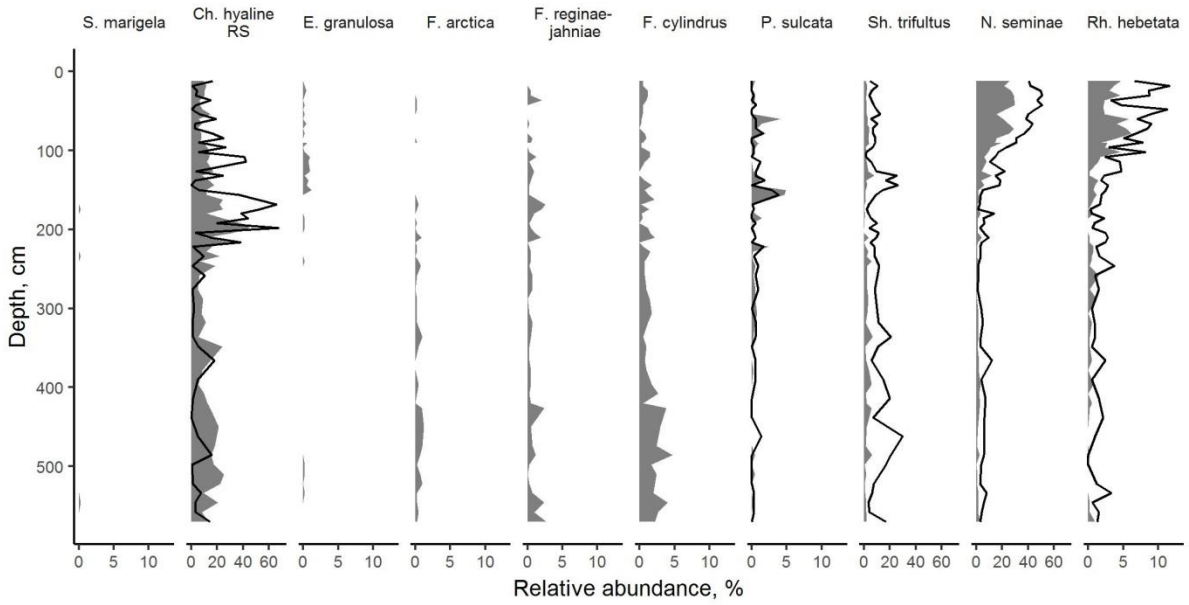

Figure 4.5. *Relative diatom abundance of the ten species counted by A. Nesterovich (gray areas) and B. Caissie (black lines) plotted against the depth. The only five species presented in both sets of counts are Chaetoceros hyaline resting spores, Paralia sulcata, Shionodiscus trifultus, Neodenticula seminae, and Rhizosolenia hebetata. The counts show similar patterns for those species. Note that the scale is different for Chaetoceros hyaline resting spores, Shionodiscus trifultus, and Rhizosolenia hebetata due their high relative abundances.*

Sea ice concentration values can indicate open ocean conditions (<15%), unconsolidated ice (15–40%), and consolidated ice (>40%) (Armand et al., 2005). Using this conversion, the GAM indicates a much longer period of consolidated spring sea ice until at least at 12.5 ka (162 cm) and a shift to ice free conditions at 7.5 ka, while the shift from consolidated to unconsolidated ice happened at approximately the same time Caissie and colleagues detected warmer water. The overall pattern of the deglaciation is nevertheless the same in both reconstructions, despite differences in timing. The differences may be due to the qualitative nature of the older reconstruction, which makes it harder to pinpoint the exact moment the concentration of ice shifts from one arbitrary category to another.

The counts themselves are also slightly different, especially in regards with pennate diatoms associated with sea ice (such as *Fossula arctica, Fragilariopsis oceanica, F.*

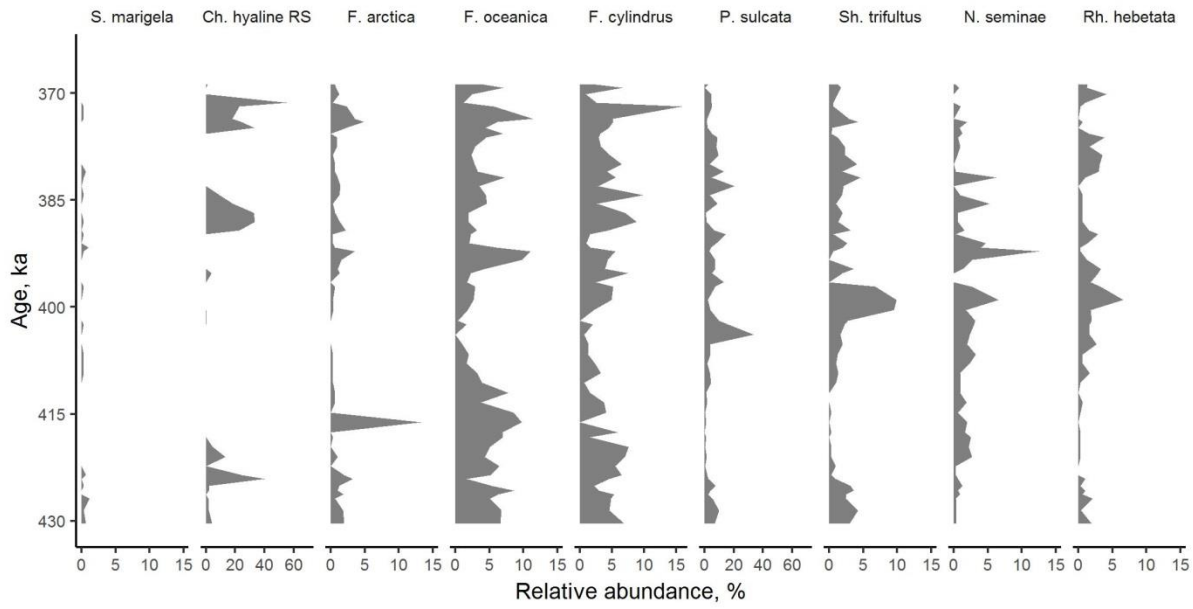

Figure 4.6. *Relative diatom abundance of the ten species counted in the core U1345. Note that the scale is different for Chaetoceros hyaline resting spores and Paralia sulcata due their high relative abundances.*

reginae-jahniae, and several others) that previously were counted together and thus cannot be compared (Fig 4.5). Different morphotaxa of *Chaetoceros* were also counted together, but due to high abundances of hyaline *Chaetoceros* resting spores relative to other morphotaxa, the new and old counts are comparable. Several species (*Shionodiscus trifultus, Neodenticula seminae,* and *Rhizosolenia hebetata*) have greater relative abundance in the old counts, probably because they include similar, rarer species. Despite these differences in diatom identifications, the two sets of counts are similar to each other.

Core U1345

MIS11, the focus of the U1345 record, is sometimes considered a good analog to the current interstadial, because it was a long interglacial with orbital parameters very similar to today's (Loutre and Berger, 2003). A previous study (Caissie 2016) and our reconstruction show that this site was under considerable influence of sea ice during the entirety of MIS11.

Caissie and colleagues (2016) point out that diatom species generally associated with warm water, such as *Shionodiscus trifultus, Neodenticula seminae*, and *Rhizosolenia hebetata*, have very low abundances in all the samples (Fig. 4.6, note that the scale for these three species on figure 4.6 is different from the scale on figure 4.5, demonstrating much lower abundances). Even though their conclusion was made qualitatively and considering whole assemblages, and our model works with abundances of only five key species, predicted sea ice concentration is in complete agreement between the two methods. Both methods indicated that the lowest sea ice concentrations during MIS11 in the Bering Sea were approximately between 410 and 391 ka, while the beginning and the end the interglacial had more sea ice in the region. Moreover, our estimates show that the North Pacific had more sea ice during entirety of MIS11 than we currently observe; the site is currently ice-free year round.

Conclusions

We have constructed an easy-to-use and accessible model for reconstructing sea ice concentration in the North Pacific based on relative abundances of diatoms in sediments using the GAM. The proxy uses relative abundance of five reliably identified diatom species: *Sinerima marigela, Fragilariospsis reginae-jahniae, Fragilariopsis cylindrus, Paralia sulcata*, and *Neodenticula seminae*. The application of the proxy to diatom counts from two cores in the Bering Sea—51JPC and U1345—resulted in a reasonable reconstruction, comparable to previously done qualitative predictions. The model reconstructs sea ice decline since the Last Glacial Maximum to present ice free conditions at the Umnak Plateau, and fluctuating, seasonal sea ice present throughout Marine Isotope Stage 11, with an excursion towards unconsolidated ice between 403 and 392 ka, in the northern Bering Sea. We argue that a quantitative model is a big improvement over qualitative predictions. The results of

such quantitative estimates can be used in oceanographic models, which need to incorporate sea ice, but until now haven't had a good way to do it beyond inputting large categories, such as permanent, seasonal, or absent ice. Diatom-based quantitative estimates can also be compared to other quantitative proxies, such as IP_{25} to improve our understanding of processes responsible for creating paleo archives.

The proxy we constructed is not only valuable, but is also relatively easy to implement. It uses only five species and does not require full counts of diatom assemblages, which makes obtaining data to run the model fast and cheap. The five species we chose are hard to confuse with any other diatoms found in the North Pacific. As an additional advantage, the archived open code used to create the model make it possible to modify and adjust our model for a new region and a new set of species.

References

Anderson, N.J., Bugmann, H., Dearing, J.A., Gaillard, M.J., 2006. Linking palaeoenvironmental data and models to understand the past and to predict the future. Trends Ecol. Evol. 21, 696–704. doi:10.1016/j.tree.2006.09.005

Belt, S.T., Massé, G., Rowland, S.J., Poulin, M., Michel, C., LeBlanc, B., 2007. A novel chemical fossil of palaeo sea ice: IP25. Org. Geochem. 38, 16–27. doi:10.1016/j.orggeochem.2006.09.013

Brown, T.A., Belt, S.T., Tatarek, A., Mundy, C.J., 2014. Source identification of the Arctic sea ice proxy IP25. Nat. Commun. 5, 4197. doi:10.1038/ncomms5197

Brown, Z.W., Arrigo, K.R., 2013. Sea ice impacts on spring bloom dynamics and net primary production in the Eastern Bering Sea. J. Geophys. Res. Ocean. 118, 43–62. doi:10.1029/2012JC008034

Caissie, B.E., Brigham-Grette, J., Cook, M.S., Colmenero-Hidalgo, E., 2016. Bering Sea surface water conditions during Marine Isotope Stages 12 to 10 at Navarin Canyon (IODP Site U1345). Clim. Past 12, 1739–1763. doi:10.5194/cp-12-1739-2016

Caissie, B.E., Brigham-grette, J., Lawrence, K.T., Herbert, T.D., Cook, M.S., 2010. Last Glacial Maximum to Holocene sea surface conditions at Umnak Plateau , Bering Sea , as inferred from diatom , alkenone , and stable isotope records. Paleoceanography 25, 1–16. doi:10.1029/2008PA001671

Collins, L.G., Allen, C.S., Pike, J., Hodgson, D.A., Weckstrom, K., Massé, G., 2013. Evaluating highly branched isoprenoid (HBI) biomarkers as a novel Antarctic sea-ice proxy in deep ocean glacial age sediments. Quat. Sci. Rev. 79, 87–98. doi:10.1016/j.quascirev.2013.02.004

Cook, M.S., Ravelo, A.C., Mix, A., Nesbitt, I.M., Miller, N. V., 2016. Tracing subarctic Pacific water masses with benthic foraminiferal stable isotopes during the LGM and late Pleistocene. Deep. Res. Part II Top. Stud. Oceanogr. 125–126, 84–95. doi:10.1016/j.dsr2.2016.02.006

Crawford, R.M., Gardner, C., Medlin, L.K., 1994. The genus Attheya. I. A description of four new taxa, and the transfer of *Gonioceros septentrionalis* and *G. armatas*. Diatom Res. 9, 27–51. doi:10.1080/0269249x.1994.9705286

Criscitiello, A.S., Das, S.B., Evans, M.J., Frey, K.E., Conway, H., Joughin, I., Medley, B., Steig, E.J., 2013. Ice sheet record of recent sea-ice behavior and polynya variability in the Amundsen Sea, West Antarctica. J. Geophys. Res. Ocean. 118, 118–130. doi:10.1029/2012JC008077

Cronin, T.M., Gemery, L., Briggs, W.M., Jakobsson, M., Polyak, L., Brouwers, E., 2010. Quaternary Sea-ice history in the Arctic Ocean based on a new Ostracode sea-ice proxy. Quat. Sci. Rev. 29, 3415–3429. doi:10.1016/j.quascirev.2010.05.024

Curran, M.A.J., van Ommen, T.D., Morgan, V.I., Phillips, K.L., Palmer, A.S., 2003. Ice core evidence for Antarctic sea ice decline since the 1950s. Science (80-.). 302, 1203–1206. doi:10.1126/science.1087888

Darby, D.A., 2008. Arctic perennial ice cover over the last 14 million years. Paleoceanography 23, 1–9. doi:10.1029/2007PA001479

Darby, D.A., Myers, W.B., Jakobsson, M., Rigor, I., 2011. Modern dirty sea ice characteristics and sources: The role of anchor ice. J. Geophys. Res. Ocean. 116, 1–18. doi:10.1029/2010JC006675

De Vernal, A., Rochon, A., Frechette, B., Henry, M., Radi, T., Solignac, S., 2013.

Reconstructing past sea ice cover of the Northern Hemisphere from dinocyst assemblages: Status of the approach. Quat. Sci. Rev. 79, 122–134. doi:10.1016/j.quascirev.2013.06.022

Eckert, C.G., Samis, K.E., Lougheed, C., 2008. Genetic variation across species' geographical ranges: the central–marginal hypothesis and beyond. Mol. Ecol. 17, 1170–1188. doi:10.1111/j.1365-294X.2007.03659.x

Edler, L., 1975. Attheya decora West (Bacillariophyceae) in the Öresund. Bot. Mar. 18, 187–189.

Ferry, A.J., Prvan, T., Jersky, B., Crosta, X., Armand, L.K., 2015. Statistical modeling of Southern Ocean marine diatom proxy and winter sea ice data: Model comparison and developments. Prog. Oceanogr. 131, 100–112. doi:10.1016/j.pocean.2014.12.001

Genuer, R., Poggi, J.-M., Tuleau-Malot, C., 2010. Variable selection using random forests. Pattern Recognit. Lett. 31, 2225–2236. doi:10.1016/j.patrec.2010.03.014

Grebmeier, J.M., Barry, J.P., 1991. The influence of oceanographic processes on pelagic-benthic coupling in polar regions: A benthic perspective. J. Mar. Syst. 2, 495–518. doi:10.1016/0924-7963(91)90049-Z

Hapfelmeier, A., Ulm, K., 2013. A new variable selection approach using Random Forests. Comput. Stat. Data Anal. 60, 50–69. doi:10.1016/j.csda.2012.09.020

Hare, C.E., Leblanc, K., DiTullio, G.R., Kudela, R.M., Zhang, Y., Lee, P.A., Riseman, S., Hutchins, D.A., 2007. Consequences of increased temperature and CO2 for phytoplankton community structure in the Bering Sea. Mar. Ecol. Prog. Ser. 352, 9–16. doi:10.3354/meps07182

Hasle, G.R., Syvertsen, E.E., von Quillfeldt, C.H., 1996. *Fossula arctica* gen. nov., spec. nov., a marine Arctic araphid diatom. Diatom Res. 11, 261–272. doi:10.1080/0269249x.1996.9705383

Hillaire-Marcel, C., de Vernal, A., 2008. Stable isotope clue to episodic sea ice formation in the glacial North Atlantic. Earth Planet. Sci. Lett. 268, 143–150. doi:10.1016/j.epsl.2008.01.012

Immonen, N., 2013. Surface microtextures of ice-rafted quartz grains revealing glacial ice in

the Cenozoic Arctic. Palaeogeogr. Palaeoclimatol. Palaeoecol. 374, 293–302. doi:10.1016/j.palaeo.2013.02.003

Jennings, A.E., Knudsen, K.L., Hald, M., Hansen, V., Andrews, J.T., 2002. A mid-Holocene shift in Arctic sea-ice variability on the East Greenland Shelf. The Holocene 12, 49–58. doi:10.1191/0959683602hl519rp

Justwan, A., Koç, N., 2008. A diatom based transfer function for reconstructing sea ice concentrations in the North Atlantic. Mar. Micropaleontol. 66, 264–278. doi:10.1016/j.marmicro.2007.11.001

Loutre, M.-F., Berger, A., 2003. Marine Isotope Stage 11 as an analogue for the present interglacial. Glob. Planet. Change 36, 209–217. doi:10.1016/S0921-8181(02)00186-8

Lundholm, N., Hasle, G.R., 2010. Fragilariopsis (Bacillariophyceae) of the Northern Hemisphere – morphology, taxonomy, phylogeny and distribution, with a description of *F. pacifica* sp. nov. Phycologia 49, 438–460. doi:10.2216/09-97.1

Lundholm, N., Hasle, G.R., 2008. Are *Fragilariopsis cylindrus* and *Fragilariopsis nana* bipolar diatoms ? – Morphological and molecular analyses of two sympatric species by. Nov. Hedwigia Beih. 133, 231–250. doi:1438-9134/08/0133–231

MacGillivary, M.L., Kaczmarska, I., 2013. Lectotypification of *Paralia sulcata* and description of *P. obscura* sp. nov. (Bacillariophyta) from the Ehrenberg Collection. Diatom Res. 28, 221–235.

McQuoid, M.R., Nordberg, K., 2003. The diatom *Paralia sulcata* as an environmental indicator species in coastal sediments. Estuar. Coast. Shelf Sci. 56, 339–354. doi:10.1016/S0272-7714(02)00187-7

Miettinen, A., Koç, N., Husum, K., 2013. Appearance of the Pacific diatom *Neodenticula seminae* in the northern Nordic Seas - An indication of changes in Arctic sea ice and ocean circulation. Mar. Micropaleontol. 99, 2–7. doi:10.1016/j.marmicro.2012.06.002

Müller, J., Wagner, A., Fahl, K., Stein, R., Prange, M., Lohmann, G., 2011. Towards quantitative sea ice reconstructions in the northern North Atlantic: A combined biomarker and numerical modelling approach. Earth Planet. Sci. Lett. 306, 137–148. doi:10.1016/j.epsl.2011.04.011

Nesterovich, A., Caissie, B.E., 2018. Taxonomy and ultrastructure of *Sinerima*, a new genus of diatoms (Bacillariophyta), with a description of a new species *S. marigela*. Phytotaxa 351, 197–209. doi:https://doi.org/10.11646/phytotaxa.351.3.1

Reid, P.C., Johns, D.G., Edwards, M., Starr, M., Poulin, M., Snoeijs, P., 2007. A biological consequence of reducing Arctic ice cover: arrival of the Pacific diatom Neodenticula seminas in the North Atlantic for the first time in 800,000 years. Glob. Chang. Biol. 13, 1910–1921. doi:10.1111/j.1365-2486.2007.01413.x A

Rontani, J.-F., Smik, L., Belt, S.T., Vaultier, F., Armbrecht, L., Leventer, A., Armand, L.K., 2019. Abiotic degradation of highly branched isoprenoid alkanes and other lipids in the water column off East Antarctica. Mar. Chem. doi:10.1016/j.marchem.2019.02.004

Sancetta, C., 1981. Oceanographic and ecologic significance of diatoms in surface sediments of the Bering and Okhotsk seas. Deep Sea Res. Part A. Oceanogr. Res. Pap. 28, 789–817. doi:10.1016/S0198-0149(81)80002-7

Selz, V., Saenz, B.T., van Dijken, G.L., Arrigo, K.R., 2018. Drivers of Ice Algal Bloom Variability between 1980 and 2015 in the Chukchi Sea. J. Geophys. Res. Ocean. 123, 1–16. doi:10.1029/2018JC014123

Serreze, M.C., Holland, M.M., Stroeve, J., 2007. Perspectives on the Arctic's shrinking sea-ice cover. Science (80). 315, 1533–1536. doi:10.1016/S0169-1317(03)00213-8

Sha, L., Jiang, H., Seidenkrantz, M.-S., Knudsen, K.L., Olsen, J., Kuijpers, A., Liu, Y., 2014. A diatom-based sea-ice reconstruction for the Vaigat Strait (Disko Bugt, West Greenland) over the last 5000yr. Palaeogeogr. Palaeoclimatol. Palaeoecol. 403, 66–79. doi:10.1016/j.palaeo.2014.03.028

Shimada, C., Burckle, L.H., Tanimura, Y., 2003. Morphological variability in *Neodenticula seminae*, a marine planktonic diatom in the North Pacific Ocean and Bering Sea. Diatom Res. 18, 307–322.

Sigler, M.F., Harvey, H.R., Ashjian, C.J., Lomas, M.W., Napp, J.M., Stabeno, P.J., Van Pelt, T.I., 2010. How does climate change affect the Bering Sea ecosystem? Eos, Trans. Am. Geophys. Union 91, 457–458. doi:10.1029/2010EO480001

St. John, K., Passchier, S., Tantillo, B., Darby, D.A., Kearns, L.E., 2015. Microfeatures of modern sea-ice-rafted sediment and implications for paleo-sea-ice reconstructions. Ann. Glaciol. 56, 83–93. doi:10.3189/2015AoG69A586

Stroeve, J., Holland, M.M., Meier, W., Scambos, T., Serreze, M., 2007. Arctic sea ice decline: Faster than forecast. Geophys. Res. Lett. 34, 1–5. doi:10.1029/2007GL029703

Sundström, B.G., 1986. The marine diatom genus *Rhizosolenia*: A new approach to the taxonomy. Lund University.

Vare, L.L., Massé, G., Gregory, T.R., Smart, C.W., Belt, S.T., 2009. Sea ice variations in the central Canadian Arctic Archipelago during the Holocene. Quat. Sci. Rev. 28, 1354–1366. doi:10.1016/j.quascirev.2009.01.013

von Quillfeldt, C.H., 2000. Common diatom species in Arctic spring blooms: Their distribution and abundance. Bot. Mar. 43, 499–516.

Von Quillfeldt, C.H., 2004. The diatom *Fragilariopsis cylindrus* and its potential as an indicator species for cold water rather than for sea ice. vie milieu 54, 137–143.

Yongqi, G., Jianqi, S., Fei, L., Shengping, H., Sandven, S., Qing, Y. an, Zhongshi, Z., Lohmann, K., Keenlyside, N., Furevik, T., Lingling, S., 2015. Arctic Sea Ice and Eurasian Climate : A Review. Adv. Atmospheic Sci. 32, 92–114. doi:10.1007/s00376-014-0009-6.1.

CHAPTER 5. CONCLUSIONS

The goal of this dissertation was to construct a quantitative proxy for sea ice concentration in the North Pacific and the Pacific sector of the Arctic Ocean. Ideally, it would be based on diatoms, the dominant component of North Pacific sediments and a natural climate archive. Compared to physical or chemical archives, biological proxies are usually harder to develop and use, because of the huge diversity of organisms that need to be identified and related to the environmental conditions the community was living in. The main objective of this work was to create a simplified, but still robust, version of a diatom-based proxy that would not require differentiation between hundreds of diatom species.

The foundation of any biological proxy are the organisms it is based on. Turning diatom records into an archive of environmental information requires an understanding of classification and taxonomy of diatoms and familiarity with the diversity of organisms in the region. While searching for diatom species that respond to sea ice conditions more strongly than to other environmental factors, I realized that the species most tied to sea ice and reaching its peak abundance at 90% sea ice concentration was not something I could find among described taxa. A closer investigation, using an SEM, revealed a set of characters unique to this taxon. As far as I know, *Sinerima marigela* is the only fultoportulate diatom without a rimoportula. Outside of the group, there are only a handful of centric diatoms that don't have a rimoportula or at least traces of once possessing it. This discovery became Chapter 2 in my dissertation, because constructing a proxy requires a solid taxonomical foundation. The species (and the new genus) needed to be described to be included in the proxy.

Chapter 3 serves as another prerequisite study for constructing a proxy. Sedimentation processes in the ocean are not fully understood and are hard to study. Ideally, we would compare phytoplankton communities and their changes throughout a year with surface sediments accumulated during that time. However, collecting phytoplankton from remote locations at regular intervals is very expensive and difficult. Thus, we are restricted to extrapolating results obtained from small freshwater lakes and using sediment traps. Despite the limitations, sediment traps present a unique opportunity to study sedimentation in progress. I found that Chukchi Sea sediment trap samples look like and cluster together with sediment samples in Principal Component Analysis,

One of the main unanswered questions that remains is, "What is happening to phytoplankton in the surface waters, as it begins to settle?" During the time I spent preparing this dissertation I had an opportunity to count phytoplankton and sea ice samples collected in the Bering Sea. I can confirm that phytoplankton samples are rich in thin, very lightly silicified, almost transparent diatoms that are mostly absent from sediment samples (and sediment trap samples). The delicate structure of those diatoms doesn't allow them to be preserved in the sediments. It is reasonable to assume that they dissolve at the very top of the water column, before they sink out of the photic zone. The processes in the photic zone and their effect on sedimentation are an area of future research. A monitoring station, where a plankton net sample would be collected once every few days for year would be an ideal material for solving the mystery of phytoplankton dissolution. In the absence of that, bucket samples from passing ships would help us answer many questions.

The set of samples I had to work with helped me solve another mystery. After counting 24 samples from a sediment trap and comparing them with sediments below, I can

say that I don't see any evidence of preferential dissolution of sea ice diatoms at the sediment-water interface as previously suggested in literature. The sea ice species, like the rest of the diatom community, are present in sediment traps and sediments in very similar relative abundances. And since we see evidence that sediment trap samples reflect changes in the surface waters to some degree, this confirms that we can infer sea ice conditions from sediment samples.

Chapter 4 is the culmination of this work, achieving the main goal of this research—constructing a diatom-based quantitative proxy for sea ice concentration in Beringia. The resulting proxy is not only quantitative, but also ecologically meaningful, since it uses only species known for their response to sea ice. Another advantage of the proxy is the ease of use. Unlike many organism-based proxies, it doesn't require full counts or identification of the whole community; rather it takes relative abundances of only five easily recognizable species. It is still not as fast as chemical proxies, but much less time-consuming than most biological proxies and cheaper than chemical ones. To make it even more appealing, I wrote a web-based application, where anyone not familiar with the R language can upload their counts and get the results in a few seconds.

The proxy developed in the course of this study is potentially useful for climate modelling. Sea ice is an influential part of the climate system, and to accurately predict future changes models need to incorporate sea ice. That, however, would require a quantitative paleo record to train the model. Thus, extending the records of sea ice back in time is very important.

APPENDIX A. CHARACTER DESCRIPTION

The states of the characters for each species were identified on SEM micrographs previously published (Fryxell & Hasle 1972, 1977, 1980, Hasle 1973, 1979, 1983; Hasle *et al.* 1971; Julius & Tanimura 2001; Makarova 1988; Park *et al.* 2016; Syvertsen & Hasle 1982, 1984) or obtained during this study. The codes used in the character table are given in parentheses after each character state. If a character is absent in a species, it was coded as '-'. If the state couldn't be determined from the available microphotographs, it was coded as ambiguous (?).

CHARACTER 1. Number of rimoportulae. Most of the Thalassiosiroid species have 1 (1) rimoportula, but there are species in our analysis without it (0), or with 2 (2) or 4 (4) rimoportulae per valve.

CHARACTER 2. Position of the rimoportula(e). The rimoportulae can be found at the valve face-mantle junction (1), on the mantle (2), or on the valve face (3).

CHARACTER 3. Rimoportula habit. This character refers to the internal opening of the rimoportula(e). We didn't differentiate between long and short stalks or raised and pinched rimoportula, so the states are either sessile (1) or stalked (2).

CHARACTER 4. Rimoportula external opening. We recognized four states of this character: a long tube (1), a short tube (2), a simple pore (3), and a rimmed pore (4).

CHARACTER 5. Position of the rimoportula(e) in relation to marginal fultoportulae. The rimoportula is usually located in a row of marginal fultoportulae, where it can be between fultoportulae (1) or take place of a fultoportula (2). When the rimoportula is located on the valve face or just outside the ring of fultoportulae, is was coded as (3).

CHARACTER 6. Central fultoportulae number. As Julius and Tanimura (2001), we separated this continuous character into discrete states: none (0), one (1), few (2), several (3), or many (4) central fultoportulae, but we also included one (5) or several (6) subcentral fultoportulae.

CHARACTER 7. Satellite pore number in the central fultoportulae. Among the analyzed species, this character has only two states, either 3 (3) or 4 (4).

CHARACTER 8. Pore cover shape in the central fultoportulae. The pore covers can be represented by a simple ridge (0), a triangular tab (1), be ball-like (2), or be absent (3).

CHARACTER 9. Internal tube of the central fultoportulae. Internally, the central tube of the central fultoportulae can be either short (1) or long (2).

CHARACTER 10. Cowling shape in the central fultoportulae. In most cases there is either no cowling (0) or it's represented by a ridge (1). Some species have complex-shaped (2) cowlings unique for a species.

CHARACTER 11. Central fultoportula tube/pore ratio. Dividing the outer diameter of the central fultoportula's internal tube by the diameter of the pore in it gives one of the three numbers among the surveyed species: 1.7 (0), 2 (1), or 3 (2). If a central fultoportula is absent, it was coded as (-).

CHARACTER 12. Position of the central fultoportula(e) in relation to areolae. It can occupy the space between areolae (0) or appear instead of them (1).

CHARACTER 13. External extension of the central fultoportula(e). Externally central fultoportulae can open as a simple pore (0), a rimmed pore (1), or a tube (2).

CHARACTER 14. Satellite pore number in marginal fultoportulae. Character states are 3 (3), 4 (4), or 5 (5).

CHARACTER 15. Pore cover shape in marginal fultoportulae. The covers of satellite pores can look like a simple ridge (0), a triangular tab (1), or be ball-like (2).

CHARACTER 16. Internal extension of the marginal fultoportulae. Internally, marginal fultoportulae have either a short (1) or a long (2) tube.

CHARACTER 17. Cowling shape in marginal fultoportulae. Similar to character 10, but refers to marginal fultoportulae. The cowling can be absent (0), be represented by a ridge (1), or have a complex shape (2).

CHARACTER 18. Marginal fultoportulae tube/pore ratio. We found that in species with both central and marginal fultoportulae the ratio is the same. However, since there is a number of species in the analysis without a central fultoportula, we decided to use this character alongside with character 11. The states are 1.7 (1), 2 (2), or 3 (3).

CHARACTER 19. Number of rows of marginal fultoportulae. Among the studied species, there can be 1 (1), 2 (2), or 3 (3) rows of fultoportulae.

CHARACTER 20. Alignment of marginal fultoportulae. In some species all fultoportulae forming a ring are in the same plane (0), whereas in others marginal fultoportulae are not perfectly aligned (1).

CHARACTER 21. External extension of the marginal fultoportulae. Externally marginal fultoportulae can open as a simple pore (0), a rimmed pore (1), a tube (2), or a complex shape with a flare, a spine or a bulb (3).

CHARACTER 22. Valve face fultoportulae presence. The studied species either have additional fultoportulae, other than central and marginal ones, scattered on the valve face (0) or they don’t (1).

CHARACTER 23. Occluded processes. The species either have occluded processes (0) or they don't (1). The processes were assumed present even if only some individuals in the species have them.

CHARACTER 24. Spines. The same as with the character 23, but refers to the presence (0) or absence (1) of solid spines, as opposed to hollow occluded processes. They were assumed present if at least some individuals in a species have them.

CHARACTER 25. Cribra position. Three character states were anticipated for this feature. Cribra can be on the inside (0), on the outside (1), or within the areolae (2). However, upon examining the species included in the analysis only the first and the last states were found.

CHARACTER 26. Cribra morphology. As with the character 25, more character states were anticipated, than eventually observed among the studied species. The cribra could be flat (0), raised (1), domed (2), or consist of rimmed pores (3), but there were no species with domed cribra.

CHARACTER 27. Foramen shape. The shape of the foramena on the outside of the valve was represented by small circles (1), large circles (2), angular shaped (3), or foramena were absent (0).

CHARACTER 28. Loculi shape. The shape of the loculi could be circular (0), hexagonal (1), irregular (2), or square (3).

CHARACTER 29. Areolae pattern can be described as bifurcating radial rows (0), fascicules with rows parallel to the central row (1), linear with straight rows (2), or eccentric rows (3).

CHARACTER 30. Outline in girdle view. We distinguished six general outlines of valves in the girdle view, though we didn't find species presenting flat valves with a bump in the centre (2). The observed states were flat valves (0), with a pit in the centre (1), domed (3), concave (4), and plicated (5).

CHARACTER 31. Layers of silica on the valve. The number of silica layers on the valve face can be either two (0), which is observed in most species, or one (1), if a species has only the basal layer.

CHARACTER 32. Cross-walls separating the poroidal layer. The presence (0) or absence (1) of cross-walls, separating individual cribra on the basal layer of the valve face.

CHARACTER 33. Radial extent of ribs on the valve face, which can end at the junction between the valve and the mantle (1) or continue to the mantle (0).

CHARACTER 34. Pattern formed by ribs on the valve face. It can be described as bifurcating radial (0), fasciculated (1), linear (2), or eccentric (3).

CHARACTER 35. Pattern formed by ribs on the mantle. We considered two character states: ribs form parallel rows (0) or not (1).

APPENDIX B. LIST OF DIATOM SPECIES IDENTIFIED IN STUDIED SAMPLES

Table B.1 *List of diatom species found in three groups of samples used in this study. The presence of species is indicated by x. Detailed counts for every samples can be downloaded from the Arctic Data Center.*

Species	Surface sediments	Sediment trap	Sediments near mooring
Achnanthes hyperboreoides	x	x	x
Achnanthes lemmermannii	x		
Achnanthes sp.1	x		
Achnanthes sp.2	x		
Achnanthes sp.4	x		
Achnanthes sp.5	x	x	
Actinocyclus cf. normanii	x		
Actinocyclus cf. subtilis	x		
Actinocyclus curvatulus	x	x	x
Actinocyclus ochotensis	x	x	x
Actinocyclus octonarius	x		
Actinocyclus radiatus	x		
Actinocyclus sp.1	x		
Actinocyclus sp.2	x		
Actinocyclus sp.3	x		
Actinoptychus senarius	x	x	
Actinoptychus sp.1	x		
Actinoptychus sp.2	x		
Actinoptychus sp.3	x		
Actinoptychus vulgaris	x		
Alveus marinus	x		
Amphora cf. gacialis	x		
Amphora sp.1	x		
Amphora sp.2	x	x	
Amphora tomiakae	x		
Asteromphalus hyalinum	x		
Asteromphalus sp.	x		
Attheya decora		x	
Aulacoseira sp.	x		
Azpeitia sp.	x		
Azpeitia tabularis	x		
Bacterosira bathyomphala	x	x	
Bacterosira bathyomphala RS	x	x	x
Bacterosira constricta	x	x	
Bacterosira constricta RS	x	x	

Species	Surface sediments	Sediment trap	Sediments near mooring
Berkeleya scopulorum	x		
Biddulphia sp.	x		
Biddulphia sp.2	x		
Cavinula sp.	x		
Centric gen. sp.1	x		
Centric gen. sp.2	x		
Centric gen. sp.3	x		
Centric gen. sp.4	x		
Chaemopinnularia cp.	x	x	
Chaetoceros Coronodiscus	x	x	x
Chaetoceros Dicladia		x	
Chaetoceros Dispinodiscus	x	x	x
Chaetoceros Gemellodiscus	x	x	x
Chaetoceros hyaline RS	x	x	x
Chaetoceros Liradiscus	x	x	
Chaetoceros Monocladia	x	x	x
Chaetoceros Peripteropsis	x	x	x
Chaetoceros Quadrocistella	x		
Chaetoceros Syndendrium	x	x	x
Chaetoceros Truncatulus	x		
Chaetoceros Vallodiscus	x	x	x
Chaetoceros vegetative cells	x	x	
Chaetoceros Xanthiopyxis	x	x	x
Climacosphenia sp.	x		
Cocconeis cf. californica	x		
Cocconeis costata	x		
Cocconeis distans	x		
Cocconeis sp.01	x		
Cocconeis sp.02	x		
Cocconeis sp.03	x		
Cocconeis sp.04	x		
Cocconeis sp.05	x		
Cocconeis sp.06	x		
Cocconeis sp.07	x		
Cocconeis sp.08	x		
Cocconeis sp.09	x		
Cocconeis sp.10	x		
Coscinodiscus cf. oculus-iridus	x	x	
Coscinodiscus cf. radiatus	x		
Coscinodiscus marginatus	x		x
Coscinodiscus sp.	x		

Species	Surface sediments	Sediment trap	Sediments near mooring
Coscinodiscus sp.1	x		
Cyclotella ocellata	x	x	
Cyclotella sp.1	x		
Cyclotella sp.2	x		
Cyclotella sp.3	x		
Cyclotella sp.4	x		
Cyclotella sp.5	x		
Cyclotella sp.6	x		
Cyclotella sp.7	x		
Cyclotella sp.8	x		
Cymbella sp.1	x	x	
Cymbella sp.2	x		
Delphineis cf. minutisima	x		
Delphineis kippae	x	x	x
Delphineis sp.1	x		
Delphineis sp.2	x		
Delphineis sp.3	x		
Delphineis surrirella	x	x	x
Detonula confervacea	x	x	x
Detonula sp.	x		
Diatomella minuta	x		
Diploneis smithii	x	x	
Diploneis sp.1	x		
Diploneis sp.2	x		
Diploneis sp.3	x		
Diploneis subcincta	x		
Dytilum brightwellii		x	
Ehrenbergiulvia granulosa	x	x	
Ehrenbergiulvia sp.	x	x	
Ellerbeckia sol	x	x	x
Encyonema sp.1	x	x	
Encyonema sp.2	x		
Encyonema sp.3	x		
Entomoneis sp.1	x	x	
Entomoneis sp.2	x		
Eucampia zodiacus	x	x	
Eunotia sp.	x	x	
Eunotogramma sp.		x	x
Fallacia minima	x		
Fallacia schaeroneis		x	
Fallacia sp.	x		

Species	Surface sediments	Sediment trap	Sediments near mooring
Fogedia geisslerae	x		
Fogedia sp.1	x		
Fogedia sp.2	x		
Fossula arctica	x	x	x
Fragilaria cf. capitata	x		
Fragilaria cf. martyi	x		
Fragilaria cf. vaucheria	x		
Fragilaria sp.01	x		
Fragilaria sp.02	x	x	
Fragilaria sp.03	x		
Fragilaria sp.04	x		
Fragilaria sp.05	x		
Fragilaria sp.06	x		
Fragilaria sp.07	x		
Fragilaria sp.08	x		
Fragilaria sp.09	x		
Fragilaria sp.10	x		
Fragilaria sp.11	x		
Fragilaria sp.12	x	x	
Fragilariopsis atlantica	x		
Fragilariopsis cf. cylindrus	x		
Fragilariopsis cf. doliolus	x		
Fragilariopsis cf. oceanica	x		
Fragilariopsis cylindrus	x	x	x
Fragilariopsis humboldtianorum	x		
Fragilariopsis nana	x	x	x
Fragilariopsis oceanica	x	x	x
Fragilariopsis pacifica	x	x	
Fragilariopsis pseudonana	x	x	
Fragilariopsis reginae-jahniae	x	x	x
Fragilariopsis reginae-jahniae RS	x	x	x
Fragilariopsis sp.1	x	x	x
Fragilariopsis sp.1 RS	x		
Fragilariopsis sp.2	x	x	
Fragilariopsis sp.3	x		
Gomphonema sp.01	x		
Gomphonema sp.02	x		
Gomphonema sp.03	x		
Gomphonema sp.04	x		
Gomphonema sp.05	x		
Gomphonema sp.06	x		

Species	Surface sediments	Sediment trap	Sediments near mooring
Gomphonema sp.07	x		
Gomphonema sp.08	x		
Gomphonema sp.09	x		
Gomphonemopsis obscurum	x	x	
Gomphonemopsis sp.1	x		
Grammatophora hamulifera	x		
Grammatophora marina	x		
Hantzschia virgata		x	
Haslea sp.	x	x	
Hyalodiscus scoticus	x		
Hyalodiscus sp.	x		
Hypodonta sp.	x		
Lyrella sp.1	x	x	
Lyrella sp.2	x		
Lyrella sp.3	x		
Lyrella sp.4	x		
Lyrella sp.5	x		
Mastogloia sp.	x		
Melosira moniliformis		x	
Melosira sp.1	x		
Melosira sp.2	x		
Meridion circulare	x		
Minidiscus sp.	x		
Navicula cf. abunda	x		
Navicula directa	x	x	
Navicula kariana	x	x	x
Navicula kariana var. detersa	x	x	x
Navicula lineola	x	x	
Navicula lineola var. lineata	x	x	x
Navicula lineola var. perlepida	x	x	x
Navicula pelagica	x		
Navicula sp.01	x		
Navicula sp.02	x	x	x
Navicula sp.03	x		
Navicula sp.05	x		
Navicula sp.06	x		
Navicula sp.07	x		
Navicula sp.08	x		
Navicula sp.09	x		
Navicula sp.10	x		
Navicula sp.11	x		

Species	Surface sediments	Sediment trap	Sediments near mooring
Navicula sp.12	x		
Navicula sp.13	x		
Navicula sp.14	x		
Navicula sp.15	x		
Navicula sp.16	x		
Navicula sp.17	x		
Navicula sp.18	x		
Navicula sp.19	x		
Navicula sp.20	x		
Navicula sp.21	x		
Navicula sp.22	x		
Navicula sp.23	x		
Navicula sp.24	x		
Navicula sp.25	x		
Navicula sp.26	x		
Navicula sp.27	x		
Navicula sp.28	x		
Navicula sp.29	x		
Navicula sp.30	x		
Navicula sp.31	x		
Navicula sp.32	x		
Navicula sp.33	x		
Navicula sp.34	x		
Navicula sp.35	x		
Navicula sp.36	x		
Navicula sp.37	x		
Navicula sp.38	x		
Navicula sp.39	x		
Navicula sp.40	x		
Navicula sp.41	x		
Navicula sp.42	x		
Navicula sp.43	x		
Navicula sp.44	x		
Navicula sp.45	x		
Navicula sp.46	x		
Navicula sp.47	x		
Navicula sp.48	x		
Navicula sp.49	x		
Navicula sp.50	x		
Navicula sp.51	x		
Navicula sp.52	x		

Species	Surface sediments	Sediment trap	Sediments near mooring
Navicula sp.53	x		
Navicula sp.54	x		
Navicula sp.55	x		
Navicula sp.56	x		
Navicula sp.57	x		
Navicula sp.58	x		
Navicula transitans	x	x	x
Navicula transitans var. derasa	x	x	x
Navicula vanhoeffenii		x	
Neodenticula seminae	x	x	
Nitzschia agnewii	x	x	
Nitzschia cf. arcuata	x		
Nitzschia cf. dubia	x		
Nitzschia cf. incrustuns	x		
Nitzschia cf. littoralis	x		
Nitzschia closterium	x		
Nitzschia frigida	x	x	x
Nitzschia gelida		x	
Nitzschia hybrida		x	
Nitzschia laevissima	x	x	
Nitzschia levidensis	x	x	
Nitzschia longissima		x	x
Nitzschia neofrigida	x	x	x
Nitzschia new-guinensis	x		
Nitzschia ovalis		x	
Nitzschia pellucida		x	
Nitzschia rorida	x		
Nitzschia sp.01	x		
Nitzschia sp.02	x		
Nitzschia sp.03	x		
Nitzschia sp.04	x		
Nitzschia sp.05	x		
Nitzschia sp.06	x		
Nitzschia sp.07	x		
Nitzschia sp.08	x		
Nitzschia sp.09	x		
Nitzschia sp.10	x		
Nitzschia sp.11	x		
Nitzschia sp.12	x		
Nitzschia sp.13	x		
Nitzschia sp.14	x		

Species	Surface sediments	Sediment trap	Sediments near mooring
Nitzschia sp.15	x		
Nitzschia sp.16	x		
Nitzschia sp.17	x		
Nitzschia sp.18	x		
Nitzschia sp.19	x		
Nitzschia sp.20	x		
Nitzschia sp.21	x		
Nitzschia sp.22	x		
Nitzschia sp.23	x		
Nitzschia sp.24	x		
Nitzschia sp.25	x		
Nitzschia sp.26	x		
Nitzschia sp.27	x		
Nitzschia sp.28	x		
Nitzschia sp.29	x		
Nitzschia sp.30	x		
Nitzschia sp.31	x	x	
Nitzschia sp.32	x		
Nitzschia sp.33	x		
Nitzschia sp.34	x		
Nitzschia sp.35	x		
Nitzschia sp.36	x		
Nitzschia sp.37	x		
Nitzschia sp.38	x		
Nitzschia sp.39	x		
Nitzschia thermaloides		x	
Odontella aurita	x	x	
Opephora sp.1	x		
Opephora sp.3	x		
Opephora sp.4	x		
Opephora sp2	x		
Paralia sulcata	x	x	x
Pauliella taeniata	x	x	x
Pennata gen .sp.9	x		
Pennate gen. sp.	x		
Pennate gen. sp.	x		
Pennate gen. sp.	x		
Pennate gen. sp.1	x		
Pennate gen. sp.2	x		
Pennate gen. sp.3	x		
Pennate gen. sp.4	x		

Species	Surface sediments	Sediment trap	Sediments near mooring
Pennate gen. sp.5	x		
Pennate gen. sp.6	x	x	
Pennate gen. sp.7	x		
Pennate gen. sp.8	x		
Pennate gen. sp.8	x		
Pennate gen. sp.9	x		
Pinnuavis sp.	x		
Pinnularia quadratarea	x	x	
Pinnularia sp.1	x	x	
Pinnularia sp.2	x		
Pinnularia sp.3	x		
Pinnularia sp.4	x		
Pinnularia sp.5	x		
Plagiogramma sp.	x		
Plagiogrammopsis mediaequatus	x		
Plagiogrammopsis vanheurchii	x		
Plagioprammopsis sp.	x		
Plagiotropsis gibberula		x	
Plagiotropsis sp.		x	
Planotidium sp.	x		
Pleurosigma sp.1	x	x	
Pleurosigma sp.2	x		
Pleurosigma sp.3	x		
Pleurosigma sp.4	x		
Pleurosigma sp.5	x		
Podosira sp.			
Porosira glacialis	x	x	x
Porosira glacialis vegetative cells	x	x	x
Porosira sp. vegetative cells	x		
Porosira sp.1	x		
Proboscia alata	x	x	x
Proboscia eumorpha	x	x	
Proboscia subarctica	x	x	
Proshkinia cf. poretzkayae	x		
Psammodiscus sp.	x		
Pseudogomphonema septentrionale		x	
Pseudopodosira sp.1	x	x	
Pseudopodosira sp.2	x		
Raphoneis amphiceros	x	x	
Rhizosolenia hebetata	x	x	x
Rhizosolenia setigera	x	x	

Species	Surface sediments	Sediment trap	Sediments near mooring
Rhizosolenia styliformis	x	x	
Shionodiscus trifultus	x		
Sinerima marigela	x	x	x
Skeletonema sp.1	x		
Skeletonema sp.2	x		
Small biraphid sp.1	x		
Small biraphid sp.2	x		
Stauroneis cf. arctica	x	x	x
Stauroneis hartzii		x	
Stauroneis radissonii	x	x	
Stauroneis sp.1	x		
Stauroneis sp.2	x		
Stauronella arctica			
Stauronella sp.	x		
Stenoneis sp.	x		
Stephanodiscus sp.	x		
Stephanopyxis turris	x		
Surrirella sp.	x		
Synedra sp.1	x		
Synedra sp.2	x		
Synedra sp.3	x		
Synedra sp.4	x		
Synedra sp.5	x		
Synedra sp.6	x		
Synedra sp.7	x		
Synedropsis hyperborea	x	x	x
Synedropsis sp.1	x		
Synedropsis sp.2	x		
Tabellaria flocculosa	x		
Thalassionema nitzschioides	x	x	x
Thalassionema sp.	x		
Thalassiosira <10um	x	x	
Thalassiosira angulata	x	x	
Thalassiosira angusta-lineata	x	x	
Thalassiosira antarctica	x	x	x
Thalassiosira antarctica vegetative cells	x		
Thalassiosira bioculata	x		
Thalassiosira bulbosa	x	x	x
Thalassiosira bulbosa vegetative cells	x		

Species	Surface sediments	Sediment trap	Sediments near mooring
Thalassiosira cf. antarctica	x		
Thalassiosira cf. bulbosa	x	x	
Thalassiosira cf. constricta	x		
Thalassiosira cf. eccentrica	x		
Thalassiosira cf. frenguellii	x		
Thalassiosira cf. hyalina	x	x	
Thalassiosira cf. jouseae	x	x	x
Thalassiosira cf. pacifica	x		
Thalassiosira cf. punctigera	x		
Thalassiosira cf. symmetrica	x		
Thalassiosira cf. trifulta	x		
Thalassiosira cf. weisflogii	x		
Thalassiosira constricta	x		
Thalassiosira decipiens	x		
Thalassiosira eccentrica	x		
Thalassiosira gravida	x	x	x
Thalassiosira hyalina	x	x	x
Thalassiosira hyperborea	x	x	
Thalassiosira lineata	x	x	
Thalassiosira nordenskioeldii	x	x	x
Thalassiosira oestrupii	x	x	
Thalassiosira pacifica	x	x	
Thalassiosira punctigera	x		
Thalassiosira sp.01	x		
Thalassiosira sp.02	x		
Thalassiosira sp.03	x	x	
Thalassiosira sp.05	x		
Thalassiosira sp.06	x	x	x
Thalassiosira sp.07	x		
Thalassiosira sp.08	x		
Thalassiosira sp.09	x		
Thalassiosira sp.10	x		
Thalassiosira sp.11	x		
Thalassiosira sp.12	x		
Thalassiosira sp.13	x		
Thalassiosira sp.14	x		
Thalassiosira sp.15	x		
Thalassiosira sp.16	x		
Thalassiosira sp.17	x		
Thalassiosira sp.18	x		
Thalassiosira sp.19	x		

Species	Surface sediments	Sediment trap	Sediments near mooring
Thalassiosira sp.20	x		
Thalassiosira sp.21	x		
Thalassiosira sp.22	x		
Thalassiosira sp.23	x		
Thalassiosira sp.24	x		
Thalassiosira sp.25	x		
Thalassiosira sp.26	x		
Thalassiosira sp.27	x		
Thalassiosira sp.28	x		
Thalassiosira sp.29	x		
Thalassiosira sp.30	x		
Thalassiosira sp.31	x		
Thalassiosira sp.32	x	x	
Thalassiosira sp.33	x		
Thalassiosira sp.34	x		
Thalassiosira sp.35	x		
Thalassiosira sp.36	x		
Thalassiosira sp.37	x		
Thalassiosira sp.38	x		
Thalassiosira sp.39	x		
Thalassiosira sp.40	x		
Thalassiosira sp.41	x	x	x
Thalassiosira sp.42	x	x	
Thalassiosira sp.43	x		
Thalassiosira sp.44	x		
Thalassiosira sp.45	x		
Thalassiosira sp.46	x		
Thalassiosira sp.47	x		
Thalassiosira sp.48	x	x	
Thalassiosira sp.49	x	x	
Thalassiosira sp.50	x		
Thalassiosira sp.51	x		
Thalassiosira sp.52	x	x	x
Thalassiosira sp.53		x	
Thalassiosira symmetrica	x	x	
Thalassiothrix longissima	x	x	
Trachyneis sp.	x	x	

APPENDIX C. TEN SPECIES CONSIDERED FOR THE PROXY

Figure C.1. *LM micrograph of Sinerima marigela.*

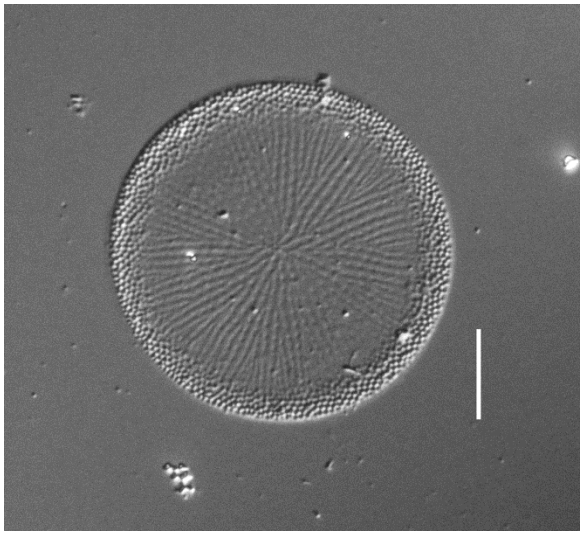

Figure C.2. *LM micrograph of Chaetoceros hyaline resting spore.*

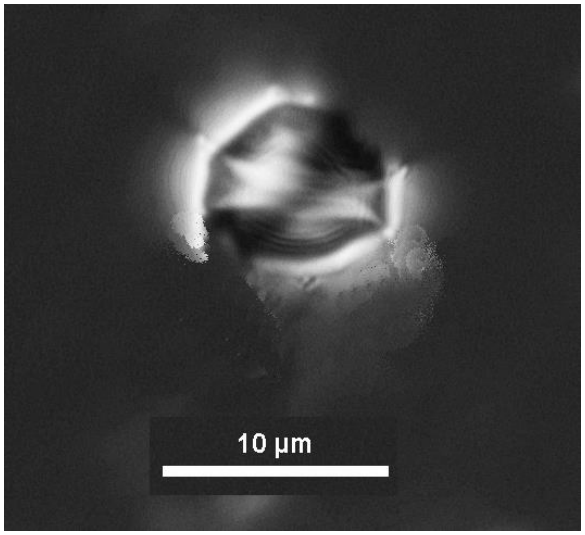

Figure C.3. *LM micrograph of Ehrenbergiulvia granulosa.*

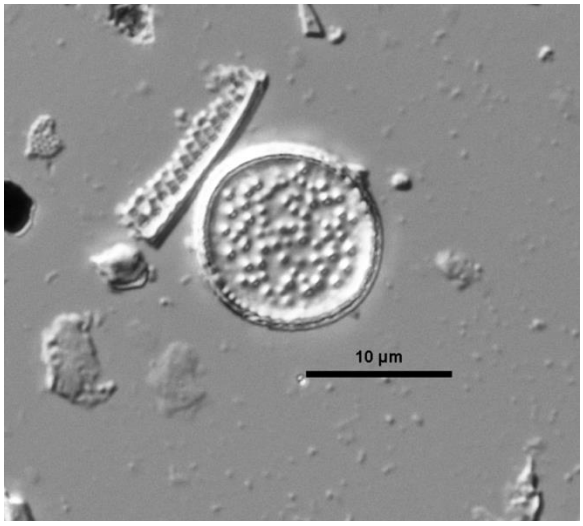

Figure C.4. *LM micrograph of Fossula arctica.*

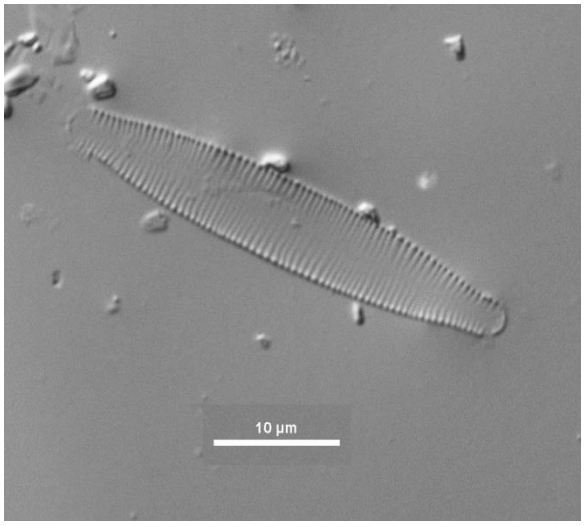

Figure C.5. *LM micrograph of Fragilariopsis reginae-jahniae. Both vegetative cells and resting spores are visible.*

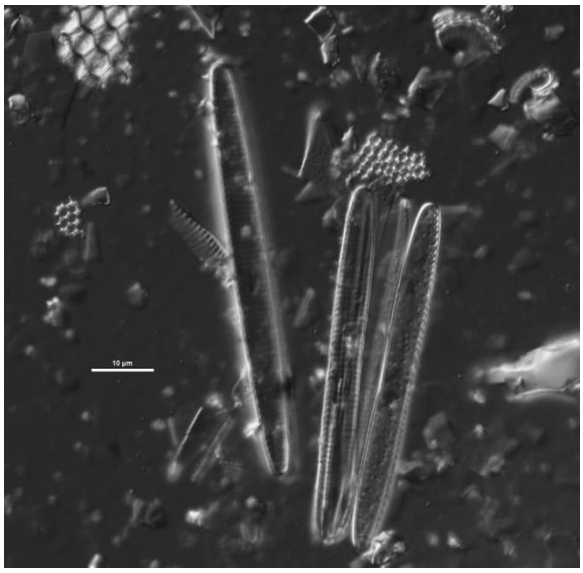

Figure C.6. *LM micrograph of Fragilariopsis cylindrus.*

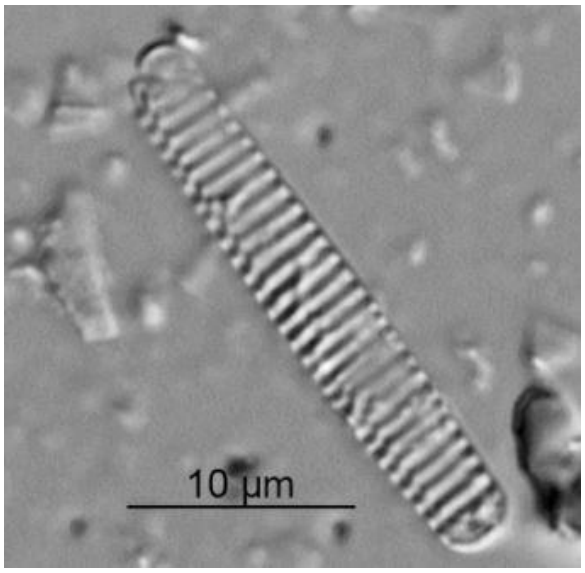

Figure C.7. *LM micrograph of Paralia sulcata.*

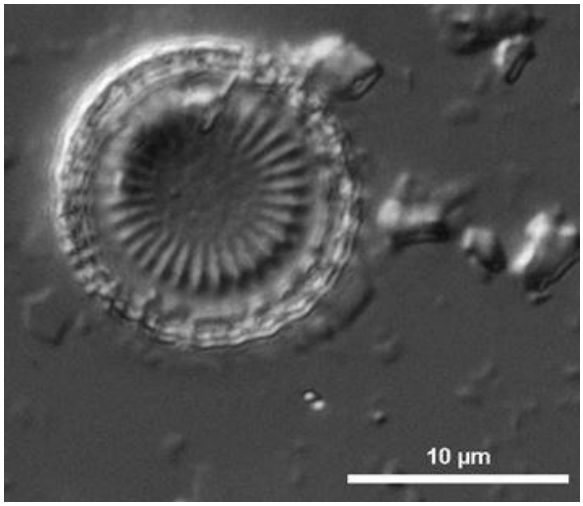

Figure C.8. *LM micrograph of Shionodiscus trifultus.*

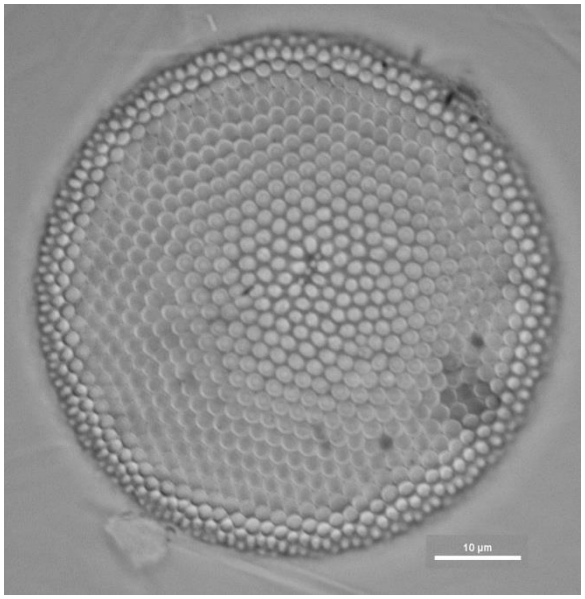

Figure C.9. *LM micrograph of Rhizosolenia hebetata.*

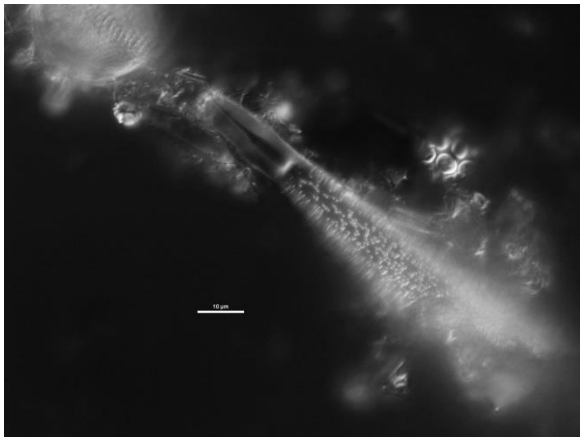

Figure C.10. *LM micrograph of Neodenticula seminae.*

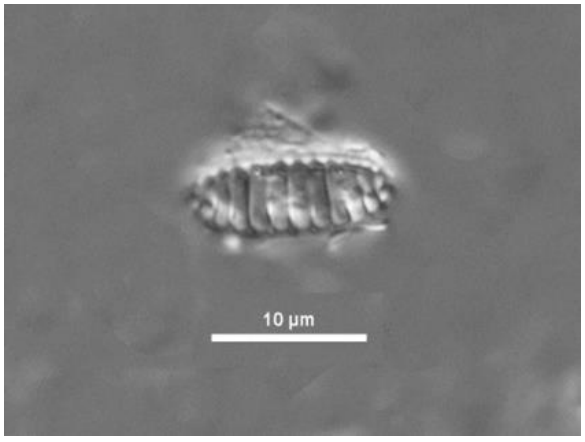

APPENDIX D. MODEL CHECKS

Figure C.1. *Standard model checks for GAM demonstrating normal distribution of residuals.*

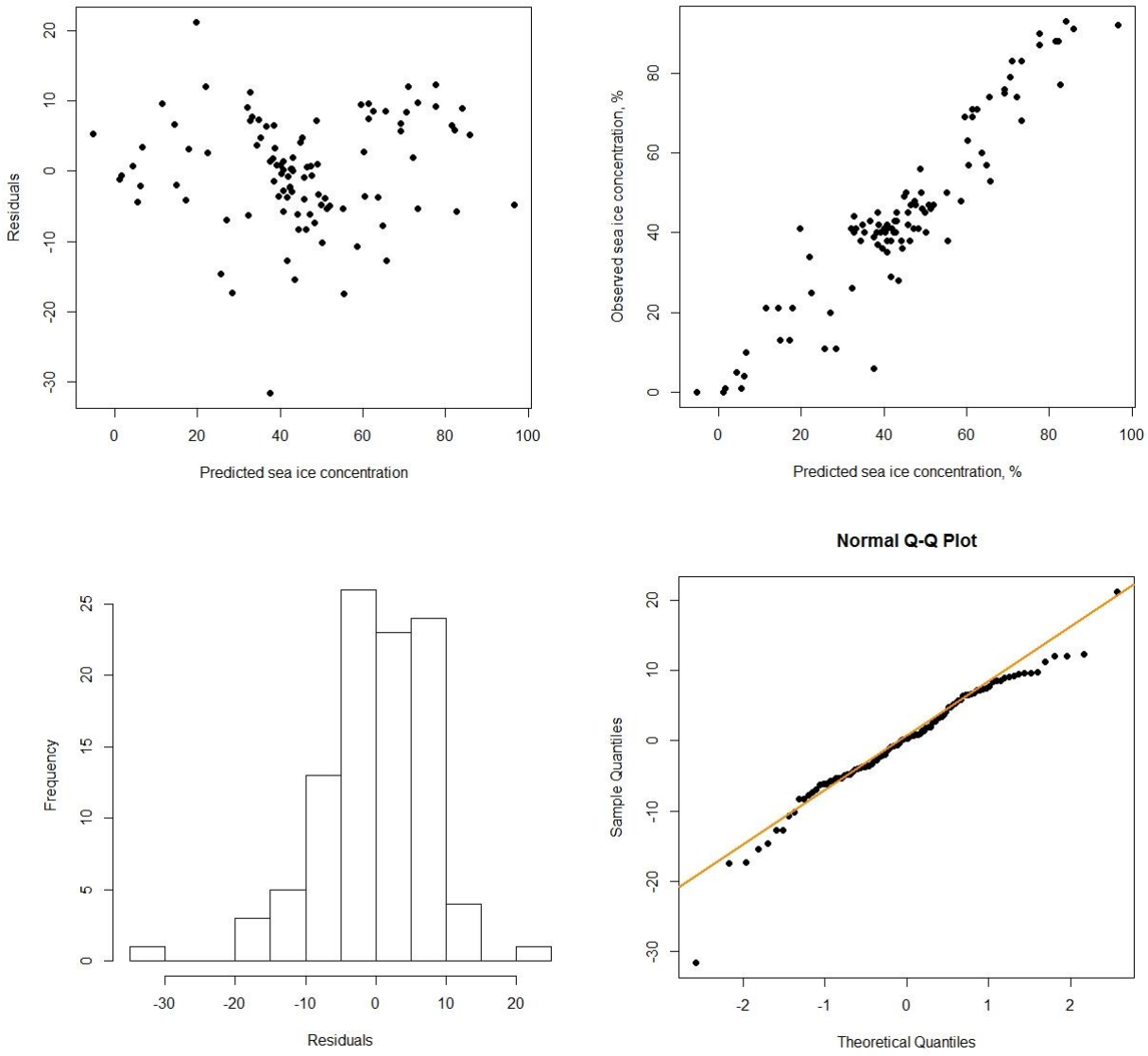

Figure D.2. *Standard model checks for GAM demonstrating independence of error terms.*

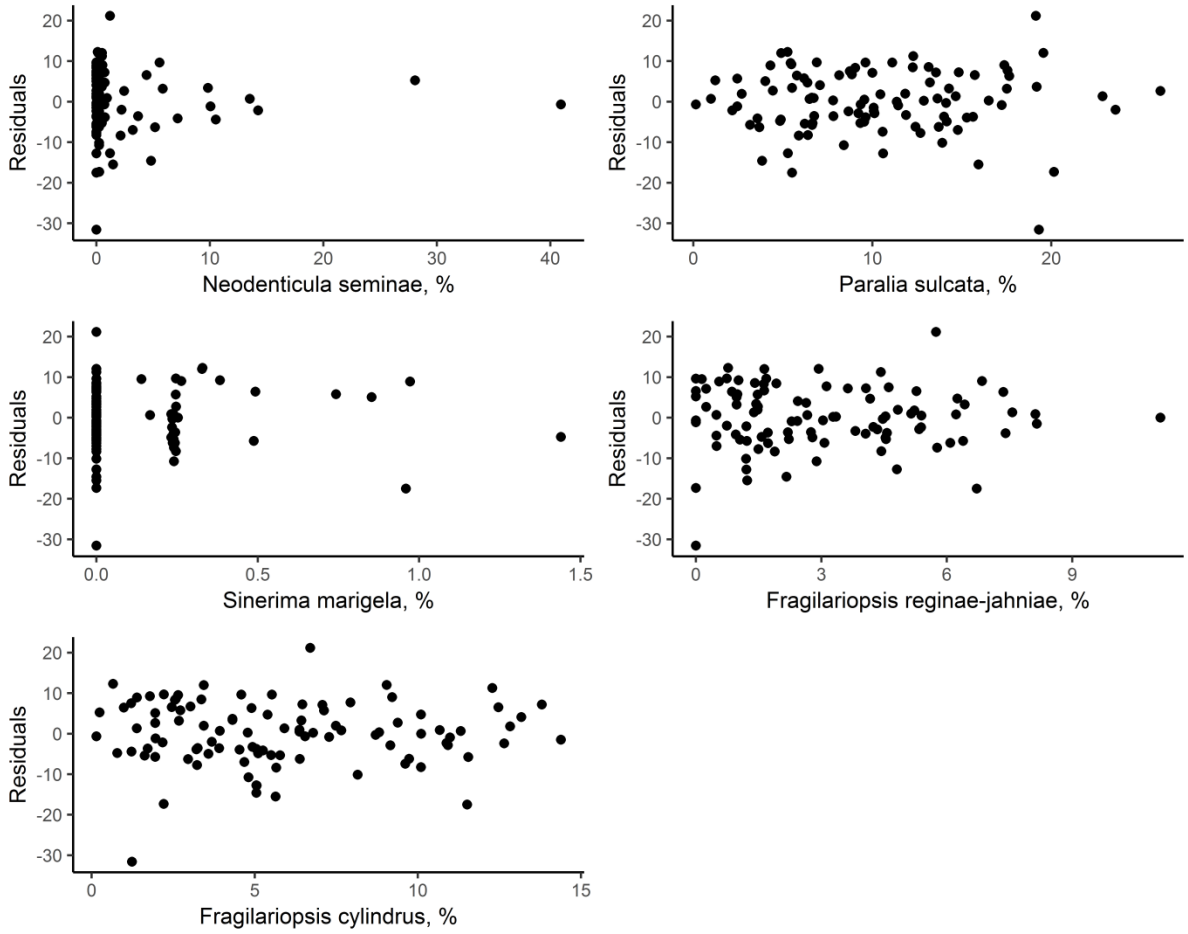

Figure D.3. *GAM residuals plotted on a schematic map of the region.*